ELECTROSPUN POLY(ε-CAPROLACTONE) - BASED NANOCOMPOSITES FOR OSTEOPOROTIC BONE DEFECT REPAIR

REMYA K.R.

Ph.D. THESIS

2017

SREE CHITRA TIRUNAL INSTITUTE FOR

MEDICAL SCIENCES AND TECHNOLOGY, THIRUVANANTHAPURAM

INDIA

ELECTROSPUN POLY(ε-CAPROLACTONE) - BASED NANOCOMPOSITES FOR OSTEOPOROTIC BONE DEFECT REPAIR

A THESIS PRESENTED BY

REMYA K.R.

TO

SREE CHITRA TIRUNAL INSTITUTE
FOR MEDICAL SCIENCES AND TECHNOLOGY,
THIRUVANANTHAPURAM
INDIA

IN PARTIAL FULFILMENT OF THE REQUIREMENTS
FOR THE AWARD OF
DOCTOR OF PHILOSOPHY

2017

CERTIFICATE

I, **Remya K.R.**, hereby certify that I had personally carried out the work depicted in the thesis entitled, **"Electrospun Poly(ε-caprolactone) - based nanocomposites for osteoporotic bone defect repair",** except where due acknowledgement has been made in the text. No part of the thesis has been submitted for the award of any other degree or diploma prior to this date.

Thiruvananthapuram

REMYA K.R.
Reg.No: 2011/PhD/04

SREE CHITRA TIRUNAL INSTITUTE FOR MEDICAL SCIENCES & TECHNOLOGY
BIOMEDICAL TECHNOLOGY WING, POOJAPPURA
THIRUVANANTHAPURAM – 695011, INDIA
(An Institute of National Importance under Govt. of India)
Phone-(91)0471-2520221 Fax-(91)0471-2341814 www.sctimst.ac.in

Dr. P. Ramesh
Scientist G & In-charge (joint)
Division of Polymeric Medical Devices
Department of Medical Devices Engineering
BMT Wing, SCTIMST
email: rameshp@sctimst.ac.in

This is to certify that **Ms. Remya K.R.**, Division of Polymeric Medical Devices, Department of Medical Devices Engineering, of this Institute has fulfilled the requirements prescribed for the Ph. D. degree of Sree Chitra Tirunal Institute for Medical Sciences and Technology, Thiruvananthapuram. The thesis entitled, **"Electrospun Poly(ε-caprolactone) – based nanocomposites for osteoporotic bone defect repair",** was carried out under my direct supervision. No part of the thesis was submitted for the award of any degree or diploma prior to this date.

Thiruvananthapuram

Dr. P. Ramesh
(Research Supervisor)

The thesis entitled

ELECTROSPUN POLY(ε-CAPROLACTONE) - BASED NANOCOMPOSITES FOR OSTEOPOROTIC BONE DEFECT REPAIR

Submitted by

Remya K.R.

for the degree of

Doctor of Philosophy

of

SREE CHITRA TIRUNAL INSTITUTE
FOR
MEDICAL SCIENCES AND TECHNOLOGY, TRIVANDRUM

Is evaluated and approved by

…….	……..
Dr. P. Ramesh	Examiner
(Research Supervisor)	

Dedicated to

GOD ALMIGHTY & MY FAMILY

ACKNOWLEDGEMENTS

It is with a deep sense of gratitude, satisfaction and with the divine blessings of Supreme God Almighty that I submit this dissertation. I take this opportunity with much pleasure to acknowledge all those who have contributed in many ways for the success of this study.

First and foremost I express my sincere gratitude and respect to my Guide Dr. P. Ramesh, Scientist G, Division of Polymeric Medical Devices, SCTIMST for his continuous advice and encouragement throughout the course of my study. He was always accessible and took significant effort for the successful completion of this endeavour.

I am grateful to Dr. Asha Kishore, Director of SCTIMST, former Director, former Head and present Head of BMT Wing, Dr. H. K. Varma for all support provided during the course of my work. I am thankful to the Dean Dr. V. Kalliyana Krishnan, Associate Dean Dr. Roy Joseph, Deputy Registrar Dr. Santosh Kumar B and all former and present members of academic division for their assistance.

I thank members of Doctoral Advisory Committee, Dr. Annie John, Scientist G, Transmission electron microscope and Dr. Roy Joseph, Scientist G, Division of Polymeric Medical Devices, for their timely suggestions, ideas and comments which helped in the improvement of the quality of this work. I express my heartfelt thanks to Dr. Annie John for her sincere help and efforts taken for drafting and revising my publication.

I am extremely thankful to Dr. Annie John, Scientist G, Transmission electron microscope for granting me the permission to use some of their lab facilities. I extend my special appreciation to Dr. Sunitha Chandran for in vitro cell cuture experiments, for being with me, helping me in analyzing my data and training me on PMMA embedding, polishing, staining and imaging. I also extent my special thanks to Ms. Susan Mani for my initial cell culture experiments. .

I express my sincere gratitude to Dr. V.S. Harikrishnan for performing in vivo surgery on rat animal model and Mr. Manoj, Mr. Anoop, Mr. Sarath, Ms Sreeja, Mr.Sunil & all staff of DLAS for timely help, support and friendship.

I thank Dr. H. K. Varma, Dr Suresh Kumar for providing nHAP for my study and Mr. Nishad Mr. Sreekumar, Mr.Sanoj and all members of Bioceramics Laboratory who helped me in ESEM and SEM analysis. I thank Dr Anil Kumar P.R, Mr Vinod, Ms Deepa for their timely help and support during my in vitro experiments. I express my heartfelt gratitude all members of Histopathology Laboratory for valuable suggestions on sample preparation for histological analysis.

I would like to acknowledge Dr. K. Sreenivasan, Dr. C. Radhakumary, Mr. Rowsen Moses and Mr. Hari of Laboratory for Polymer Analysis for ATR-FTIR, DSC, TGA and GPC analysis; Dr. V. Kalliyana Krishnan, Ms. Lakshmi, Mr. Satheesh and Dr. Priya of Dental Products Laboratory for Micro CT and ATR-FTIR analysis; Dr. Prabha D Nair, Ms. Geetha, Ms. Nimmy, Mr. Dhanesh and staff, Division of Tissue Engineering & Regenerative Technology for contact angle and conductivity measurements.

I also acknowledge Er.V Ramesh Babu, Mr. Subash and Staffs of Precision Fabrication Facility for developing punches for cutting the scaffolds.

I express my sincere gratitude to Dr. M. C. Sunny for his guidance, support and encouragement during the course of my tenure. I am extremely thankful to my dear friends in the campus for their help and whole-hearted cooperation during the study. I thank Dr. Mayuri, Dr. Priya, Dr. Arjun, Dr. Kiran, Dr. Sudhin, Mr. Susanth, Ms. Vibha, Dr. Shanti, Ms. Rakhi, Dr. Rethikala, Dr. Soumya Columbus , Mr. Harilal, Ms. Dhanya C. S., Ms. Jincy, Ms. Darsana, Ms. Sreelakshmi, Dr. Parvathy, Dr. Anupama, Ms. Nayana, Ms. Reshmi, Mr. Arungovil, Dr. Titash, Ms. Soorya, Mr. Sreeraj, Mr. Athiyappan, Mr. Sarath, Ms. Anitha, Ms. Anuja, Mr. Krishnachandran, Ms. Deepthi, Mr. Berwin Singh, Mr. Syam, Ms. Dhanya Thyagarajan, Mr. Arunkumar, Dr. Praveen, Mr. Riju, Mr.Kumaran, Mr. Sreevisakh, Ms. Lakshmi, Dr.Vidhu, Mr. Dhanesh, Dr. Finosh Ms. Christina and Ms. Sini for their friendship which relieved my stresses and made those days memorable.

I am extremely grateful to all my teachers within the campus who were involved in my PhD course work. Co-operation from staff of various administrative departments and library of the Institute is fondly remembered.

I wish to acknowledge Sree Chitra Tirunal Institute for Medical Sciences & Technology, India for providing me prestigious SCTIMST Institute fellowship during the course of study.

I have no words to express gratitude to my family members who provided the most precious support. I am indebted to my parents and my sister, for their unconditional love, support, encouragement and prayers.

God almighty, I bow before you for providing me strength, courage and health for completing this work and for being with me in all my good and hard times.

Remya K.R.

TABLE OF CONTENTS

LIST OF FIGURES

LIST OF TABLES

ABBREVIATIONS

ADMSC	Adipose derived mesenchymal stem cells
ALD	Alendronate disodium pentahydrate
ASC	Adult stem cells
BMD	bone mineral density
BMPs	bone morphogenetic proteins
BPs	Bishosphonates
CEC	poly(ε-caprolactone) –polyethyleneglycol - poly(ε-caprolactone) copolymer
cLSM	confocal laser scanning electron microscope
ECM	extracellular matrix
ESC	Embryonic stem cells
ESEM	Environmental scanning electron microscopy
FTIR	Fourier Transform Infrared Spectroscopy
FDA	Food and Drug Administration
FGF	fibroblast growth factors
GPC	Gel permeation chromatography
HA	hyaluronic acid
ICMR	Indian Council for Medical Research
IOF	International Osteoporosis Foundation
IGF I/II	insulin growth factor I and II
MSC	mesenchymal stem cells
μ-CT	Micro CT
nHAP	nanohydroxyapatite
NBF	neutral buffered formalin
OVX	ovariectomised
PGA	poly(glycolic acid)
PLA	poly(lactic acid)
PLGA	poly(lactic-co-glycolic acid)
PCL	poly(ε-caprolactone)
PEG	Polyethylene glycol
PDS	pamidronate disodium pentahydrate

SYNOPSIS

Bone could be considered as a 'smart tissue' having an intrinsic capacity to heal and regenerate even without leaving a scar. Even though bone being strong, it often undergoes defects or damages resulting either from traumatic situations or from pathological conditions. Osteoporosis is one of the most prevalent metabolic bone disorders which is characterized by low bone mineral density, reduced bone mass, and poor bone strength leading to skeletal fragility and increased susceptibility to fractures. As per worldwide statistics of International Osteoporosis Foundation, osteoporosis causes more than 8.9 million fractures annually, resulting in an osteoporotic fracture in every 3 seconds.

The major clinical consequence of osteoporosis is fracture and the current clinical treatment modalities include the use of either surgical interventions such as autografts/allografts/ bone grafts based on biomaterials or the use of pharmacological agents such as antiresorptive /anabolic agents. The limitations of surgical interventions include limited availability of donor tissue, donor site morbidity, risk of infection, immune rejection, long term hospitalization etc and that of pharmaceutical agents is their poor bioavailability and undesired toxic side effects.

There are only a few reports available on antiresorptive agents incorporated biomaterial scaffolds used for osteoporotic defect regeneration. However, developing scaffolds with appropriate combination of mechanical support and morphological guidance for cell proliferation and attachment while at the same time serving as matrices for sustained delivery of pharmaceutical agent is a major challenge.

Poly(ε-caprolactone) (PCL) is one of the widely explored polymers in biomedical field as scaffolding material for bone regeneration application owing to its inherent properties such as biodegradability and biocompatibility. One major drawback of PCL which limit its use as a functional scaffold is its hydrophobic nature which is unfavourable for better cellular response. Hence strategies to improve the hydrophilicity of PCL scaffolds are essential.

Hypotheses put forward on the basis of current knowledge are:

(1) Incorporation of a hydrophilic polymer to PCL can modify its surface wetting property, improve its biodegradability and provide better cellular response

(2) Nanohydroxyapatite (nHAP) incorporation can improve the mechanical properties and the osteogenic potential of PCL based scaffolds

(3) Incorporation of pamidronate disodium pentahydrate (PDS), an antiresorptive agent used for osteoporotic treatment, in PCL based scaffolds can improve the biofunctionality of the scaffolds and can be used for osteoporotic fracture repair

In order to prove the hypotheses, a 5-pronged approach was employed which includes:

- Synthesizing a hydrophilic copolymer based on ε-caprolactone and polyethylene glycol (CEC)
- Fabricating scaffolds based on PCL and its blend with CEC filled with and without nHAP particles using electrospinning technique
- Physical and biological characterization of scaffolds to prove its usefulness in orthopaedic application
- Fabricating PDS incorporated PCL based scaffolds and evaluating the effect of PDS on physical and biological properties of PCL

- *In-vivo* osteogenic efficacy evaluation of PDS incorporated scaffolds in a rat calvarial osteoporotic model

The work is presented in six chapters. The chapter 1 begins with an introduction to bone, followed by detailing about osteoporosis, its pathophysiology, current treatment modalities and challenges. It also briefly introduces the requirements for an ideal scaffolding material and relevance of electrospinning for scaffold fabrication. Properties of biodegradable polymer employed as scaffolding material, antiresorptive agents used and animal models employed for osteoporosis treatment are also described.

In Chapter 2, an exhaustive literature review highlights the current status of bone grafts used for orthopaedic applications. The topics reviewed include history of bone grafts, various scaffold fabrication strategies, osteoporotic drug incorporated scaffolds and electrospun polymeric scaffolds as bone regeneration scaffolds. Review also summarises about the animal models used for osteoporotic fracture treatments.

In Chapter 3, the experimental design in order to achieve the proposed objectives of the study is presented. This includes detailed description of the materials employed, experimental protocols, instruments utilized and development of rat animal model. The chapter is classified into different sections. The section 1 discusses in detail the procedure for synthesis of copolymer CEC, fabrication of scaffolds by electrospinning and modification of PCL scaffolds with copolymer CEC as well as nHAP incorporation. The fabrication of PDS incorporated PCL based scaffolds is detailed in section 2. The physico-chemical characterization of synthesized copolymer CEC and the fabricated scaffolds is explained in Section 3.

The details of biological evaluation of fabricated scaffolds under *in vitro* conditions using L929 mouse fibroblast cell lines, human osteosarcoma and adipiose derived mesenchymal stem cells are discussed in Section 4. The section 5 elaborates the *in vivo* evaluation of fabricated scaffolds in rat animal model. This section details the development and validation of rat osteoporotic model and *in vivo* osteogenic efficacy assessment in osteoporotic rat calvarial defect models.

Chapter 4 presents the results of the studies described using figures, tables and graphs. The synthesized copolymer CEC was characterized in terms of molecular weight using GPC, chemical structure by NMR and FTIR techniques. The electrospinning parameters for scaffold fabrication, PCL/CEC blend ratio and nHAP wt% were optimized. Both CEC and nHAP incorporation improved the surface wettability, biodegradability as well as both static and dynamic mechanical properties of PCL scaffolds. Comparative evaluation of both physical and biological properties of PCL, PCL/CEC and their nHAP filled composites suggested that PCL/CEC/nHAP composite scaffolds would be the best owing to the presence of hydrophilic copolymer CEC and osteoconductive nHAP. The antiresorptive drug PDS was successfully incorporated on PCL, PCL/CEC and PCL/CEC/nHAP scaffolds which was reflected by the decreased fiber diameter, improved surface wettability and enhanced mechanical properties of the bare scaffolds. *In-vitro* release studies showed sustained release of PDS for the PCL/CEC/nHAP composite scaffolds. *In vitro* cell culture studies proved cytocompatibility of PDS incorporated scaffolds towards human osteosarcoma cell lines (hOS). Change in cell morphology observed for higher amount of PDS 5wt%. The PCL/CEC/nHAP-PDS3 scaffolds were chosen for *in vivo* evaluation based on *in vitro* release behavior, mechanical

property and cellular response. Prior to implantation in rat animal model, *in vitro* cytocompatibility of scaffolds proved using rat adipose derived mesenchymal stem cells (rADMSCs) using MTT assay, environmental scanning electron microscopy (ESEM) and actin staining. Osteoporotic animal model was successfully developed and micro computed tomography analysis, histology evaluation and serum analysis confirms the osteoporotic model induction. Results of *in vivo* studies showed better osseous tissue integration within PDS loaded scaffolds after 12 weeks as depicted by X-ray radiographic, micro CT analysis, histology and histomorphometry analysis suggesting the potential of fabricated PCL/CEC/nHAP-PDS3 scaffolds for the repair of osteoporotic bone defects.

In Chapter 5, results are discussed and analyzed with the aid of current literature. The concept of local delivery of antiresorptive drug PDS at the implant site using electrospun PCL based scaffolds has showed improved osteogenesis in osteoporotic condition in rat animal model. The importance of present study has also been highlighted.

Chapter 6 summarises the results and conclusions which are drawn from the study. Studies with PCL/CEC/nHAP-PDS scaffolds suggest that the above drug-scaffold composite system has the ability to promote bone healing especially in osteoporotic trauma.

CHAPTER 1

INTRODUCTION

Bone forms the major building block of human musculoskeletal system and plays diverse role in our body. They serves both structural as well as reservoir functions which includes protecting various vital internal organs, helping in locomotion, providing mechanical support, act as store house of essential minerals and produce principal blood components. Bone has the unique ability to heal and remodel without leaving a scar. Though bone is considered as one of strongest tissue, it often undergoes defects or damages resulting either from traumatic or pathological conditions such as accidents, congenital abnormalities, infection, tumor resection, surgery, osteoporosis, etc. Though nature has elegantly designed our body with an inbuilt mechanism for repair and regeneration, the potential to heal may not be always sufficient.

Osteoporosis represents a metabolic bone disorder which is a worldwide emerging health care issue and socioeconomic threat characterized by reduced bone mass, and poor bone strength which results in fragile bones which are much susceptible to fractures (Sartori *et al.,* 2008). The clinical features of osteoporosis are pain, fracture and deformity and the three major classic locations of fracture are hip, spine and wrist. These fractures will lead to disability and reduce the quality of life and cause morbidity and mortality especially in the elderly people. It is estimated that over 200 million people are affected by osteoporosis worldwide. This figure will rise in future as the life expectancy of ageing population is increasing and this will enhance the worldwide eco-

nomic cost. It has been reported that, the worldwide economic cost of osteoporosis in 1998 was US$34.8 billion, which is expected to rise to $131.5 billion by 2050 (Cauley *et al.,* 2014).

The treatment for osteoporotic fractures involves use of surgical interventions such as autografts, allografts, bone grafts based on biomaterials (internal or external fixatives such as screws, pins, intramedullary nails, braces) as well as pharmaceutical agents (anabolic and catabolic agents). Since osteoporosis results in weakened bones which are unable to heal on its own, it is often difficult to achieve a stable bone-implant construct with the use of metallic implants. The pharmaceutical agents are usually provided as a measure to prevent and treat osteoporotic fractures. However their poor bioavailability and the undesirable side effects caused by routine administration is a major concern. Hence localized delivery of these agents at the defect site is a possible solution so as to enhance their bioavailability and efficacy.

Tissue engineering approaches utilizing scaffold, cells, growth factors or bioactive drugs at the implant site can be a promising strategy for treating osteoporotic bone fractures. The strategy adopted in the present study is to combine a biodegradable scaffold with a pharmaceutical agent so as to develop an appropriate scaffolding material for osteoporotic bone defect repair. In order to construct an ideal scaffold for bone defect repair under osteoporotic condition, a thorough understanding about bone anatomy, bone remodeling process, osteoporosis its types, causes, treatment modalities and challenges is necessary, which is outlined below. This introductory chapter briefly discusses the significance of tissue engineering in osteoporosis, requirements of an ideal

scaffolding material, the relevance of electrospinning technique for scaffold fabrication, properties of biodegradable polymer, ceramic and the antiresorptive drug employed for the study.

1.1. Bone

Bone is considered as a complex, dynamic and highly vascularized tissue having huge variations of skeletal shapes in different regions of the body. Based on shape, bones can be grouped into different categories such as long (e.g. femur, tibia, and humerus), short (e.g. tarsus and carpus), flat (e.g. ribs and cranial bones), and irregular (e.g. vertebrae of the spine) bones. Despite these variations in skeletal shapes, macroscopically all bones are similar.

1.1.1. Bone macrostructure

In human body, there are two kinds of bone such as primary and secondary bone. Primary bone also known as non woven bone is the initial bone which is formed during the development and regeneration process. It comprises of large number of osteocytes and irregularly arranged collagen fibers. Secondary bone also known as mature bone is formed by replacement of the primary bone over time, and is present throughout a fully developed human and is characterized by its dense mineralization and organized structure.

The two types of secondary bones present in the body are cortical/compact bone and cancellous/trabecular bone. The proportion of these bones varies at different locations of the skeleton. The cortical bone accounts for 80 % of the human adult skeleton which is almost solid and is of only 10 % porous. They are mostly found in the

outer part of long bones and in flat bones and are of about ~ 80-90 % mineralized. They provide mechanical support and protect various delicate internal organs. The trabecular bone accounts for rest 20% of the adult skeleton and is having a higher porosity of 50-90% which makes their modulus and ultimate compressive strength around 20 times inferior than that of the cortical bone. Their primary function is metabolic in nature as they serve as the reservoir of calcium and phosphate ions. They are seen mostly in metaphysic of long bones which are covered by cortical bone and also in the vertebral bodies.

1.1.2. Bone matrix

Bone is a natural composite consisting of two phases, an organic (protein) contributing about 25–30% of the total matrix and a inorganic (mineral) phase contributing 65–70% of matrix. The mineral phase of the bone is calcium phosphate in the form of crystalline hydroxyapatite, $Ca_{10}(PO_4)_6(OH)_2$. It also contains other mineral ions such as magnesium, strontium, carbonate, citrate, and fluoride. The bone protein is mainly composed of Type I collagen, which acts as a structural framework in which plate-like tiny crystals of HAP are embedded to strengthen the bone. Non-collagenous proteins constitute about 10 to 15% of total bone protein and make up approximately 3-5% of the bone and it includes osteocalcin and glycoproteins including alkaline phosphatase (ALP), osteonectin etc. This unique composition of bone ECM enables the bone to provide mechanical support for the skeleton.

1.1.3. Bone cells

Bone tissue is populated mainly by four different cell types-osteoprogenitor cells, osteoblasts, osteoclasts and osteocytes. Each cell type has defined task and they act unanimously to maintain a healthy bone tissue. Osteoprogenitor cells originate from mesenchymal stem cells and undergo osteogenic differentiation into osteoblasts. They are most active during development of the skeletal system, but are frequently reactivated during the normal bone turnover process and large numbers are activated during fracture repair.Osteoblasts are metabolically active bone forming cells which originates from bone marrow derived stem cells. They are cuboidal in shape when they are active and become flattened out during inactive phase (resting). During the resting phase, they are known as bone lining cells. They are involved in synthesizing collagenous as well as non collagenous proteins and alkaline phosphatase which initiates the matrix mineralization.Osteocytes are mature osteoblasts which are trapped within the bone matrix and are responsible for its maintenance. Osteoclasts are multinucleated ruffle bordered cells which are found on bone surfaces. They originate from monocytes and macrophages and are responsible for the bone resorption process. The ruffled border morphology of these cells enables them to attach to the bone surface and secrete acid and enzymes into the mineralized bone, which results in the demineralization of the bone.

1.2. Bone remodeling

Bone is a dynamic and metabolically active tissue which undergoes remodeling throughout the entire life so as to maintain healthy skeleton and mineral homeostasis

(Kumar and Bhaskar, 2012). This process is controlled by the activity of osteoblasts (bone formation) and osteoclasts (bone resorption). The remodeling process involves continuous removal of discrete packets of old bone by osteoclasts followed by replacing these packets with newly synthesized proteinaceous matrix, and subsequent mineralization of the matrix to form new bone by the osteoblasts. During childhood and adolescence period, remodeling is a balanced process where the rate of bone resorption and bone formation is equal. After attaining the peak bone mass at adulthood, this balance is maintained with small variations until the age of 50. After that, resorption exceeds bone formation and loss of bone mass initiates. The bone loss increases with age in both men and women and rate of bone loss is more in postmenopausal women.

1.3. Osteoporosis: A look into the problem

Osteoporosis is a global public health problem affecting millions of people worldwide and its impact is pervasive in most of the nations which is associated with significant morbidity, mortality, and socioeconomic burden (Aggarwal *et al.,* 2011). It is a silently progressing; multifactorial, age-related metabolic bone disease which is characterized compromised bone strength predisposing to increased risk of fracture. Bone strength reflects integration of two main features- bone quality and density. In osteoporosis, both bone quality and density is affected. Morphological features of normal and osteoporotic bone is represented in Figure 1.

As per World health organization (WHO), osteoporosis is diagnosed when the value for the bone mineral density (BMD) is 2.5 standard deviations or more below the mean of the young adult reference range. In India, it is estimated that about 50 million

are either osteoporotic (T-score lower than -2.5) or have low bone mass (T- score between -1.0 and -2.5) (Mithal *et al.,* 2014).

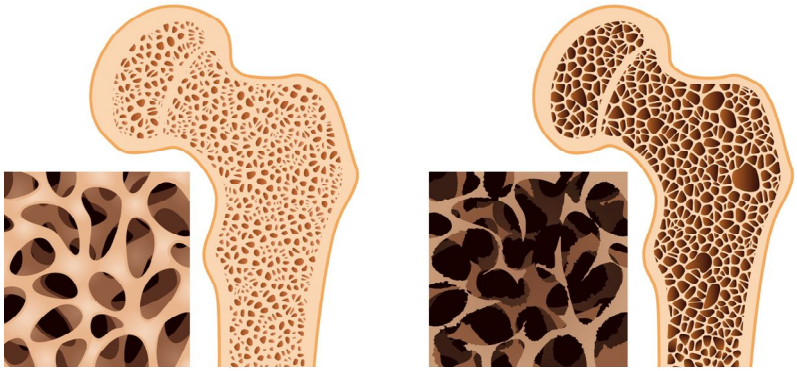

Normal bone **Osteoporotic bone**

Figure 1. Morphological features of normal and osteoporotic bone

(adapted from http://www.medguidance.com/thread/What-Causes-Osteoporosis.html)

Osteoporosis can be grouped into two categories based on their causes - Primary and secondary. Primary osteoporosis related to estrogen deficiency and is termed as Type I and generally affects women, particularly those who have undergone menopause or ovariectomy. It is also known as post-menopausal / estrogen-induced osteoporosis as it occurs due to the reduced level of estrogen hormone. Primary osteoporosis related to ageing is known as Type II or senile or age-related osteoporosis. It affects both men and women and is characterized by trabecular thinning, reduction in cortical thickness, and increase in cortical porosity. Though these two types represents the most common causes of osteoporosis in humans, their main difference is that in post-menopausal osteoporosis, trabecular bone loss predominates over cortical bone loss whereas in age-related osteoporosis there is a decline in both cortical and trabecular bone density.

Secondary osteoporosis results from external factors such as medications, endocrine disorders, chronic renal disease, hematopoietic disorders, immobilization, nutrition and gastrointestinal (GI) disorders and connective tissue disorders

The incidence of osteoporosis is more prominent in women due to their lower peak bone mass and hormonal changes. Approximately one in two women and one in four men over the age of 50 will have osteoporosis related fracture (Gudena *et al*., 2011). This increased incident rate in women occurs due to the hormonal changes during menopause, inadequate physical activity and low calcium intake. In aging population, osteoporotic vertebral fractures are becoming more frequent and the increased incident rate is associated with significant morbidity and mortality.

1.4. Osteoporosis epidemics in India

In India, fractures associated with osteoporosis is common in both men and women, however owing to the lack of facilities for measuring of bone mineral density (BMD), very little population-based research has been done in India (Anburajan *et al.,* 2011). As per Indian Council for Medical Research (ICMR) report on population based studies, the prevalence of osteoporosis in male is of 3% and that of female is 8% (Sreedevi & Ragi, 2016). Based on census data, out of 163 million aged people, 20% percent of women and 10-15% of men were affected by osteoporosis (Malhothra & Mithal, 2008). International Osteoporosis Foundation (IOF) Asian Audit, estimated that about 50 million people in India are osteoporotic (T-score lower than - 2.5) or have low bone mass (T score between -1.0 and -2.5). Studies by ICMR revealed that the lower BMD values observed in Indians when compared to the western countries is due to the

genetic differences, nutritional deficiency and smaller skeletal size. The other factors which contribute for poor bone health and osteoporosis in India are low intake of calcium, high rate of vitamin D deficiency, lack of physical activity, sex inequality, increasing longevity, lack of diagnostic facilities, poor knowledge on bone health, and early menopause. The high rate of vitamin D deficiency in Indians is attributed to low sun exposure, inadequate dietary vitamin D intake, and lack of food fortification with vitamin D, pigmented skin, environmental pollution, and traditional dress code (Mithal *et al.,* 2013, Thulkar & Singh, 2015).

1.5. Pathogenesis of osteoporosis

Osteoporosis results mainly due to the imbalance in bone remodeling process, which is determined by the activities of osteoblasts and osteoclasts. During normal bone remodelling cycle, process of bone resorption and bone formation occurs in a coordinated fashion. In case of osteoporosis, bone resorption exceeds bone formation.The skeletal fragility associated with osteoporosis is due to various factors such as (a) inadequate skeletal peak mass and strength during growth; (b) excessive bone resorption resulting in decreased bone mass and micro architectural deterioration of the skeleton and (c) an inadequate bone formation in response to increased resorption during bone remodeling (Raisz, 2005).

In the case of post-menopausal osteoporosis, estrogen deficiency is a significant cause of accelerated bone loss. Postmenopausal women are at the highest risk for developing osteoporosis as their estrogen levels decline naturally which induce the excessive proliferation of early osteoblast progenitors, which fuels excessive bone

turnover. Other factors affecting bone mass includes - Physical activity tends to increase bone mass, whereas immobilization leads to increased bone loss. Obesity is associated with higher bone mass. Typical patients who have osteoporosis tend to be thin and possess less muscle mass. Low dietary intake of calcium, phosphorous, and vitamin D are associated with age-related bone loss.

1.6. Treatment modalities for osteoporosis

Treatment of osteoporosis targets at reducing the fracture rate by means of increasing bone strength which depends on bone mineral density (BMD) and bone quality. Hip, wrist and spine are the three classic location of osteoporotic fracture. Fractures occur mostly in skeletal regions with large proportion of cancellous bone such as the vertebral body in the spine or the metaphyseal region of the long bones.

Non surgical, surgical and pharmacological approaches are used for osteoporotic fracture treatment. Non-surgical approach involves immobilization which is mostly used for elbow and knee fractures and is becoming less frequent (Larsson S, 2002). Surgical interventions include use of intramedullary nails, bone impaction, buttress fixation, fixed-angle devices, bone augmentation and joint replacement. Bone augmentation involves use of bone autografts or allografts, bone cement or bone substitutes. Pharmaceutical approach involves anabolic agents that stimulate bone formation [eg, parathyroid hormone (PTH)] or antiresorptive agents that inhibit bone resorption [eg, bisphosphonates, calcitonin, raloxifene, and estrogen] to slow down the progression of disease (Malhothra & Mithal, 2008). And for most of these drugs, major concern is their poor bioavailability and the long term use of these drugs has been often associated with

adverse side effects. Therefore, better strategy is to deliver these drugs locally at defect site using drug loaded implants.

1.7. Challenges in osteoporotica fracture treatment

Fractures associated with osteoporosis are different from normal fracture and the management of these fractures is challenging. The failure rates of fracture fixation in osteoporotic bone range from 10% to 25% (Goldhahn *et al.,* 2012). Even though strategies for prevention and treatment for osteoporosis is available, the incidence of fractures continues to rise with increasing aging population and is a major cause of morbidity and mortality especially in elderly people. The implants developed for normal bone fracture tend to fail in that of osteoporotic fractures. According to preclinical evidence, fracture healing is delayed in osteoporotic patients due to the impaired mechanosensitivity of osteoporotic bone (Jakob *et al.,* 2013). The major challenge in osteoporotic fracture treatment is to achieve a proper fixation and stability of implants. The standard fracture fixating devices such as pins, intramedullary rods, plates and screws often fails due to the inability of osteoporotic bone to hold them. The likelihood of forming cavities in the area where devices are secured results in implant loosening which also results in treatment failure (Lyet, 2006). The fixation strength of implants is affected by the decreased thickness and increased porosity of the cortical bone, as well as the rarefaction of the trabecular network (Schneider *et al.,* 2005). The other factors effecting fixation strength is changes in the remodelling cycle associated with osteoporosis which results in the delayed fracture healing and high risk of non union.

Besides surgical interventions, pharmacological approaches involves using bioactive agents which regulates bone remodeling process are used in preventing and treating osteoporosis. However their poor bioavailability and undesirable side effects is a major concern. Hence strategies for developing therapies which enables improved bone repair, fracture healing, and implant fixation is essential in reducing osteoporosis associated fractures.

1.8. Tissue engineering approach in osteoporosis

The development of tissue engineering constitutes a new platform for translational medical research. Tissue engineering evolved as a result of lack of availability of tissues and organs for transplantation and the inconvenience associated with their transplantation such as donor site morbidity, immune rejection and pathogen transfer (Subia *et al.,* 2010). Tissue engineering approach utilizing biomaterial scaffold represents a promising alternative for traditional osteoporosis therapies. The scaffold based tissue engineering enables the delivery of cells, growth factors as well as bioactive drugs at the defect site which aids in better bone formation and bone strength. Scaffolds not only provide structural support to the growing tissue, but also play key role as a construct in guiding tissue regeneration. Therefore the physical and chemical properties of the scaffold, such as material composition, architecture, mechanical strength, pore size and porosity, must be carefully designed which is the key challenge for the success of tissue engineered bone grafts.

1.8.1. Scaffold requirements significant for bone tissue engineering

The key requirements for scaffolding material include non-immunogenicity, non-toxicity, biocompatibility and biodegradability. Scaffold act as a temporary matrix to deliver cells, growth factors as well as bioactive drug molecules and provide structural support and serve as the template for cellular interactions and extracellular matrix (ECM) formation. They should have a three dimensional architecture which favour the growth and attachment of cells which has been cultured on it. Scaffolds must be highly porous with interconnected pores and adequate pore size that allows cell in-growth and proper cell distribution throughout the porous structure. Porosity and interconnectivity is essential for diffusion of nutrients and gases and removal of metabolic waste resulting from the cellular activity. The recommended pore size for bone tissue engineering purposes lies within the range of 200–900 μm (Yang *et al.,* 2001). Surface properties such as surface chemistry and hydrophilicity govern *in vitro* and *in vivo* cellular response. The mechanical properties of scaffolds should ideally match to that of the living bone. The degradation rate of scaffolds must match with the neotissue growth rate.

1.8.2. Biodegradable polymers and polymer-ceramic composites as scaffolds

The design and development of scaffold matrix from appropriate biocompatible polymers with desired properties is the key challenge for the success of tissue engineering. Natural as well as synthetic biodegradable polymers can be employed as scaffolding material. Natural biodegradable polymers derived from natural sources possess better biocompatibility and low immunogenic potential and the widely used

polymers includes collagen, fibrinogen, chitosan, starch, hyaluronic acid (HA) and poly(hydroxybutyrate) (PHB). The inferior mechanical properties and the batch-to-batch variation in properties associated with the natural polymers is a major drawback.

Synthetic polymers widely used for tissue engineering are aliphatic polyesters such as poly(glycolic acid) or PGA, poly(lactic acid) (PLA), poly(lactic-co-glycolic acid) (PLGA), poly(ε-caprolactone) (PCL) etc. These polymers have US Food and Drug administration (FDA) approval and are already been used for clinically established products such as implantable devices and sutures. These polymers also possess excellent mechanical properties and their degradation behaviour could be tuned by blending with other polymers or copolymers. However, they lack cell binding sites which results in poor cell-material interaction. Currently, composite materials are being prepared using biodegradable polymer and bioactive ceramic phase with the aim of increasing the mechanical performance and bioactivity of the scaffolds. The most widely used bioactive ceramics includes calcium phosphate ceramics such as hydroxyapatite (HAP), tricalcium phosphate (TCP) , biphasic calcium phosphate (BCP) and bioactive glasses (BAG).They have strong affinity to bind to the surrounding osseous tissue and enhance bone tissue formation (Puppi *et al.,* 2010).

1.8.3. Relevance of electrospinning technique for scaffold fabrication

Electrospinning is an enabling technique that allows fabrication of fibrous scaffolds with well-defined architecture, controlled pore size, fiber diameter and topography which favours cell growth and closely resembles the *in vivo*-like architecture of ECM (Fischer *et al.,* 2012, Kim *et al.,* 2004). The unique feature of electrospinning

technique is its simplicity which enables fabrication of scaffolds in the required architecture using appropriate polymer. Now researchers are increasingly interested in developing drug delivery systems using electrospinning technique by incorporating bioactive drugs in order to enhance the biofunctionality of the scaffolds. Drug molecules can be embedded in the fiber either through dissolution or dispersion in the polymer solution (Xie *et al.,* 2010). The highly fibroporous architecture of electrospun fibers along with their very high surface area enables the drug molecules to diffuse out from the polymeric matrix. One major advantage of using drug loaded scaffolds is that, they can be directly implanted on the defect site and thereby allows higher drug bioavailability, improved therapeutic efficacy and reduced toxic side effects.

Advantages of using electrospinning technique for scaffold fabrication:

- Process is a simple, straightforward, and cost-effective
- Fibers with diameters ranging from microns down to few nanometers can be obtained.
- Scaffolds obtained is highly porous with interconnected pores and have extremely large surface- area-to-volume ratio
- Allows use of a variety of polymers, blends of different polymers, and inorganic materials as well as incorporation of additives, biomolecules, and living cells for tailoring different application requirements

1.8.4. Cell requirements significant for bone tissue engineering

The cell source should be non-immunogenic and could be easily isolated and expandable (Heath, 2001).The osteoblast, owing to their non-immunogenicity is the first

choice and is usually isolated from biopsies of the patients (autologous cells). Their usage is limited since their isolation is time consuming and only few cells with low expansion rates could be obtained. Cells from non-human donors (xenogeneic cells) are used as an alternative, to solve the problem of low cell number yields. However, the associated immunogenicity and chance of transmission of infectious agents is a major drawback.

Stem cells are more promising candidate in bone tissue engineering. They are un-specialized cells that can self-renew indefinitely and can also differentiate into more mature cells with specialized functions. They possess high proliferation capability and multilineage differentiation. Embryonic stem cells (ESC) and adult stem cells (ASC) are mostly used in bone tissue engineering (Salgado *et al.,* 2004).There has been special interest in use of mesenchymal stem cells (MSC) for bone tissue engineering applications. Their source of isolation includes bone marrow, adipose tissue, muscle tissue, amniotic fluid and periosteum. The advantage of using MSCs includes:

- Can be easily harvested and propagated
- Multipotent- Can differentiate to different lineages
- High proliferation rate
- Adherent to tissue culture plate
- Easily expanadable for long time without losing their osteogenic potential

1.8.5. Growth factors /bioactive drugs used in bone tissue engineering

Growth factors are cytokines that are secreted by many cell types and function as signalling molecules Binding of a growth factor to its receptor initiates intracellular

signalling that will lead to promotion and/or prevention of cell adhesion, proliferation, migration and differentiation by up-regulating or down-regulating the synthesis of several proteins, growth factors and receptors. Bone morphogenetic proteins (BMP), transforming growth factor beta (TGFb), fibroblast growth factors (FGFs), insulin growth factor I and II (IGF I/II), and platelet derived growth factor (PDGF) are the most commonly used growth factors.

The class of drugs used in bone tissue engineering includes antimicrobial agents (Gentamicin, Tetracyclin, Vancomycin, Ciprofloxacin, silver ions), anti inflammatory drugs (steroids such as dexamethasone and non steroids like ibuprofen) and bisphosphonates (alendronate, zolendronate, pamidronate, Clodronate).

1.9. Role of bisphosphonates in treatment of osteoporosis

Bishosphonates (BPs) belong to the family of antiresorptive agents and are the first-line medications for osteoporosis treatment being taken by millions of patients worldwide, predominantly postmenopausal women (Gieger *et al.,* 2013).

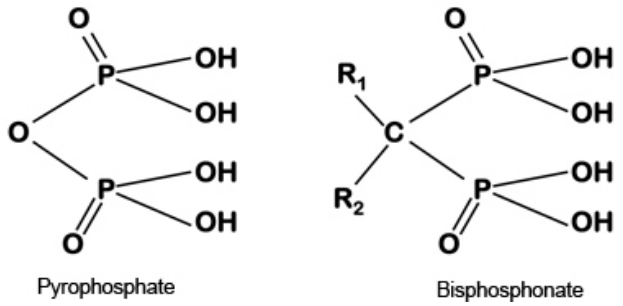

Figure 2. Structure of pyrophosphate and bisphosphonate

They are carbon-substituted analogues of pyrophosphate that act as powerful inhibitors of osteoclastic activity. The structural difference between pyrophosphates and

bisphosphonates is the substitution of the oxygen connecting the two phosphates by a carbon atom (Figure 2). The major site of action of bisphosphonate is bone. At any time, approximately 10% of the adult skeleton undergoes active remodelling whereas the remaining 90% is quiescent. Bisphosphonates have strong affinity for calcium in hydroxyapatite. The calcium bound drug will be dissolved under the acidic conditions created by osteoclasts during resorption. The solubilised bisphosphonate is then taken up by the osteoclasts where they trigger various biochemical effects. At the molecular level, nitrogen containing BPs inhibits the melvonate pathway which perturbs cell activity and can induce apoptosis. At the cellular level, osteoclast recruitment and adhesion is reduced and the loss of ruffled border on the osteoclasts makes it inactive for further resorption resulting in shallow resorption sites. In addition to its effect on osteoclasts, they promote osteoblasts proliferation and maturation. The net result is reduction in bone resorption and net gain in bone density.

1.10. Need for animal models in osteoporosis research

Animal models provide uniform experimental material and allow extensive testing of potential therapies. The osteoporosis research in particular is one of the most common areas where animal models are necessary. Osteoporosis occurs naturally only in humans and in nonhuman primates. Hence in other animal models, osteoporosis has to be induced in the experimental setting by various approaches such as ovariectomy, change of diet, use of drugs, immobolization etc. The performance of the tissue engineering construct has to be evaluated in animal models prior to its evaluation in humans. The Food and Drug Administration (FDA) guidelines recommends two

preclinical animal models, the ovariectomised (OVX) rat and a second non-rodent model, to demonstrate the efficiency and safety of agents which is intended to use for osteoporosis therapy (Thompson *et al.,* 1995). Preclinical trials in smaller animals are initially carried out as a proof of concept. If promising results are observed, further the preclinical studies are extended to larger animals. The experimental animal model must be carefully selected to evaluate the performance of the tissue engineering construct and is critical for the success of the studies.

1.11. Rationale for choosing Poly (ε-caprolactone), Nanohydroxyapatite and Pamidronate for the study

1.11.1. Poly (ε-caprolactone) (PCL)

PCL is the material of choice for the current study. The unique properties of PCL are attributed to its chemical structure which consists of five non-polar methylene groups and a single relatively polar ester group arranged in repeated fashion. The presence of the olefinic group provides structural properties similar to polyolefin while the hydrolytically liable ester group is responsible for the degradation property.

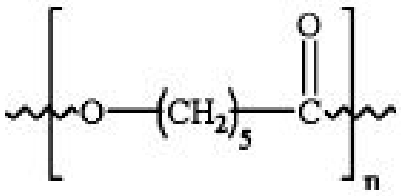

Figure 3. Structure of PCL

PCL has been intensively studied for tissue engineering applications owing to its non toxicity, biodegradability and biocompatibility. It is a semi-crystalline polymer with

glass transition temperature of -60 °C and melting temperature of 58-63 °C which makes it suitable for processing into various shapes with much ease. PCL degrades mainly by hydrolysis of its ester linkages under enzymatic and hydrolytic conditions and hence they received great deal of attention as an implantable material. The enzymatic degradation occurs through the hydrolysis of their ester linkages by lipase, cholesterol esterase, and carboxyl esterase (Gan *et al.,* 1997*,* Labow *et al., 2002).* The nontoxic nature of its degradation product i.e, caproic acid, a natural fatty acid of human skin makes it an attractive candidate for biomedical applications. The complete resorption of PCL requires more than 2 years (Yang *et al*., 2001).The versatility of PCL is due to the fact that, it allows modification of its physical, chemical and mechanical properties by co-polymerization or blending with many other polymers efficiently. It has been observed that co-polymerization alters the chemical property that indirectly affects all other properties such surface wettability and degradation behavior resulting in a modified polymer with improved properties.

1.11.2 Significance of Nanohydroxyapatite (nHAP)

Nanohydroxyapatite (nHAP) has been widely used in biomedical implants for bone regeneration due to its structural similarity to the mineral component of the bone. The excellent biocompatibility, bioactivity, osteoconductivity and direct involvement in bone cell differentiation and mineralization makes nHAP especially suitable for bone tissue engineering. Moreover, HAP has the ability to induce mesenchymal stem cells differentiation towards osteoblasts. Studies show that nanosized HAP particles (nHAP) enhance protein adsorption and cell adhesion to the internal surfaces of the scaffold and

improve both mechanical and biological properties. However, the use of HAP alone is limited due to its inherent brittle nature. Hence studies involving composites based on HAP and biodegradable polymers are being carried out extensively with the aim to confer high bioactivity and adequate mechanical properties to the scaffolds.

1.11.3. Role of Pamidronate (PDS)

Pamidronate disodium pentahydrate (PDS) belongs to the family of amino bisphosphonates. Bisphosphonates (BPs) are important class of drugs which has been widely used since 1970s for the management of various metabolic bone disorders such as Paget's disease, osteoporosis, hypercalcemia of malignancy as well as inflammation related bone loss. They are stable analogues of pyrophosphates which are natural modulators of bone metabolism. BPs binds strongly to hydroxyapatite mineral in bone where they retain for many years, thereby providing potent pharmacological effects on target tissue and act as potent inhibitor of osteoclast mediated bone resorption.

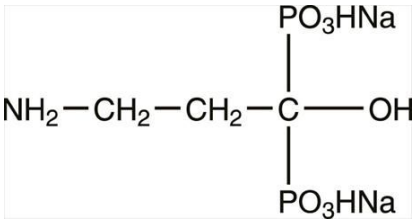

Figure 4. Structure of pamidronate

Studies have shown that administration of PDS seems to improve the bone mineral density and helps in preventing bone loss associated with various bone related disorders. However owing to its poor bioavailability, high dosage of PDS is necessary

which may result in various side effects. Hence localized delivery of PDS from polymer matrix can increase the bioavailability and its therapeutic efficacy.

1.11.4. Rat as osteoporotic animal model

Rats are the most commonly used and excellent model for studying osteoporosis. The choice of rat animal model is advantageous as they are quite inexpensive, easy to house and maintain. They grow rapidly and have a well characterized skeleton. They have cancellous bone remodeling with remodeling sites very similar to those seen in human cancellous bone. Their short life span helps in studying the effect of ageing on bone. Though rats do not experience natural menopause, an artificial menopause can be induced by ovariectomy (Wronski *et al.,* 1985). Ovariectomized animals are frequently used as models for studying postmenopausal osteoporosis. Ovariectomy in rats results in significant trabecular bone loss within 3-6 months (Bagi *et al.,* 1997, Jee and Yao, 2001). The rapid loss of cancellous bone mass and strength observed in rats after ovariectomy (OVX) mimic the bone changes following menopause in humans.

1.12. Hypothesis

The treatment of osteoporotic fractures are challenging due to the poor bone quality which leads to higher rate of implant failure. Compared to the traditional treatment modalities, biomaterial scaffold based tissue engineering approach is a promising strategy for osteoporotic bone defect repair. On literature reviewing, only very few studies has been focussed on the repair of critical-sized bone defects using biomaterial scaffold based approach under osteoporotic condition. Similarly pharmacological agents has been widely used for the treatment of osteoporosis and

fracture prevention, however less attention has been placed on the development of pharmaceutical agent incorporated biomaterial scaffolds. Hence designing an appropriate scaffold material that can effectively deliver pharmaceutical agents locally at the defect site may be an effective strategy to promote osteoporotic bone repair.

Poly (ε-caprolactone) has been widely explored for bone tissue regeneration application owing to it inherent biodegradability and biocompatibility. However, the inherent hydrophobic nature of PCL limits its use as a functional scaffold owing to its poor cellular response. This present study aims to investigate whether critical-sized calvarial bone defects created in an osteoporotic rat animal model could be repaired using an bisphosphonate based tissue engineering (TE) approach. In this context, the hypothesis put forward is as follows:

(1) Incorporation of a hydrophilic polymer to PCL can modify its surface wetting property, improve its biodegradability and provide better cellular response

(2) Nanohydroxyapatite (nHAP) incorporation can improve the mechanical properties and the osteogenic potential of PCL based scaffolds

(3) Incorporation of pamidronate disodium pentahydrate (PDS), an antiresorptive agent used for osteoporotic treatment, in PCL based scaffolds can improve the biofunctionality of the scaffolds and can be used for osteoporotic bone defect repair

1.13. Objectives of the study

The main objective of the research study is to develop and characterize electrospun PCL based nanocomposite scaffolds for osteoporotic bone defect repair. The study focussed

on validating the applicability of scaffolds under *in vitro* conditions and *in vivo* conditions.To prove the hypothesis following objectives was defined:

1. To fabricate polymeric scaffolds based on biodegradable poly (ε-caprolactone) (PCL) by electrospinning technique.
2. To improve the surface wettability and degradation behaviour of PCL by blending with hydrophilic polymer and to evaluate its effect on the physical and biological properties of PCL.
3. To fabricate bioactive scaffolds by incorporating nanohydroxyapatite (nHAP) and to evaluate its effect on the physical and biological properties of PCL.
4. To fabricate and characterize pamidronate disodium pentahydrate (PDS) incorporated PCL based scaffolds.
5. To evaluate the release profile of PDS and to determine the effect of PDS release on cytocompatibility.
6. To develop an osteoporotic rat animal model by ovariectomy in female Wistar rats.
7. To evaluate osteoporosis induced rat animal model.
8. To evaluate the osteogenic efficacy of PDS loaded PCL based scaffolds in calvarial defects in rat osteoporotic model.

CHAPTER 2

LITERATURE REVIEW

The main goal of the study is to develop electrospun poly(ε-caprolactone) based nanocomposite scaffolds with appropriate combination of mechanical support and cellular response for osteoporotic bone defect repair. To develop an appropriate scaffold, thorough knowledge of the current progress in this field is essential. This chapter elaborates in detail the history of bone grafts and its current status, significance of tissue engineering approach in osteoporosis, scaffold fabrication techniques in tissue engineering. The chapter details the use of electrospun poly(ε-caprolactone) polymer as bone regenerative scaffolds, studies on bisphosphonate incorporated polymeric scaffolds and animal models used for osteoporotic fracture treatments. Thus with the aid of published literature, experimental design strategies for the present study has been deduced.

2.1. Bone grafts: History and current status

After blood, bone is the second most transplanted human tissue with approximately 3.5 million bone graft procedures performed each year (Elsalanty and Genecov, 2009). The concept of tissue transplantation is very ancient, dating back to the early Christian era. The twin saints, St. Cosmas and St. Damian, who were surgeons in the third century, were regarded as the pioneers of bone transplantation. They have successfully removed the malignant and gangrenous limb of an aged sacristan of the church and transplanted the leg of a deceased Ethiopian Moor to the sacristan.

In the modern era, bone grating began with the work by Dutch surgeon Job van Meekeren, in 1668, who has repaired the traumatic defect in a soldier's cranium using dog's skull (Blitch and Ricotta, 1996). It was in 1674, the Dutch scientist Anton van Leeuwenhoek described the structure of bone. Ten years later, illustrations on callus formation was also reported. The role of periosteum in bone formation was established from the works of Duhamel in 1742. The first clinical autologous bone grafting was performed by Dr. Philip von Walter in Germany in 1821, who replaced part of a skull surgically removed after trephening the bone.Later in 1880, the first allograft implantation was performed by Scottish surgeon Macewen on a four year old boy whose infected humerus was reconstructed with a tibia graft taken from another child.

In 1915, Albee in his classical work concluded that the most suitable tissues for transplantation are those originated from the connective tissue such as bone, fat and fascia. The works on bone grafting and periosteum by Ollier, Barth and Axhausen has laid the foundation for other researchers in this area. The works of Phemister and Albee has elucidated the important factors in bone grafting which paved the way for the recent work that has delineated the importance of osteoconductive scaffolding, osteoinductive growth factors, and osteogenic progenitor stem cells in bone graft healing. Even with such an extensive scientific history and various products available, till now, an ideal bone graft substitute has not yet developed.

The demand for bone grafts is high in clinical practice for the substitution of bone defects and recovery of atrophic bone regions. Based on the source, bone grafts can be categorized as autografts, allografts and synthetic grafts.

2.1.1. Autografts

Autograft is one in which the source of the graft is from the same person i.e., the donor bone is harvested from the patient itself. They are the primary material used in bone grafting and is considered as the golden standard for replacing bone loss associated with trauma, infection, tumor resection, revision arthroplasty, and arthrodesis (Williams and Szabo, 2004). The main source of autograft bone is iliac crest of the patients and the other site includes distal radius, proximal and distal tibia, and ribs. Since they are harvested from the patient's own body, they are highly accepted by the patient and eliminate the risk of disease transmission. As the autograft bone is osteoconductive, osteoinductive and provides osteogenic cells, faster bone formation at the implant site can be easily achieved.

Though autografts provide best replacement alternate, its drawbacks may sometimes outweighs its benefits. This includes pain and injury associated with harvesting procedure, quality as well as quantity of the harvested bone, high cost involved in the surgical procedure, the need for second surgery and the associated morbidity.

2.1.2. Allografts

Allograft is one in which the source of the graft (donor bone) is from another person but of the same species. The concept of using allograft is as old as autograft and the allograft procedure become well established in 1960s by the works of Burwell which led to the development of reliable bone banks. Bone allografts are being widely used in the field of dentistry, orthopedics and craniofacial surgery. The main source of allogenic

bone is the femoral head which is obtained during hip arthoplasty. Based on the processing, the allogenic bone grafts can be of two types-mineralized and demineralized allografts. Mineralized allograft is available in fresh, frozen or freeze dried forms. Demineralised allografts (mineral component of bone removed) comprises of collagen, non collagenous proteins and some growth factors which provides it an osteoinductive capacity.

The use of allografts is associated with various advantages such as it is available in adequate quantities and eliminates the need for additional donor site surgery thus relieving the patient from pain and injury. However, host incompatibility, and potential risk of disease transmission from donor to recipient and the high cost requirement for maintaining bone banks is a major concern (Laurencin *et al.,* 2006)

2.1.3. Synthetic grafts

Synthetic bone grafts evolved as a result of the limitations associated with autografts and allografts such as donor shortage, chance for rejection or transmission of infectious disease. However, synthetic bone grafts are selected based on the nature and complication of the bone defects as well as choice of available bone grafts.

2.1.3.1. Metals

Metals have been used in clinical orthopedics since early 1900s. Due to their good mechanical durability, high strength and ductility metals are normally used for load bearing applications such as pins, plates and femoral stems. The most commonly used implants are based on austenitic stainless steel, cobalt-chromium alloy, titanium and its alloys. Implants based on stainless steel have been the tradition metal which is used as

screws, plates and nails for bone fixation. Cobalt-chromium alloys based implants have better corrosion resistance, wear resistance and have higher elastic modulus. The elastic modulus of stainless steel and Co–Cr alloys is higher than that of natural bone, i.e., about 10 times greater which results in mechanical incompatibility. Titanium and its alloys (e.g., Ti–6Al–4V) are now widely used in load-bearing applications due to its excellent biocompatibility, light weight and good mechano-chemical properties. The elastic modulus of these materials is much lesser than other metals and is found to be about 5 times greater than natural bone. They are used mainly for prostheses to replace large joints such as hip and knee. Their poor shear strength makes it less desirable for bone screws, plates and similar applications which can be overcome by alloying with other metals such as aluminium and vanadium.

Although metals have superior mechanical properties, problems such as elastic modulus mismatch with host tissue, no active bonding to the tissue, low biocompatibility, inflammatory and allergic reactions is of major concern.. The corrosive nature of metals also weakens the implant and the corroded products may escape into the tissue resulting in undesirable effects. Biodegradable magnesium alloys with low density and mechanical properties closer to bone has been developed by researchers. However the degrade rapidly and resulted in loose integrity prior to bone formation (Staiger *et a*l.,2006).

2.1.3.2. Ceramics

Ceramics are refractory, polycrystalline compounds usually inorganic, including silicates, metallic oxides, carbides and various refractory sulphides and selenides. Specially designed ceramics for the repair, reconstruction and replacement of diseased or damaged parts of the body are termed "bioceramics" (Laverna and Schoenung,1991). They were introduced to orthopedics during 1960s. They have high compressive strength and hardness and highly biocompatible and tissue responsive. Based on tissue response, they are classified into three types; nearly bioinert (e.g., alumina and zirconia), bioactive (e.g., hydroxyapatite (HA) and bioglass), and bioresorbable (tri-calcium phosphate (TCP)

The first clinically used bioceramic material was alumina in 1970 owing to its excellent biocompatibility, hardness, strength to resist fatigue, and corrosion resistance. Zirconia has been in use in orthopedics since 1985 and they exhibits fracture toughness greater than alumina. Alumina and zirconia are predominantly used as femoral heads of total hip joints. Due to exceptional bioactivity, HAP and bioglasses are frequently used as bone graft substitute and as coating-agent on biometallic or biocomposite implants. They elicit a strong interfacial interaction with host tissue due to their bioactivity; thereby they are considered to provide osteointegrative stimuli. However, they are very less bioresorbable. TCP is widely used as a bioresorbable bone graft. However, the rate of bioresorption of TCP is unpredictable and they have certain drawbacks, which include poor mechanical properties (e.g., brittleness and low toughness). Therefore, they are used only in low-weight bearing orthopedic applications. Overall, the ceramics have

many advantages that include biocompatibility, easy availability, shapeability, non-toxic, and non-immunogenic.

2.1.3.3. Polymers

Polymers are relatively new class of materials which is widely used as bone graft substitutes owing to their biocompatibility, design flexibility, functional groups availability, surface modifiability, light weight, and ductile nature (Hollinger and Battistone, 1985). The category of polymers used as bone graft substitutes includes biodegradable and non-biodegradable polymers. Collagen, gelatin, poly (ε-caprolactone), poly (lactic acid) (PLA), poly (glycolic acid) (PGA) and their copolymers poly(lactic-co-glycolic acid) (PLGA) belongs to the class of biodegradable polymers and poly(ethylene) (PE), poly(ethylene terephthalate) (PET), and Poly(methyl methacrylate) (PMMA) belongs to that of non-biodegradable polymers. The first synthetic polymer used in clinical practice was of PMMA in 1937. Since then, numerous polymers has been developed and used in orthopedic and other medical applications. Ultra high molecular weight polyethylene is used to fabricate acetabular cups and used in total hip arthoplasty. The acrylic cements are used alone or in combination with HAP for cementing the metallic implants to natural bone.

The extensive interest in polymers is mainly due to their design flexibility and the biodegradability of certain polymers at body pH which has resulted in the use of polymers as scaffolding material for bone tissue engineering (BTE) applications. Both natural as well as synthetic polymers are used as scaffolds for the delivery of cells, growth factors or bioactive drugs to the site of injury. The most widely studied of natural

polymers includes collagen, gelatin, chitosan, silk, alginate, hyaluronic acid, and peptides and that of synthetic polymers are polyesters such as poly glycolic acid, poly lactic acid, and their copolymer of poly lactic-co-glycolic acid.

2.1.3.4. Polymer nanocomposites as bone grafts

Nanocomposites could play a pivotal role in bone grafting as a new class of bone graft material, which uses a combination of several nanoscale bone graft materials and/or in conjunction with osteoinductive growth factors and osteogenic cellular components (Murugan and Ramakrishna, 2005).The term nanocomposite can be defined as a heterogeneous combination of two or more materials in which at least one of those materials should be on a nanometer-scale. Since bone is a typical example of a nanocomposite, designing bone graft in the form of nanocomposite is perceived to be beneficial. Polymer ceramic composites are the most investigated class for bone tissue repair as they mimic the organic-inorganic hybrid nature of native bone tissue. Nanocrystalline HA promotes osteoblast cells adhesion, differentiation, and proliferation, osteointegration and deposition of calcium containing minerals on its surface thus enhancing the formation of new bone tissue within a short period. Studies have shown that incorporation of nano HA on polymer enhances the mechanical property as well as tissue interactions.

2.2. Role of tissue engineering in treating osteoporotic bone fractures

Tissue engineering strategies may be adopted for osteoporotic fracture treatments, wherein the cellular part of the scaffold helps in bone regeneration and the scaffold/implant helps to maintain the contour and aesthetics of the fractured bone.

Effective therapies for bone tissue engineering typically employ the coordinated manipulation of cells, biologically active signaling molecules, and biomimetic, biodegradable scaffolds. Studies have been reported that reported that in aged and osteoporotic patients the number as well as proliferation and differentiation potential of MSCs will be lower. Hence this approach may be particularly beneficial for osteoporotic patients for whom the number and renewal capability of osteoprogenitors cells is poor. Manipulation of the local fracture environment in terms of application of growth factors, scaffolds, MSCs or agents promoting bone formation and bone strength have been considered as a treatment option from which promising results may arise.

2.3 Scaffold fabrication techniques in tissue engineering

Based on the specific requirements, various techniques can be adopted for fabricating scaffolds based on appropriate material for tissue engineering applications. While choosing the processing technique, it must be ensured that it will not adversely affect the materials properties, especially the biocompatibility. The conventional techniques employed for scaffold fabrication involves solvent casting and particulate leaching, phase separation, gas foaming, melt moulding, fiber bonding and textile methods such as electrospinning. Advanced techniques based on computer-aided designing (CAD) or computer aided modelling (CAM) includes three-dimensional printing, stereolithography, fused deposition modelling, selective laser sintering. Among these various techniques, electrospinning technique can be employed to fabricate fibrous structures consisting of macro/nano fibers. Due to the high resemblance to the extra cellular matrix (ECM), scaffolds fabricated using electrospinning is considered as

potential candidates for temporary templates in tissue engineering. The simplicity of this technique also allows encapsulation of bioactive drug molecules and hence can be used as drug delivery device.

2.3.1. Electrospinning

Electrospinning is a unique and facile technique for producing ultrafine micron / nano fibers from polymer solution or melts. A wide range of polymeric materials had been electrospun for various applications. In order to develop materials with specific functional applications, predominantly for bone tissue engineering composite nanofibers based on polymeric materials incorporated with inorganic nanoparticles has been mostly used. In a typical electrospinning process, when a high potential is applied to a polymeric solutions or melts from few to tens of kilovolts (depending on the electrospinnability of the material), an electrical field is simultaneously induced between the spinneret and collecting device. The ball-shaped drop pendent on the nozzle exit is then deformed, as a consequence of the force interactions between the coulombic force (exerted by the external electric field) and the surface tension of the polymer solution, into a conical shape termed as the Taylor cone. When the electric field strength is increased to a threshold value, the electrostatic forces overcome the surface tension, resulting in an ejection of a polymer liquid jet. This jet is then subjected to an extremely high ratio of stretching and rapid evaporation of solvents, leading to the formation of nano-/micro- meter sized fibers on the collecting device The mechanism of forming nanoscale polymeric fibers with electrospinning has recently been identified as a result of the bending instability or whipping of the charged jet, which was previously

described phenomenally as splitting or splaying. To date, with the electrospinning process, more than 100 different types of materials have been electrospun into ultrafine fibers with diameters ranging from a few nanometers to tens of micrometers.

2.4. Role of polycaprolactone as scaffolds in tissue regeneration

Poly (ε-caprolactone) (PCL) was synthesized in early 1930s by the Carothers group (Van Natta et al., 1934). It can be synthesized either by ring-opening polymerisation of ε-caprolactone using a variety of anionic, cationic and coordination catalysts or via free radical ring-opening polymerisation of 2- methylene-1-3-dioxepane (Pitt., 1990). PCL is semi-crystalline and hydrophobic in nature with a polar ester group and five non-polar methylene groups in its repeating unit. The high olefin content imparts polyolefin-like properties to PCL (Kim *et al.,* 2004). PCL exhibits molecular weight (Mw) ranging from 1000 to over 100,000 (Chen *et al.,* 1998; Fields *et al.,* 1974; Tang *et al*., 2004) and its melting point (*Tm*) depends on Mw and can range from 45 ºC to 60 ºC. PCL exhibits glass transition temperature (*Tg*) around -60ºC. The low melting point along with its solubility in wide range of solvents, and exceptional blend-compatibility has stimulated extensive research in its potential application in the biomedical field.

During the resorbable-polymer-boom of the 1970s and 1980s, PCL and its copolymers were used in a number of drug-delivery devices. Attention was drawn to these biopolymers owing to their numerous advantages over other biopolymers in use at that time. These included tailorable degradation kinetics and mechanical properties, their

ease of shaping and ease of manufacture enabling appropriate pore sizes conducive to tissue in-growth, and the controlled delivery of drugs contained within their matrix.

Polycaprolactone has been modified by researchers in order to enhance its surface wettability, mechanical properties, degradation behavior and biocompatible properties. Blending techniques have been widely used to modify physical and chemical properties of PCL. Numerous studies have been carried out on blends and composites based on PCL for biomedical applications especially in the area of tissue engineering and drug delivery. PCL has been blended with both natural as well as synthetic biodegradable polymers. Prabhakaran et al has reported that PCL blended with chitosan showed improved wettability, tensile property and cellular response (Molamma et al., 2008). The studies by Kim et al suggested that PCL blended with water-soluble poly(N-vinyl-2-pyrrolidone) (PVP) exhibited with tunable fiber surface morphology and controllable degradation rates. The washing out of hydrophilic PVP resulted in formation of nanopores on fiber surface leading to enhanced porosity which would facilitate their use in tissue engineering (Kim *et al.,* 2013). Aghdam *et al* modified PCL with different concentration of PGA and observed improved wettability and mechanical properties (Aghdam *et al.,* 2011). The PCL/PMMA blend scaffold (7/3 wt ratio) developed by Son et al exhibited improved growth of MG-63 osteoblast cells under *in vitro* conditions *and* promoted bone formation of calvarial defect in Sprague Dawley under *in vivo* conditions (Son *et al.,* 2013).

Studies have shown that mechanical properties and biocompatibility of PCL can be improved with of incorporation of ceramic (Wutticharoenmongkol *et al.,* 2006).

Calcium phosphate based ceramics are widely used as fillers to overcome the mechanical inferiority of the polymeric scaffolds (Xu, and Simon, 2005). The various class of calcium phosphate based ceramics used in bone tissue engineering includes Hydroxyapatite (HAP), beta-tricalcium phosphate (β-TCP), octa calcium phosphates (OCP) and biphasic calcium phosphates (BCP) (Bose and Tarafder., 2012).

Among these, nano-sized hydroxyapatite (nHAP) particles are the most promising filler which has been mostly incorporated in polymers owing their structural similarity to the inorganic phase of the bone. Polymer composites are made either by the direct incorporation of nanohydroxyapatite (nHAP) within polymeric matrices or by the mineralization of nHAP on the surface of polymeric substrates (Liao et al., 2008). The biologically beneficial characteristics of nHAP, includes the similarilty to the major inorganic component of bone matrix, specific affinity to many adhesive proteins, and direct involvement in the bone cell differentiation and mineralization processes which make nHAP especially suited for utilization in the bone regeneration field.

Wutticharoenmongkol *et al* has observed improved tensile properties, enhanced viability of human osteoblasts and highest ALP activity on PCL scaffolds incorporated with 1wt% nHAP particles (Wutticharoenmongkol *et al.,* 2006). Comparative evaluation of attachment, proliferation, and alkaline phosphatise (ALP) activity of human osteoblasts cells (SaOS2) on electrospun scaffolds and solvent casted films based on PCL and PCL/nHAP revealed that fibrous scaffolds promoted much better adhesion and proliferation than the corresponding film scaffolds (Wutticharoenmongkol *et al.,* 2006). Studies by Shalumon et al have shown that PCL nanofibers appear to show a significant

disposition towards initiating cell attachment and spreading than the micro-fiber geometries. They observed that incorporation of nHAP (1.5wt %) into the nanofibrous PCL scaffold enhanced the adhesion of human osteoblastic cell line (MG63) and protein adsorption which was due to the high surface activity of nHAP.

2.5. Controlled release of bisphosphonates from polymeric scaffolds

Bisphosphonates (BPs) were discovered by the Theodor Salzer in 1894 and have been used in textile and oil industries as corrosion inhibitors and complexing agents (Petroianu., 2011).However the pharmacological activity of BPs was discovered in the late 1960s by Herbert Fleisch (Giger *et al,* 2013). The works by Fleisch in collaboration with Francis at Procter & Gamble revealed the high affinity of BPs for hydroxyapatite which later resulted in their use for treating various bone diseases such as osteoporosis, Paget's disease, bone metastases, malignancy-associated hypercalcemia, etc (Giger *et al,* 2013).

Now BPs is the first-line medications for osteoporosis treatment and is being taken by millions of patient's worldwide, predominantly postmenopausal women. They are powerful inhibitors of osteoclastic bone resorption and reports are available regarding their ability to proliferate bone-building osteoblast cells (Fleisch.,1998, von Knoch *et al.,* 2005, Im *et al.,* 2004, Reinholz *et al.,* 2000). The oral bioavailability of the bisphosphonates is low (1–6%) and drug absorption decreases dramatically in the presence of food as they form insoluble complexes with calcium or iron which is a major concern. In fact, oral absorption ranges from about 0.7% (for alendronate and risedronate) to only 6% (for etidronate and tiludronate).Studies have shown the

localized, controlled delivery of bisphosphonates has the potential to improve drug efficacy and reduce the side effects by targeting the site of action. It avoids the inconvenience of fasting and the patient morbidity associated with gastrointestinal disturbance or musculoskeletal pain associated with the systemic delivery of these drugs.

Clinically, bisphosphonates effectively increase bone density, prevent bone loss and reduce the risk of vertebral and non-vertebral fractures (Verron *et al,* 2010). Studies have shown that local delivery of bisphosphonates can improve bone growth around dental and orthopedic implants. In most of these studies, bisphosphonate has been applied either topically into the implant cavity or as a drug coating on the implant itself, but neither of these approaches affords controlled drug release. Only limited number of reports is available on the development and characterization of polymer-based, controlled-release delivery systems for bisphosphonates. Though polymeric microspheric preparations of bisphosphonates clodronate, alendronate and pamidronate have been reported, only very few reports are available on biodegradable films for controlled and localized delivery of bisphosphonates (Table 1).

Literature review shows that very few works has been reported on the fabrication and characterization of electrospun polymeric scaffolds for the delivery of bisphosponates. Puppi *et al* has reported on the development of bioactive composite scaffolds using three-arm branched-star poly(ε-caprolactone) (PCL), hydroxyapatite nanoparticles(HNPs) and clodronate (CD) and evaluated their physico-chemical characteristics (Puppi *et al.,*2011) . Lu *et a*l has fabricated sandwich like nanofiber meshes using polylactic acid and polyethyleneoxide for the controlled delivery of

zolendronic acid. Their results demonstrated that the drug release speed and initial burst release were controllable by adjusting the thicknesses of electrospun barrier mesh and drug-loaded mesh. Similarly, Yun *et al* has evaluated the effect of alendronate (Aln) loading on in-vitro osteogenic differentiation of adipose-derived stem cells (ADSC) on electrospun PCL scaffolds. They also investigated the *in-vivo* bone regenerative capability of scaffolds in rat calvarial defect model and their results suggested that Aln/PCL nanofibrous scaffolds enhanced the osteogenic differentiation of ADSCs *in vitro* and bone formation *in vivo (*Yun *et al.,*2014).

Polymer used	**Fabrication**	**Bisphosphonate**	**Author**
PCL	Electrospun	Alendronate	Yun *et al.,*2014
Chitosan and hydroxypropylmethyl cellulose (HPMC)	Solvent cast	Risendronate	DhrubojyotiMukherjee *et al.,* 2013
Three-arm branched-star PCL / hydroxyapatite	Electrospun	Clodronate	Doustagni *et al.,*2011
Three-arm branched-star PCL / hydroxyapatite	Electrospun	Clodronate	Puppi *et al.,*2011
PLA	Electrospun	Zolendronate	Jian *et al.,* 2011
PDLLA	Solvent casted	Pamidronate	Yu *et al.,*2010
PLGA/PLLA-methoxy PEG	Solvent casted	Alendronate	Long *et al.,*2009

Table 1. Bisphosphonate incorporated polymeric membranes

2.6. Studies based on pamidronate for bone tissue regeneration

Studies based on pamidronate on evaluating their efficacy on clinical studies especially in post menopausal women are reported by various researchers. Reid *et al*

demonstrated improvements in bone mineral density throughout the skeleton of postmenapausal women as a result of continuous daily therapy with pamidronate dosage of 150 mg/day (Reid *et al.,* 1994). Morabito *et al* showed the effect combined use of cyclic use of intravenous pamidronate and fluoride produced continuous increases in BMD, at the lumbar level in post menopausal women (Morabito *et al.,* 2004). The treatment of postmenopausal osteoporotic women with intermittent intravenous pamidronate increased bone mass at spine, hip and radius, and also potentially reduced the incidence of new fractures (Thiebaud *et al.,* 1994).The effectiveness of intravenous doses of pamidronate in the prevention of femoral neck and lumbar spine bone loss in men during the first 12 months after renal transplantation has also been reported (Stanley *et al.,* 2000).

Surface modifications of dental and orthopedic implants have been carried out to improve the biological properties of implant materials. The surface properties of implants play vital role in tissue acceptance and cell survival and modification of the metallic implant surface can improve initial mechanical fixation and can increase bone-to-implant bonding. The studies by Kajiwara *et al* demonstrated more new bone formation around the pamidronate-immobilized titanium implant than around the calcium-immobilized and pure titanium implants (Kajiwara *et al.,* 2004). Studies by Ponader et al has demonstrated the effectiveness of pamidronate-containing sodium silicate coatings in enhancing the *in vitro* bioactivity, osteoblast attachment, proliferation and vitality of cellulose-based scaffolds in terms of *in vitro* bioactivity and osteoblast attachment, proliferation and vitality (Ponader *et al.,* 2008). Shin et al has

fabricated pamidronate immobilized TiO_2/HA nanofiber mats and studied the adhesion and proliferation of osteoblasts on nanofibers. The results indicated better cellular response of TiO_2/HA-P composite nanofiber mats than bare TiO_2/HA composites (Shin *et al.,* 2013).Very few studies have been reported on *in vitro* and *in vivo* analysis of pamidronate incorporated polymeric scaffolds for osteoporotic treatment. Local co-delivery of bone morphogenic protein (BMP) with via biodegradable poly-D, L-lactic-acid (PDLLA) polymer implanted in the hind limbs of female C57BL6/J mice shows that with appropriate dosing, local pamidronate may have the potential to improve BMP-induced bone formation.

2.7. *In vivo* studies on rat animal model

Preclinical studies in animal models are essential in order to evaluate the potential of developed materials which are intended to use in humans so as to confirm its safety and efficacy. Ovariectomized animal model is widely recognized to closely represent the pathophysiological situations of postmenopausal osteoporosis. Laboratory ovariectomized rats are FDA-recommended models for osteoporosis research. The endocrine gland ovary is responsible for the estrogen production. In cases of early menopause, late menarche and ovariectomy, the level of estrogen secretion is decreased which results in uncontrolled bone remodelling characterized by reduced deposition of calcium and phosphorus in bone. These alterations will damage bone microarchitecture, predisposing to the occurrence of osteoporosis (Cunha *et al,* 2010).

On literature reviewing, very few studies are reported on the use of polymeric scaffolds in ovariectomised rats. Shen *et al.* has reported reduction in estrogen

concentration of ovariectomized rats which resulted in decreased bone mineral density and biomechanical changes in the femur (Shen *et al.,* 2000). Zhang *et al* has developed strontium-incorporated mesoporous bioactive glass (Sr-MBG) scaffolds and implanted in critical size femur defects created in ovariectomized rats so as to evaluate the *in vivo* osteogenic efficacy. The results revealed improved ability of Sr-MBG scaffolds to regenerate osteoporotic bone defects (Zhang *et al*., 2013) The studies by Cheng et al on the evaluation of the efficacy of pure silk and hybrid CaP/silk scaffolds in treating critical sized defects created in distal femoral epiphysis suggested enhanced osseointegration with the use of hybrid CaP/silk scaffolds. Chandran et al has reported the osteogenic efficacy of Strontium incorporated hydroxyapatite (SrHA) microgranules in treating 3mm cortical bone defect in ovariectomised rats. Their findings suggest that the improved osteogenesis observed with SrHA can be attributed to the released Sr^{2+} in the defect site (Chandran *et al.,* 2016).

To summarize, though significant progress has been made in the area of developing bone graft substitutes. The development of an ideal bone graft with adequate properties for osteoporosis bone defect repair still remains as a challenge. The present work is an initiative in this area of research utilizing the advantage of the biodegradable polymer PCL and the bisphosphonate drug pamidronate. The study focus on showing how electrospun nanofibrous scaffolds based on PCL and PDS with adequate properties can serve the purpose and efforts are being taken to achieve this goal.

CHAPTER 3

MATERIALS AND METHODS

In this study, efforts were made to develop an appropriate scaffolding material based on PCL based nanocomposite for osteoporotic bone defect repair. The study involves (1) development of biodegradable and bioactive scaffolds based on PCL with improved hydrophilicity, biodegradability and better cell viability (2) development and characterization of PDS incorporated PCL based scaffolds (3) *In vivo* evaluation of PDS incorporated PCL based scaffold in a rat animal model to corroborate its applicability.

Electrospinning technique was employed for scaffold fabrication. PCL scaffolds were modified by blending with synthesized copolymer polycaprolactone–polyethyleneglycol–polycaprolactone (CEC) and by incorporating nanohydroxyapatite (nHAP) particles and were evaluated for their applicability in bone tissue engineering. The amino bisphosphonate PDS incorporated PCL based scaffolds were fabricated and characterized to evaluate the effect of PDS on physical and biological properties of scaffolds. The experimental procedure related to copolymer CEC synthesis and scaffold fabrication based on PCL is detailed in section 3.1. Fabrication of PDS incorporated scaffolds is described in section 3.2. The section 3.3 details about characterization of CEC copolymer and physico-mechanical property evaluation of scaffolds. The *in vitro* cytocompatibility evaluation and cell culture studies on scaffolds using mesenchymal stem cells (MSCs), L929 and human osteosarcoma cell lines (hOS) is described in

section 3.4. The *in vivo* evaluation of developed scaffolds in rat animal model is detailed in section 3.5.

3.1. Synthesis of poly(ε-caprolactone) – polyethyleneglycol - poly(ε-caprolactone) copolymer (CEC)

3.1.1. Commercial reagents for copolymer synthesis

ε-Caprolactone (ε-CL) and tin (II) 2-ethylhexanoate (stannous octoate) were purchased from Sigma-Aldrich Chemical Company Inc., USA and polyethylene glycol (PEG, Mn 2000) was procured from Merck, Germany.

3.1.2. Synthesis of CEC

The copolymer CEC was synthesized by polymerizing the monomer ε-caprolactone monomer using polyethyleneglycol as the macro initiator and tin (II) ethylhexanoate as the catalyst at a temperature of 130^{o}C for 3 h. The triblock copolymer formed was dissolved in dichloromethane and then precipitated in petroleum ether and dried under vacuum at 40 ^{o}C.

3.2. Development of PCL based scaffolds with improved hydrophilicity, biodegradability and better cell viability

3.2.1. Materials used for scaffold fabrication

Poly(ε-caprolactone) (PCL) with number average molecular weight Mn 80,000 was procured from Sigma Aldrich, USA, Synthesized triblock copolymer PCL–PEG– PCL (CEC) with number average molecular weight (Mn 7500) determined by GPC, Spray dried nanohydroxyapatite (nHAP) particles with average particle size of 89 nm

provided by Bioceramics laboratory, SCTIMST, Trivandrum, India. The solvents dichloromethane (DCM) and N,N-dimethyl formamide (DMF) (puris AR grade) were purchased from Spectrochem, India.

3.2.1.1. Fabrication of scaffolds by electrospinning technique

Scaffolds were fabricated by electrospinning technique using PCL, PCL/CEC blend (80/20 wt%) and their nHAP (2 wt%) filled composites in a solvent mixture of 80:20 (v/v) of dichloromethane (DCM) and dimethyl-formamide (DMF). Prior to electrospinning, conductivity of spinning solution was measured using PC Scan 300 conductivity meter (Eutech instruments). Electrospinning was performed at a predetermined condition of 10% solution concentration, applied potential of 12-15 kV with a feed rate of 1 mL/h. The desired solutions were loaded into a 10 ml syringe, the opening end of which was connected to a 21 gauge stainless steel needle that was used as the nozzle. A mandrel rotating at 500 rpm was used as the collector and was placed at a distance of 13-15 cm from the needle tip. A high-voltage power supply ((Gamma High Voltage Research, Inc.,U.S.A.) was used to generate a high DC potential. A syringe pump (Holmarc opto-mechatronics,Kochi, India) was used to control the feed rate of the polymer solution.. After the process, the electrospun fibers were dried in a vacuum oven at 40℃ for about 48 h to remove the residual solvent.

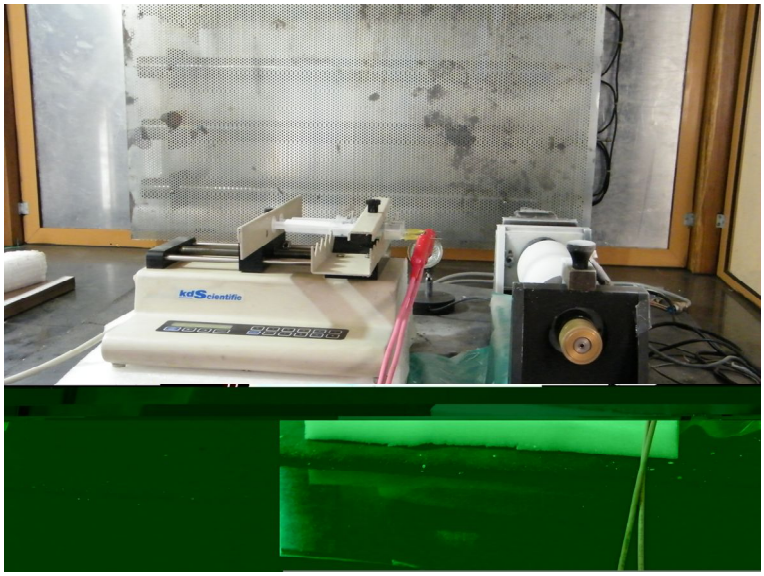

Figure 5. Electrospinning setup for scaffold fabrication

Sample Code	Wt %		
	PCL	CEC	nHAP
PCL	100	-	-
PCL/CEC	80	20	-
PCL/nHAP	100	-	2
PCL/CEC/nHAP	80	20	2

Table 2. Scaffold composition used for the study

3.2.2. Development of pamidronate incorporated PCL based scaffolds

3.2.2.1. Materials used and scaffold composition

Poly (ε-caprolactone) (PCL) , PCL–PEG– PCL (CEC), spray dried nanohydroxyapatite (nHAP) , pamidronate disodium pentahydrate (PDS). The drug PDS was supplied as a gift sample by JPN Pharma limited (Bangalore).

3.2.2.2. Fabrication of PDS incorporated PCL based scaffolds

Scaffolds were fabricated as described in section 3.2.1.1. The drug PDS (1, 3 and 5 wt %) was incorporated in the spinning solution and the drug loaded scaffolds based on PCL, PCL/CEC and PCL/CEC /nHAP scaffold were fabricated. The scaffold details are described in Table 3-

Sample Code	Wt %	
	PCL	PDS
PCL-PDS 1	100	1
PCL-PDS 3	100	3
PCL-PDS 5	100	5

Table 3. Scaffold composition of PDS incorporated PCL scaffolds

Sample Code	Wt %		
	PCL	CEC	PDS
PCL/CEC-PDS 1	80	20	5
PCL/CEC-PDS 3	80	20	5
PCL/CEC-PDS 5	80	20	5

Table 4. Scaffold composition of PDS incorporated PCL/CEC scaffolds

Sample Code	Wt %			
	PCL	CEC	nHAP	PDS
PCL/CEC/nHAP - PDS1	80	20	2	1
PCL/CEC/nHAP - PDS3	80	20	2	3
PCL/CEC/nHAP - PDS5	80	20	2	5

Table 5. Scaffold composition of PDS incorporated PCL/CEC/nHAP scaffolds

3.3. Characterization of copolymer and scaffolds

3.3.1. Characterization of copolymer CEC

3.3.1.1. Fourier transform infrared spectra (FTIR)

The structural characterization of copolymer CEC was recorded using Thermo Nicolet 5700 spectrometer with a diffused reflectance sample mode (Thermo Scientific, Germany). The sample was mixed with optical grade KBR and scanned in the range of 400 and 4000 cm^{-1}.

3.3.1.2. ^{1}H- Nuclear Magnetic Resonance spectra (NMR)

^{1}H-NMR spectra of the synthesized copolymer CEC was recorded using 500-MHz spectrophotometer (Bruker Avance DPX 300) in deuterated chloroform ($CDCl_{3)}$, containing small amount of tetramethylsilane (TMS) as internal standard.

3.3.1.3 Gel permeation chromatography (GPC) analysis

The molecular weight distribution and weight average molecular weight of the synthesized copolymer CEC was determined by gel permeation chromatography (GPC, Waters HPLC system, 600 series pump Milford, USA) with THF as the mobile phase

with a flow rate 1mL/min. Polystyrene standards used for relative calibration was of Mp-100000, 34300, 1470. The mobile phase was THF with a flow-rate of 1 mL /min. The injection volume was usually 100 ml of stock solutions (0.1–0.5 w/v %).

3.3.2. Characterization of nanohydroxyapatite (nHAP).

3.3.2.1. Particle size analysis

Particle size of nHAP was measured using particle size analyzer, Zetasizer (Nano ZS-90, Malvern Instruments, UK). For DLS measurements, nHAP was re-dispersed in de-ionized water. The temperature was kept at 25^{o}C during the measuring process and measurements were recorded as the average of three test runs. The particle size was measured with regard to the volume of particles in the sample. On volume basis the average particle size is taken to be the size of particles occupying the maximum volume.

3.3.2.2 TEM Analysis

TEM analysis of nHAP was performed on a Hitachi H-7650 (Tokyo, Japan) at an acceleration voltage of 80 kV. The suspension of nHAP was administered onto a 200 mesh copper grid coated with a formvar film and air dried prior to imaging.

3.3.3. Characterization of pamidronate (PDS)

3.3.3.1 FTIR spectra

FTIR analysis of PDS was carried out as described in section 3.3.11.

3.3.3.2. Particle size analysis

Particle size analysis of PDS was carried out as described in section 3.3.2.1.

3.3.4. Characterization of Electrospun scaffolds

3.3.4.1. Scanning Electron Microscopy (SEM)

The 3D morphology of the electrospun fibrous scaffolds was observed by scanning electron microscopes (Hitachi-model-S-2400, JEOL, JSM-6390, model 7582, Japan). The samples were sputter coated with gold palladium and imaged in order to study the fiber morphology and average fiber diameter. The fiber diameter was measured using Image J software.

3.3.4.2. Microcomputed Tomography (μ-CT) Analysis

Percentage porosity, pore size distribution, 3D structure and architecture of the fibrous scaffolds were evaluated by microcomputed tomography (μ-CT) analysis using Scanco 40 equipment (μ-CT 40, Scanco Medicals, Switzerland). A series of about 302 2D slices with a scanning resolution of 6 μm were obtained by irradiating the specimen with penetrative X-rays of 45 keV. CT tomography V5.5 was used as image processing software and CT Evaluation Programme V6.0 was used as evaluation software. The porosity along the scaffolds was also evaluated by 2D histomorphometric analysis using a threshold 27 (Th 27).

3.3.4.3. Porosity analysis by liquid intrusion

The porosity of the scaffolds was measured using liquid intrusion method. Scaffolds (n = 6) were weighed prior to immersion in ethanol (liquid intrusion) and the scaffolds were left overnight on a shaker table to allow diffusion of ethanol into the void volume. The scaffolds were taken out, blotted with a wipe and reweighed. The porosity was calculated by dividing the volume of intruded ethanol (as determined by the change

in mass due to intrusion and the density of ethanol, 0.789 g/mL) by the total volume after intrusion (i.e., volume of the intruded ethanol combined with the volume of the PCL fibers determined from the initial mass of the PCL scaffold and the density of PCL, 1.145 g/mL)

3.3.4.4. Surface wettability

3.3.4.4.1. Static Contact Angle Measurements

Surface wettability of the scaffolds (n=3) was estimated with Goniometer (Data Physics OCA 15 plus Germany). A drop of distilled water (5 l) was automatically dropped onto a specially prepared plate of substratum and the image was immediately sent via the camera to the computer and imaged using Imaging SCA20 software.

3.3.4.4.2. Dynamic contact angle measurements

The scaffolds (n=6) were cut to the dimensions 4 cm x 1.5 cm. The samples were cleaned in a sonicate bath prior to the measurements. The contact angle was determined in water using Wilhelmy method using KSV sigma 701 tensiometer. The immersion depth was set to 10 mm with the speed of immersion of 5 mm/min. The initial 2 mm length from each samples were ignored during the measurements. Six measurements from each sample were recorded and the average of consecutive three values from each samples were taken.

3.3.4.5. Static mechanical properties

The static mechanical properties were determined with universal testing machine (Instron 3345, single column, UK) with the use of a 10 N load cell under a cross-head speed of 10 mm/min (gauge length 20 mm) at ambient conditions. Dump bell specimens

as per ISO 527-2 was employed for the test. At least six set of specimens were tested for each type of electrospun fibrous scaffolds.

3.3.4.6. Dynamic mechanical properties using DMA

The dynamic mechanical properties of scaffolds were assessed using Tritec 2000 B (Triton Technology Limited, UK). Samples were tested under tensile mode at a frequency of 1 Hz, and temperature range from −100 ºC to 40 ºC.

3.3.4.7. In-vitro release studies in PBS

Scaffolds (n=5) having 8 mm diameter and 0.2 mm thickness were in placed a vial filled with 2 ml phosphate buffer solution (PBS). The release study of PDS was carried out by keeping the samples at a temperature of 37 °C in a thermostatic shaking incubator (Julabo SW22). At different time intervals, the drug eluted medium (2ml) is taken and then the same volume of fresh PBS was added as replacement. The amount of PDS released was quantified by Ninhydrin assay and evaluated using UV visible spectrophotometer (SHIMADZU1500) at the wavelength of 568 nm.

3.3.4.8. In vitro Hydrolytic Degradation Studies

3.3.4.8.1. Mechanical property evaluation using UTM

Dumb-bell specimens as per ISO 527-2 were placed in closed bottles containing 30 mL phosphate buffer solution (pH: 7.4) and incubated *in vitro* at 37 ºC for different time periods. At the end of each degradation period, the aged specimens were characterized for mechanical properties using universal testing machine (Instron 3345, single column, UK).

3.3.4.8.2 Morphology evaluation by ESEM analysis

The morphological changes of scaffolds in PBS after a period of 14 days were observed using scanning electron microscope (Hitachi-model-S-2400).

3.4 *In vitro* studies

3.4.1. Ethical statement

In vitro cell culture studies using rabbit and rat derived mesenchymal stem cell research work was carried out with the approval of Institutional Committee for Stem Research and Therapy (ICSCRT) - Approval No:– SCT/IC-SCRT/28/Jan 2016.

3.4.2. Sterilization of scaffolds

Prior to cell culture studies, scaffolds (8 mm disc) were sterilized by immersing in 70% alcohol under the laminar air flow over 2 h. Alcohol is then drained off and samples were exposed to UV overnight.

3.4.3. *In vitro* cytocompatibility evaluation using L929 cell line

3.4.3.1. MTT assay

The MTT assay was performed to measure the metabolic activity of cells to reduce yellow coloured tetrazolium salt 3-(4,5-Dimethylthiazol-2-yl)-2,5-diphenyl tetrazolium bromide to purple coloured formazan. Material extract was prepared by incubating test material with culture medium containing serum at 37 ± 2 ºC for 24 to 26 h at an extraction ratio of 6 cm^2/ ml. The extract (100%) was diluted to 50% and 25% with culture medium. A 100% extract prepared using HDPE was considered as negative control. Extract and control medium were added to subconfluent monolayer of mouse fibroblasts L929 cells in triplicate in a 96 well culture plate and incubated at 37 ± 2 °C

for 24 ± 2 h. Extract and control medium were replaced with 200 µl fresh culture medium to which 50 µl MTT (1mg/ml in serum free medium) was added. Cells were incubated at 37 °C for 2 h. After discarding the MTT medium, 200 µl of isopropanol was added to all wells and mixed. The color developed was quantified by measuring absorbance at 570 nm using a microplate reader (Biotek).

3.4.4. *In vitro* cell culture studies using human osteosarcoma (hOS) cell lines

The hOS cells obtained from National Centre for Cell Science, Pune were cultured in Dulbecco's modified Eagle's medium (DMEM, Sigma) supplemented with 10 % (v/v) fetal bovine serum (Sigma) and 1% (v/v) antibiotic/antimycotic solution at 37 °C in a humidified, 5 % CO_2 atmosphere. After harvest, cells were seeded at a concentration of 1x 10^4 cells/cm on each sterilized scaffolds.

3.4.4.1. Live/dead assay

The morphology and viability of hOS cells was observed using DM 6000 fluorescence microscope (Leica, Germany, 20x objective, equipped with DFC 300 FX digital camera). Fluorescein diacetate (FDA) / propidium iodide (PI) staining was carried out to visualize viable and dead cells on scaffolds.

3.4.4.2. MTT assay

MTT assay was carried out to measure the proliferation of hOS on scaffolds. Scaffolds were incubated at 37 °C in 5 % CO_2 for 4 h in serum-free a-minimum essential medium supplemented with 0.5 g of 3-(4,5-dimethylthiazol-2-yl)2,5-diphenyltetrazolium bromide and the purple formazan was extracted using 0.04 M HCl in 2-propanol. The extracted solution was measured at 570 nm using a UV-VIS spectrophotometer.

3.4.5. *In vitro* cell culture studies using rabbit adipose derived mesenchymal stem cells (RADMSCs)

3.4.5.1. Cell Adhesion

The sterilized scaffolds were conditioned in α-MEM (alpha Mini-mum Essential Medium, Invitrogen) for one hour prior to cell seeding. The cell seeded scaffolds were maintained in osteogenic medium (α-MEM supplemented with 15% FBS, 10 mM glycerophosphate, 10^{-8} M dexamethasone and 0.05 mg/ml L-ascorbic acid-Sigma) for a period of 5 days. Each of the scaffolds were then retrieved at 2^{nd} hour, 4^{th} hour, 1^{st} day and 5^{th} day respectively, then fixed in 3% gluteraldehyde and processed for SEM (Hitachi-model-S- 2400) to evaluate the cell morphology and cell spreading over the scaffold.

3.4.5.2. Live/dead assay

The viability of RADMSCs on the scaffolds was determined using LIVE/DEAD viability/cytotoxicity kit (Molecular Probes, Eugene). After 5 days in osteogenic medium, the cell loaded scaffolds were incubated with DMEM containing 4 mM acridine orange and 2 mM ethidium homodimer for 30 min. The non fluorescent acridine permeates the intact membrane of living cells and appears bright green fluorescent. The ethidium homodimer enters damaged cells and is fluorescent when bound to nucleic acids. The cell-seeded scaffolds were washed with phosphate buffered saline (PBS) thrice and imaged using Confocal Laser Scanning Microscope (cLSM). Calcein flu- orescence was excited with the Ar+ laser at 495 nm, and ethidium homodimer excitation was carried out using 528 nm HeNe laser.

3.4.5.3. Alkaline Phosphatase assay (ALP activity)

The cell-seeded scaffolds on day 5 were washed with PBS and fixed with 3.7% paraformaldehyde. After permeabilizing with 0.2% Triton-X-100 in PBS, the samples were blocked with 3% bovine serum albumin in PBS and stained with ELF-97 endogenous phosphatise detection kit (Molecular probes) and viewed under cLSM (Carl Zeiss LSM 510 Meta) for ALP activity.

3.4.5.4. LDH assay

The viability of osteogenic induced cells after 14 and 28 days of cultivation were determined by measurement of cytosolic LDH activity using Cytotox96 kit (Promega, Madison, USA). An aliquot of each cell lysate (50 µl) and LDH substrate (50 µl) were allowed to react at 37 °C and the enzymatic reaction was stopped after 30 min with 0.1 M acetic acid. The absorbance was read at 492 nm (Hidex, Chamaleon). A calibration line was plotted with an increase in the concentration of cells.

3.4.5.5. Picogreen assay

The DNA content of the cells after 14 and 28 days of cultivation were determined using Picogreen® dsDNA Quantitation reagent (Molecular probes) according to manufacturers instructions. The intensity of fluorescence was measured (Hidex, Chamaleon) at an excitation and emission wavelength of 485/535 nm. Relative fluorescence units were correlated with cell number using a calibration line constructed from cell suspensions with increasing concentrations of cell numbers.

3.4.6. *In vitro* cell culture studies using rat adipose derived mesenchymal stem cells (rADMSCs)

3.4.6.1. MTT Assay - un induced rADMSCs

MTT assay of un induced rADMSCs after 24h was performed as discussed in section 3.4.3.1.

3.4.6.2. Cell adhesion - un induced rADMSCs

Cell adhesion of un induced rADMSCs after 24h were performed as discussed in section 3.4.5.1.

3.4.6.3. Live/dead assay –un induced rADMSCs

Live/ dead of un induced rADMSCs were performed as discussed in section 3.4.4.1.

3.4.6.4 Cell adhesion – osteogenic induced rADMSCs

Cell adhesion of osteogenic induced rADMSCs after 14 days were performed as discussed in section 3.4.5.1.

3.5. In vivo studies in rat animal model

Ethical statement

Animal surgical procedures were carried out at Division of Laboratory Animal Science (DLAS), BMT Wing, SCTIMST. All experimental procedures and protocols were conducted as per the guidelines and recommendations of Committee for the Purpose of Control and Supervision of Experiments on Animals (CPCSEA), India and with the approval of the Institutional Animal Ethics Committee (IAEC), B Form No: 98/PO/bc/99/CPCSEA

Animals were housed in individually ventilated cages (IVC, Citizen Industries, India) at 22±2°C and 55±10% Relative Humidity (RH). Light levels measured at 1 meter height less than 300 Lux and a 12:12 hour dark: light was maintained. Animals were fed with standard pelleted rat feed and drinking *ad libitum*. The health of animal colony was monitored as per Federation of European Laboratory Animal Science Associations (FELASA) guidelines for parasitology and was stamped negative of any infectious agents. All operations were carried out under sterile conditions with minimal invasive surgical technique.

3.5.1. Development of osteoporotic rat animal model

3.5.1.1. Surgical procedure

Three month old female wistar rats weighing approximately about 250g were selected for the study. In order to develop osteoporosis, rats were subjected to interventional bilateral ovariectomy. The surgery was carried out under general anaesthesia using xylazine (Xylaxin, Neon Lab, India) at a rate of 5mg/kg body weight and Ketamine (Anket, Neon Lab, and India) at a rate of 70 mg/kg body weight as intraperitoneal injections.The abdominal skin was shaved and the area for surgical intervention was clipped and prepared with 5% povidone iodine solution (Win Media care, India) prior to surgery. The incisions were made on flank on both sides laterally towards the dorsal plane. The peritoneal fat pad was exposed and was exteriorized to view the ovary and uterine horn on each side using a pair of fine tweezers. The ovary was clamped using mosquito forceps an excised. The distal region of the uterine horn was also clamped and a portion of the uterine horn was excised. Clamps were removed

and ascertained that haemostasis was achieved. The fat pad was retracted to the peritoneal cavity using the blunt end of a vascular forceps and skin and muscle wounds were closed using braided silk sutures 3-0 (Mersilk, Johnson Johnson, USA). Povidone iodine solution was applied daily for 7 post operative days until the sutures were removed. Post operatively; animals received subcutaneous injection of Analgesic-Meloxicam (Melonex, Indian Immunologicals Ltd, India) @ 1mg/kg twice daily and Buprenorphine (Buprigesic, Neon Lab, India) @ 0.05 mg/Kg i/m (intra muscular) twice daily for 7 days. The animals were maintained for 4 months post induction to develop osteoporosis.

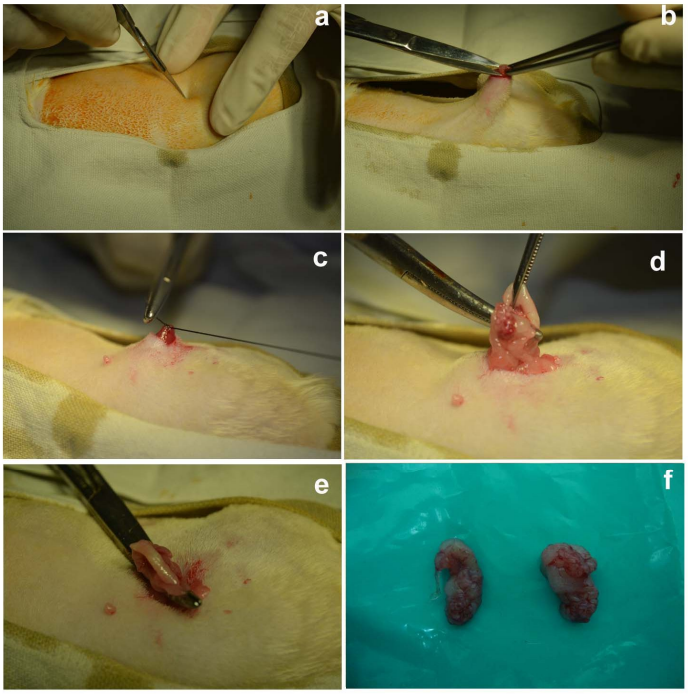

Figure 6. Surgical procedure for rat ovariectomy

[a-incision made on lateral side of abdomen**, b-**external oblique muscle exposed**, c-**peritonial space and adipose tissue surrounding ovary exposed**, d-**removal of ovaries**, e-**suturing the incision]

3.5.2. Evaluation of rat osteoporotic model

3.5.2.1. Histology of excised ovarian tissue - Haematoxylin & Eosin staining

The ovarian tissue collected during ovariectomy procedure were fixed in 10% neutral buffered formalin (NBF) and stored at room temperature until histological evaluation. The formalin fixed ovaries were further processed in series of alcohol followed by embedding in paraffin to prepare 4 μm thick paraffin sections for haematoxylin and eosin staining.

The processing steps involves dehydrating the formalin fixed ovaries in series of alcohol - 80% isopropyl alcohol (2 hours), 95%isopropyl alcohol (2 hours), 95% isopropyl alcohol (1 hour), 100% isopropyl alcohol for 1 hour –(three changes) followed by clearing in xylene for 45 min (three changes) and infiltrated in paraffin wax for 1 h (two changes) followed by 2 h (one change). The tissues capsules were then placed in cassettes which were then put in a tissue processor. The paraffinized tissues were removed from the tissue processor and were then formed into blocks. Thin paraffin sections of approximately 4 micron thickness were collected using rotary microtome (RM 2255, Leica, Germany). Sections were placed in hot air oven at 37°C for one day.

The hematoxylin and eosin (H & E) staining protocol involves deparaffinising the sections by immersing it in xylene for 15 min (2 times) followed by processing the sections in descending series of isopropanol (100%, 80% and 70% for 3 min each. After washing with running tap water for 5 min, stain with Haris Hematoxylin (Sigma chemicals, India) for 12 min and brought to running tap water (5 min). Sections were then dipped in 1% acid alcohol (twice) followed by incubation in 0.2% ammonia water

solution for 2 min. Sections were counterstained with Eosin (sigma chemicals, India) (5 min) and underwent dehydration in ascending series of alcohol – 95% and 100% (2 min each); three changes of xylene wash (15 min) and mounted using DPX. H & E stained sections were then viewed and micrographed using DM 6000 microscope.

3.5.2.2. Micro Computed Tomography analysis-Assessment of trabecular bone loss

Micro CT analysis was carried out to confirm the osteoporotic model induction by evaluating both qualitatively and quantitatively the trabecular bone loss by examining the metaphyseal cancellous bone area. The ovariectomised rats after 4 months of post induction (n=3) and normal rats (n=3) of same age group were sacrificed and their proximal tibia was retrieved. The metaphyseal cancellous bone at the tibial head region was scanned using micro-CT desktop scanner CT 40, Scanco Medical AG which was operated at 70 kVp and 114 μA. Three dimensional model reconstructions were performed using in built software V6.5 by selectively contouring approximately 200 slices of 20μm thickness from the volume of interest. The various parameters like trabecular number (Tb.N.), trabecular spacing (Tb.Sp.), bone volume per total volume (Bv/Tv) and trabeculat thickness (Tb.Th) were automatically determined which enables the confirmation of osteoporotic model induction.

3.5.2.3. Weight monitoring before and after model induction

In order to assess the effect of ovariectomy on weight of normal and ovariectomised rats (n=5) were weighed at definite time periods.

3.5.2.4. Biochemical analysis of blood serum - Calcium, Phosphorus and ALP assay

Blood samples were collected from rats (n = 6) before and after ovariectomy at definite time period 0, 2 and 4 months was isolated from the animals by centrifugation at 1500 rpm at 37 °C for 10 min and stored in freezer until analysis.

Isolated serum were then analyzed for calcium concentration based on the Arsenazo III method end point as per protocol (Cat No: BLT0001 Erba, Germany) (1 ml reagent mixed with 20 µl sample and absorbance read at 630 nm against blank). Calcium concentration was calculated as:

Calcium (mg/dl) = (absorbance of test/absorbance of standard) x concentration standard (mg/dl)

Phosphorus concentration was analysed based on molybdate assay as per protocol (Cat No: BLT00047 Erba, Germany) (1 ml reagent mixed with 10 µl sample, incubate for 5 min. at 37 °C and absorbance read at 340 nm against blank) Phosphorus concentration was calculated as:

Phosphorus (mmol/l) = (absorbance of test/absorbance of standard) x concentration standard (mg/dl)

ALP concentration was analysed based on molybdate assay as per protocol (Cat No: BLT00003 Erba, Germany) (1 ml reagent mixed with 20 µl sample, incubate for 1 min. at 37°C and absorbance read at 405nm against blank). ALP concentration was calculated as:

ALP (U/l) = (absorbance of test/absorbance of standard) x concentration standard (mg/dl).

3.5.3. Development of calvarial defect and scaffold implantation

3.5.3.1. Surgical procedure

The 8 mm critical size defect was created in calvaria of post osteoporotic rats (n=21). The animals were weighed and housed singly in cages from one day before the surgery. All the equipment used for surgery were sterilized by autoclaving. The surgery was performed under general anaesthesia using xylazine at a rate of 5 mg/kg body weight and Ketamine at a rate of 70 mg/kg body weight as intraperitoneal injections. The surgical site was shaved and scrubbed with povidone iodine solution. Under aseptic precautions, incision was made in the sagittal plane across the cranium. A full-thickness flap including the periosteum was reflected, exposing the calvarial bone. Then a critical-size (8 mm diameter) circular defect will be created on the cranium by using a saline-cooled trephine drill without damaging the meninges and neural tissues. The polymeric scaffold will be implanted on the defect in test group and the defect area will be kept as such in sham group. The incisions will be finally closed by using 3-0 catgut sutures. The wound will be cleaned and will be dressed using betadine ointment daily. The skin sutures will be removed after 7 days of surgery. Animals will receive antibiotic ampicillin-cloxacillin at a rate of 10mg/kg bid intramuscular injection and analgesic Meloxicam at a rate of 1.0 mg/kg body weight subcutaneously once daily and Buprenorphine at a rate of 0.1 mg/kg BID intramuscular as injections for a period of 5 post operative days.

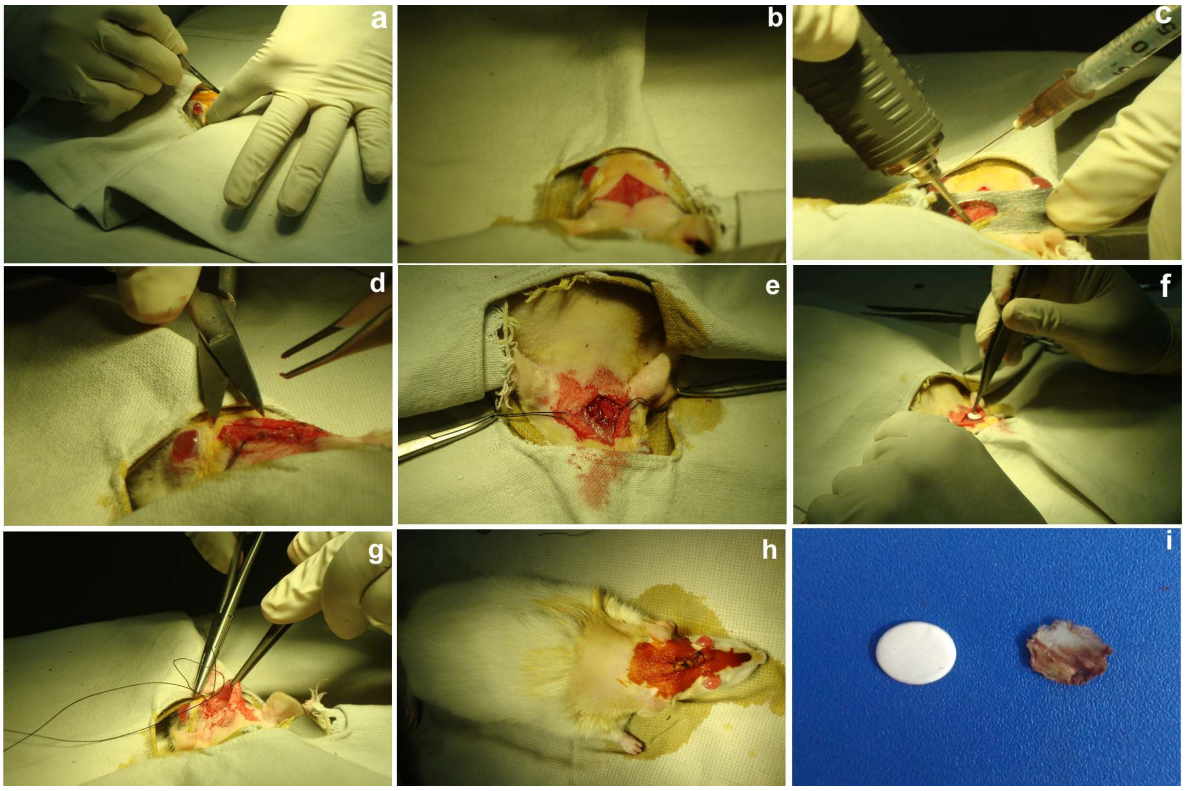

Figure 7. Surgical procedure for calvarial defect and implantation

[a-incision on skin**, b-** exposing calvarial bone**, c-**drilling to create 8 mm CSD**, d-** removal of calvarial bone**, e-**CSD created, **f-**placing 8 mm scaffold, **g-**suturing incision area, **h-**sutured defect area, **i-** scaffold used and removed calvarial bone]

3.5.4. Osteogenic efficacy assessment of scaffolds in osteoporotic rat animal model

The osteogenic efficacy of PDS loaded scaffolds was evaluated through histology (Stevenal's blue and vanGieson's picrofuchsin staining), histomorphometry, radiographic and micro-CT.analysis

3.5.4.1. Gross evaluation of explants:

Animals were euthanized at definite time periods of 3, 6 and 12 weeks post implantation. The implant site along with the adjacent host bone of each animal was desected and fixed in 10% NBF. Prior to any other evaluations, gross examination of retrieved explants was carried out.

3.5.4.2. Radiographic evaluation

Radiographic analysis of explants containing test and control at different post implantation periods (3,6 and 12 weeks) was carried out at standard conditions using X- ray film unit and imaging CR -30X (AGFA, USA) .

3.5.4.3. Micro CT evaluation:

The effect of bone healing ability was assessed from the formalin fixed samples of 3, 6 and 12 weeks implantation studies. The explants were scanned using desktop μCT (μCT 40, Scanco Medical AG, Brüttisellen, Switzerland). The 2D and morphometry images generated from micro CT were assessed for evaluating the overall healing efficacy. *In vivo* healing in the test was compared with of control animal post 12 weeks of implantation. The *de novo* bone formation and *de novo* bone mineralization was assessed from the density histograms (included host bone and *de novo* bone) generated from 2 D 61 of control and test group. Mineralization was estimated from the density drawn on corresponding 2D slices.

3.5.4.4. Histological evaluation – PMMA embedding and staining

Prior to histological evaluation, the formalin fixed explants (3, 6 and 12 weeks) were dehydrated in graded ascending series of isopropyl alcohol

(Finar, India) (70% isopropyl alcohol for 4 days, 80% isopropyl for 4 days, 96% isopropyl alcohol for 4 days, 100% isopropyl alcohol for 2 days, 100% isopropyl alcohol for 1 day). Samples were then infiltrated in methyl methacrylate (MMA) (Merck,India) for 6 days (2 changes) and finally embedded in MMA containing 1% peroxide under vacuum in desiccator. The plastic sections of about 130-150 microns thickness were sliced from PMMA embedded blocks using high-speed precision saw (Isomet TM 2000 Precision Saw, Buehler, USA) and polished down manually to 70–90 microns using variable speed grinder polisher (Ecomet 3000, Buehler, USA). The PMMA sections stained with Stevenal's blue and van Gieson's picrofuchsin. The staining protocol involves incubating PMMA sections in hot water for 3 min followed by immersing in pre-heated Stevenal's blue stain (stain filtered and heated to a temperature of 60-65°C for 5-15 min. The section is then water wash and counter stained with van Gieson's Picrofuchsin for 3- 5 min at room temperature. The sections were then viewed under light microscope (Leica DM6000). Stevenal's blue stains cells and extracellular structures in a subtle gradation of blue tones and van Giesen's picrofuchsin colours collagen fibres (green or green blue), bone (orange or purple) and osteoid matrix (yellow green).

3.5.4.5. Histomorphometry analysis - QWin software

Histomorphometry analysis was carried out to assess the osteointegrative and osteogenic efficacy of scaffolds. The analysis was performed on three consecutive sections of each implant and analyzed using image analyzing software (Leica Qwin, Germany). The Stevenal's blue and van Gieson's picrofuchsin stained sections were

scanned for determining and the area of newly formed bone using the Quips programme of QWin software of the microscope (Leica DM 6000). Bone formation indices were evaluated within the defect boundaries alone. Regeneration efficiency (RE) of implant was calculated and expressed as ratio of new bone formed to total defect area. Measurements were taken from equidistant sites across sections under same magnification.

3.6. Statistical Analysis

Data of all non-biological studies presented in this work were the mean of 6 samples. All the biological studies were done in triplicate. Data is reported as mean ± SD. Statistical analysis was performed with one way ANOVA using Microsoft excel 2007 version or using Graph pad prism (Version 6.01). The values for which $p<0.05$ were considered as statistically significant.

CHAPTER 4

RESULTS

The results obtained from the current study are detailed in Chapter 4 which is further divided into four subsections. The first section discusses the synthesis and characterization of materials used for scaffold fabrication. The second section details the fabrication and characterization of nHAP and CEC incorporated PCL scaffolds. The fabrication and characterization of PDS incorporated PCL based scaffolds are discussed in third section. The *in vivo* evaluation of scaffolds in an osteoporotic rat animal model is detailed in section four.

4.1. Material Characterization

This section details the synthesis and characterization of copolymer CEC, nHAP and drug PDS used for scaffold fabrication.

4.1.1. Synthesis & characterization of PCL-PEG-PCL triblock copolymer (CEC)

4.1.1.1. Synthesis of CEC

The PCL-PEG-PCL (CEC) triblock copolymer was synthesized by the ring-opening polymerization of ε-caprolactone monomer using PEG as macro initiator, whose hydroxyl end group initiated the ring opening. The schematic representation of the copolymer synthesis is shown in Figure 8. The yield obtained was about 90%.

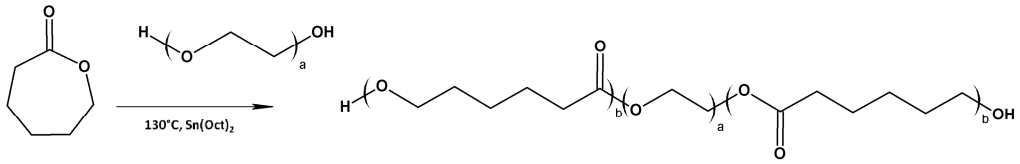

Figure 8. Schematic representation of copolymer synthesis

4.1.1.2. Fourier transform infrared spectroscopy

The chemical structure of synthesized copolymer was confirmed by the characteristics bands observed using FTIR spectroscopy (Figure 9).

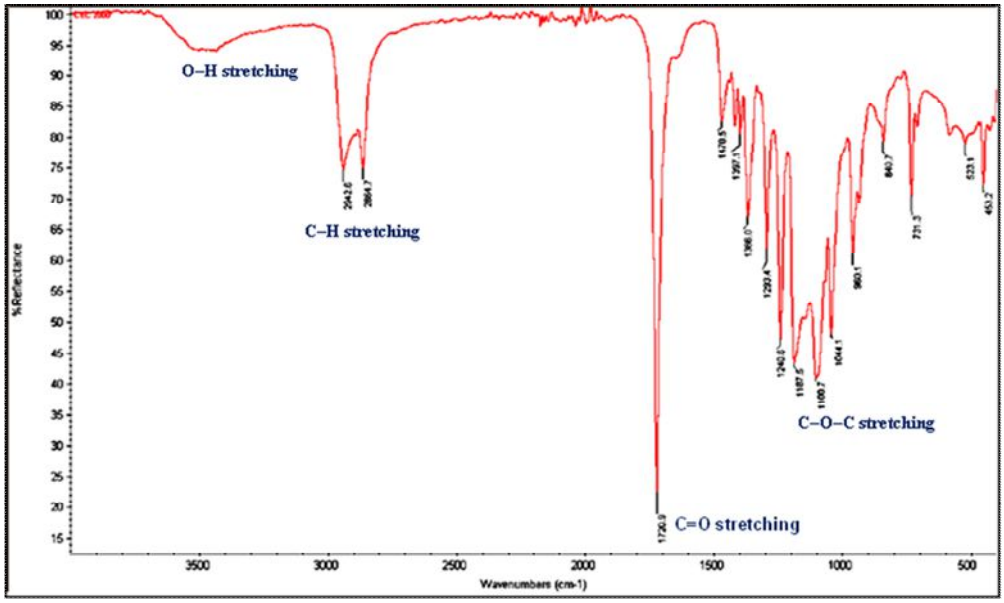

Figure 9. FTIR spectra of copolymer CEC

The FTIR analysis of CEC copolymer exhibited characteristic peaks of both PEG and PCL. The absorption band at 1720 cm^{-1} is attributed to the C=O stretching vibrations of the ester carbonyl group. The absorption bands at 1100 cm^{-1} and 1240 cm^{-1} are attributed to the characteristic C–O–C stretching vibrations of the repeated $–OCH_2CH_2$ units of PEG and the –COO- bonds stretching vibrations, respectively. The absorption

band at ~3450 cm^{-1} is assigned to terminal hydroxyl groups in the copolymer. All the C–H stretching bonds are centered at 2942 cm^{-1} and 2864 cm^{-1}.

4.1.1.3. ^{1}H- Nuclear Magnetic Resonance spectroscopy

The chemical structure of CEC was further fortified with ^{1}H NMR spectra (Figure 10).

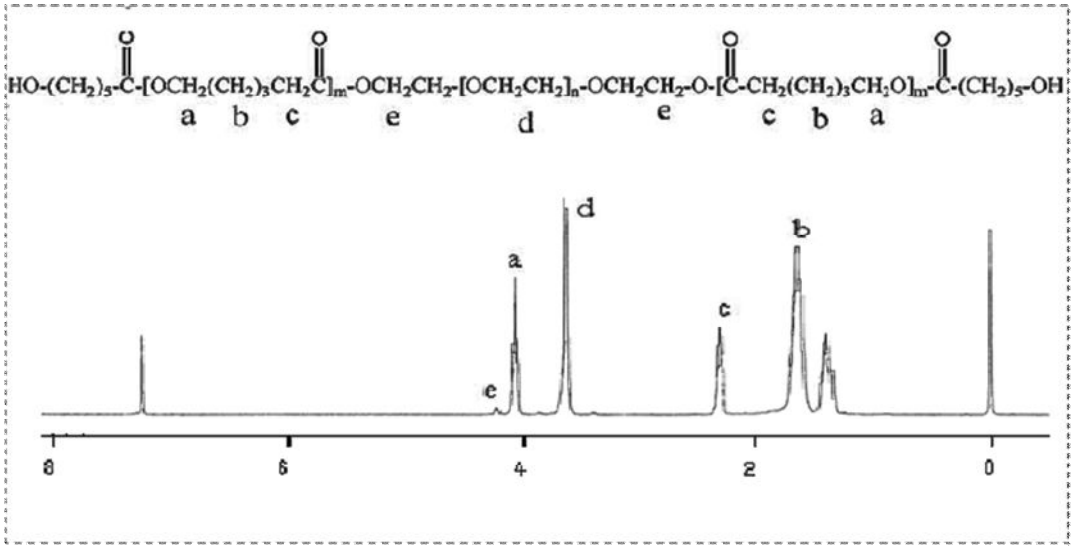

Figure 10: ^{1}H NMR spectra of copolymer CEC

The peaks at 1.62 ppm corresponds to methylene protons of - $(CH_2)_3$ - in PCL units, 2.34 pmm to that of methylene protons of –$OCCH_2$– in PCL units, and 4.09 ppm to that of methylene protons of –CH_2OOC– in PCL units respectively. The sharp single peak at 3.66 ppm is attributed to the methylene protons of homosequences of the PEG oxyethylene units. Peak at 7.26 is the peak for small amount of $CHCl_3$ present in $CDCl_3$.

4.1.1.4. GPC analysis

The copolymer CEC showed narrow molecular weight distribution with PDI 1.33 (Figure 11). The number average (Mn) and weight average (Mw) molecular weights obtained are 5508 and 7305 respectively.

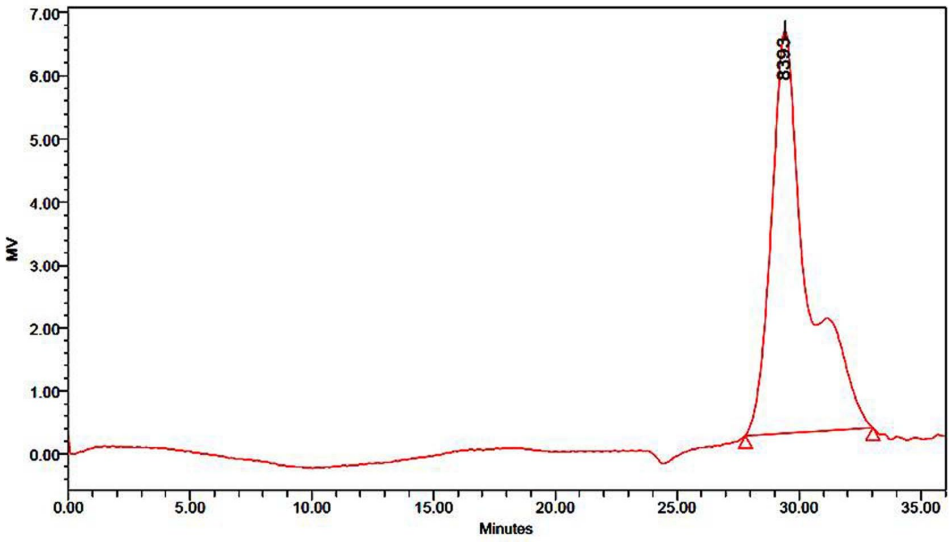

Figure 11. GPC analysis of copolymer CEC

4.1.2. Characterization of nHAP

4.1.2.1. Particle size analysis

The average particle size of nHAP particles was found to be 90 nm and the polydispersity index was 0.292 as measured by particle size analyzer (Figure 12).

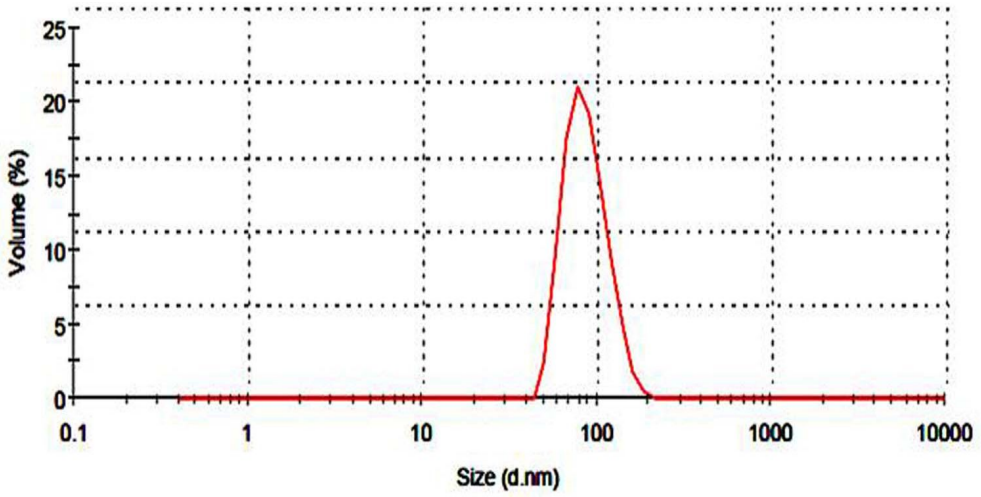

Figure 12. Particle size distribution of nHAP

4.1.2.2. TEM analysis

TEM analysis of nHAP showed rod shaped particles and the size was found to be in the range of 12-35 nm width and 90-120 nm length (Figure 13).

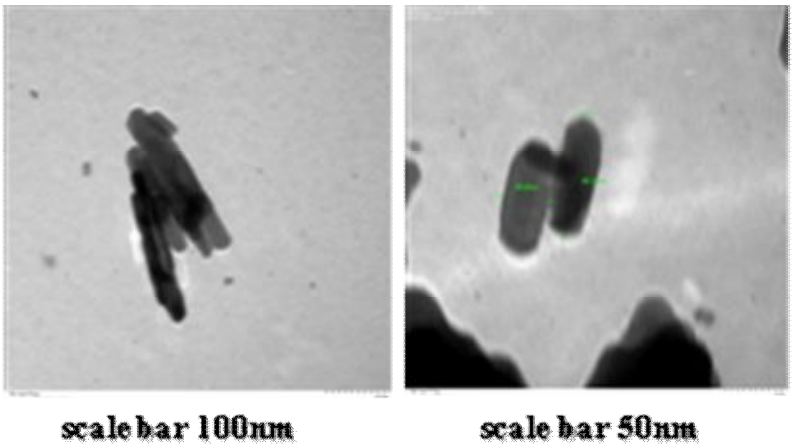

Figure 13. TEM image of nHAP

4.1.3. Characterization of PDS

4.1.3.1. Fourier transform infrared spectroscopy

The FTIR analysis (Figure 14) revealed that the drug amino bisphosphonate PDS showed strong absorption bands for their characteristic N-H stretching vibrations at 3386 cm^{-1}, N-H bending vibrations at 1651 cm^{-1} and that of the O-H stretching at 3122 cm^{-1} respectively. The broad band at 1062 cm^{-1} is attributed to the vibrational band for the PO_3 group of PDS and the sharp bands at 1178 cm^{-1} and 921 cm^{-1} are assigned to P=O and P–OH stretching vibrations respectively .

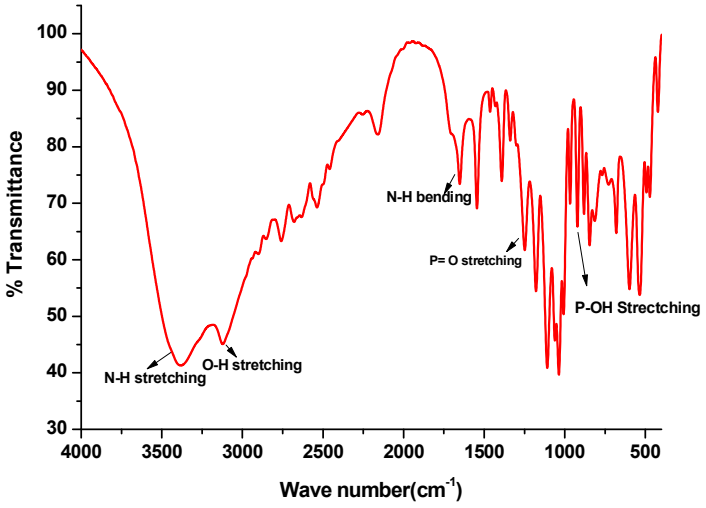

Figure 14. FTIR spectra of PDS

4.1.3.2. Particle size analysis

The size of PDS drug particles analysed using particle size analyzer (Figure 15) was found to be in the range of 162nm with PDI value of 0.433.

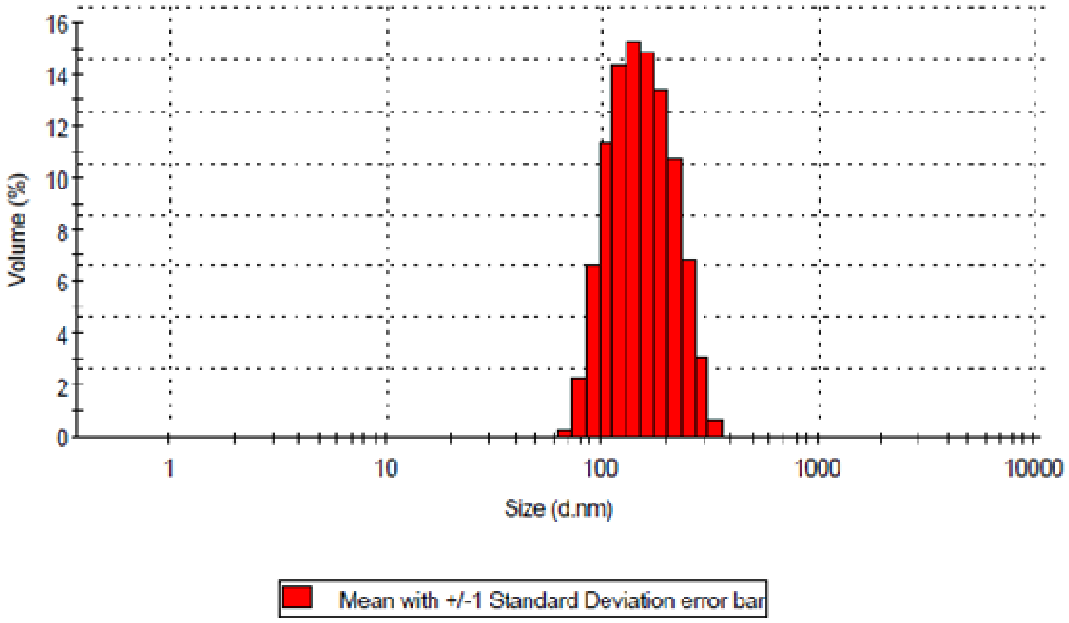

Figure 15. Particle size distribution of PDS

4.2. Development of biodegradable and bioactive scaffolds based on PCL with improved hydrophilicity, biodegradability and better cell viability

4.2.1. SEM analysis

Electrospun PCL, PCL/CEC blend and their nHAP filled composite scaffolds exhibited fibrous morphology as revealed by the SEM micrographs (Figure 16).

Samples	Average fiber diameter (µm)	Conductivity(µS/cm^{-1})
PCL	1.53 ± 0.53	0.98 ± 0.05
PCL/CEC	0.40 ± 0.10	2.87 ± 0.15
PCL/nHAP	0.66 ± 0.16	4.80 ± 0.14
PCL/CEC/nHAP	0.37 ± 0.09	9.20 ± 0.05

Table 6. Conductivity & average fiber diameter of scaffolds

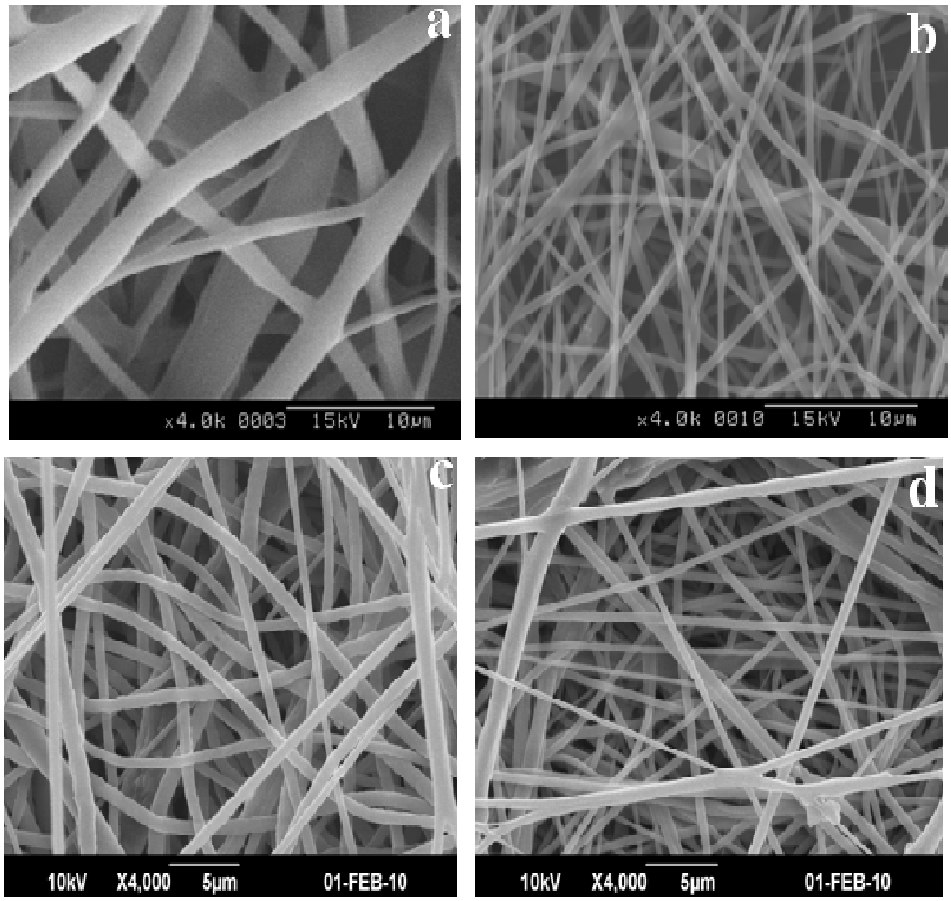

Figure 16. SEM micrograph showing fibrous morphology of (a) PCL (b) PCL/CEC (c) PCL/nHAP and (d) PCL/CEC/nHAP

The analysis of fiber diameter using Image J revealed that the fiber diameter varied among all the scaffolds (Figure 17.). Electrospun PCL exhibited non uniform fibers with an average diameter of 1.53 µm. Significant decrease in fiber diameter exist among all the scaffolds (p value <0.0002). PCL/CEC blend scaffold had diameter of about 0.40 ± 0.1µm. PCL/nHAP composite scaffolds exhibited rough surface with average fiber diameter around 0.66 ± 0.16 µm. The PCL/CEC/nHAP composite scaffold

showed an average fiber diameter of 0.37 ± 0.09 μm. The conductivity and average fiber diameter is summarized in Table 6.

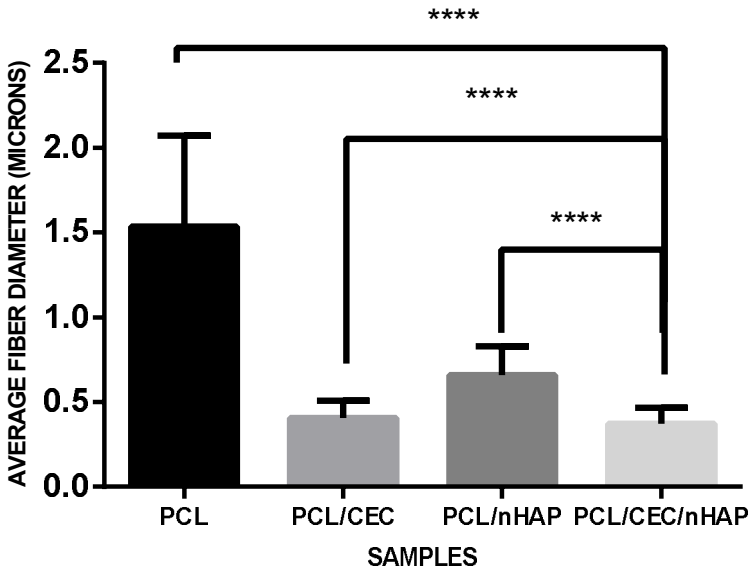

Figure 17. Average fiber diameter of scaffolds

4.2.2. Micro CT analysis

The 3D morphometry of scaffolds analyzed using μ-CT (Figure 18) revealed the porous nature of the scaffolds. All the scaffolds were found to be porous in nature with PCL scaffolds having percentage porosity of about 92%. The incorporation of both CEC and nHAP reduced the porosity to about 80%. The fibrous scaffold PCL/CEC/nHAP showed a percentage porosity of 48%.

The pore size distribution of scaffolds is shown in Figure 19. The average pore size for PCL, PCL/CEC, PCL/nHAP and PCL/CEC/nHAP composite scaffolds were 48, 40, 34 and 20 μm respectively. This reduced pore size can be due to the decreased fiber diameter of both CEC and nHAP incorporated scaffolds.

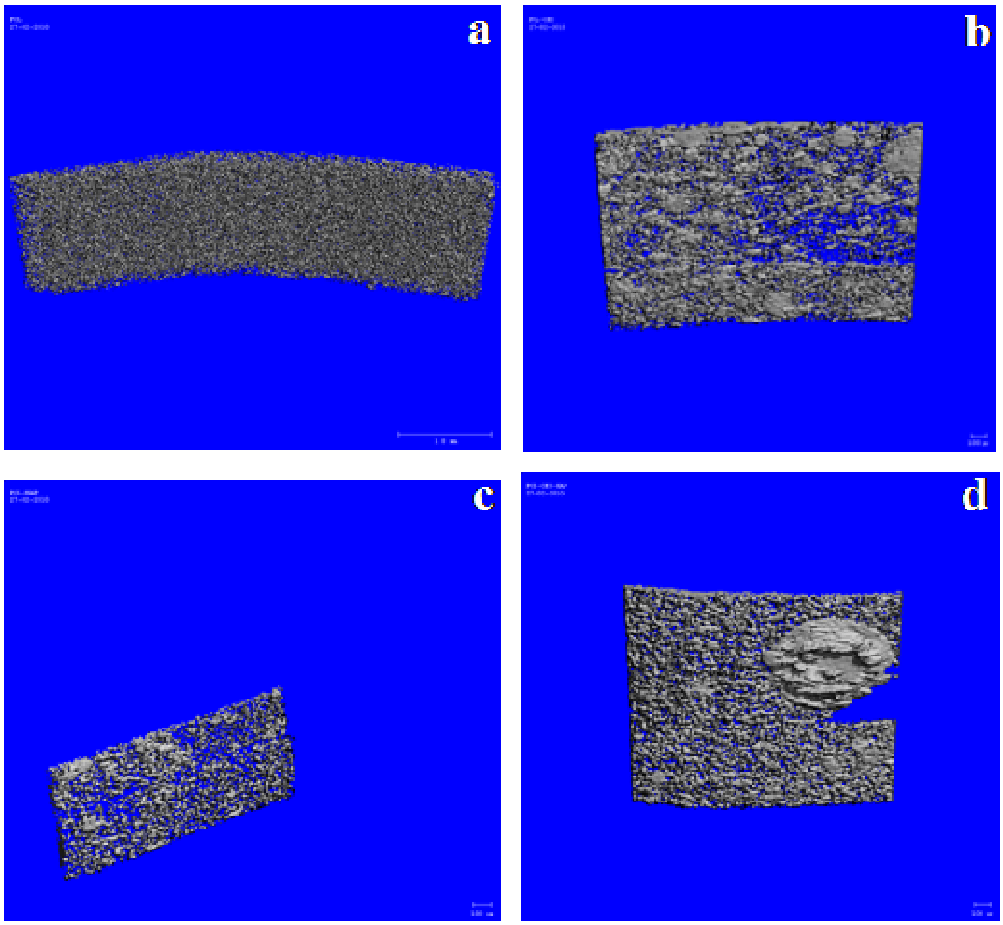

Figure 18. Micro CT analysis showing 3D morphometry of scaffolds (a) PCL (b) PCL/CEC (c) PCL/nHAP and (d) PCL/CEC/nHAP

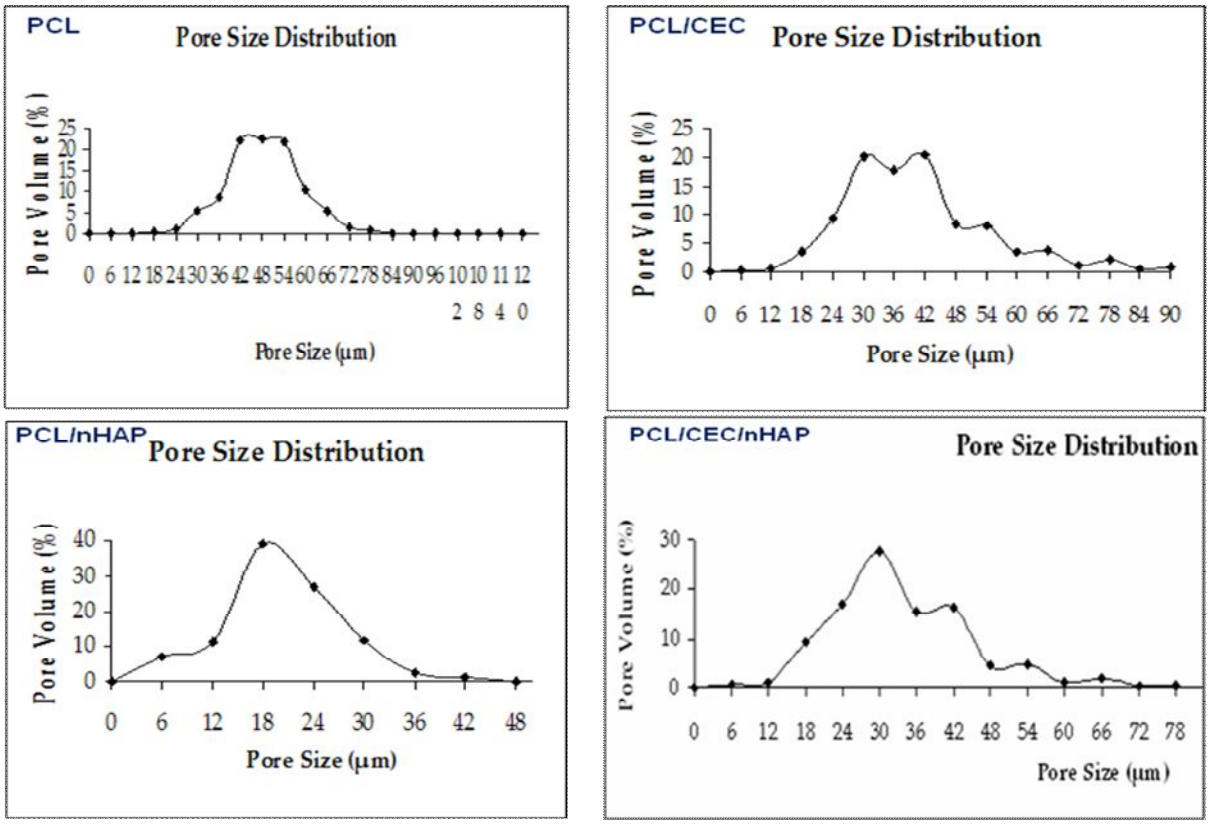

Figure 19. Pore size distribution of PCL, PCL/CEC, PCL/nHAP and PCL/CEC/nHAP scaffolds

4.2.3. Contact Angle Measurements

The results of contact angle measurements showed a higher water contact angle of 119 ± 2° and 112±1° for PCL and PCL/nHAP scaffolds indicating their inherent hydrophobic nature (Figure 20). The contact angle of copolymer blended scaffolds dropped to zero suggesting that the incorporation of hydrophilic CEC resulted in changes in the surface wettabilty.

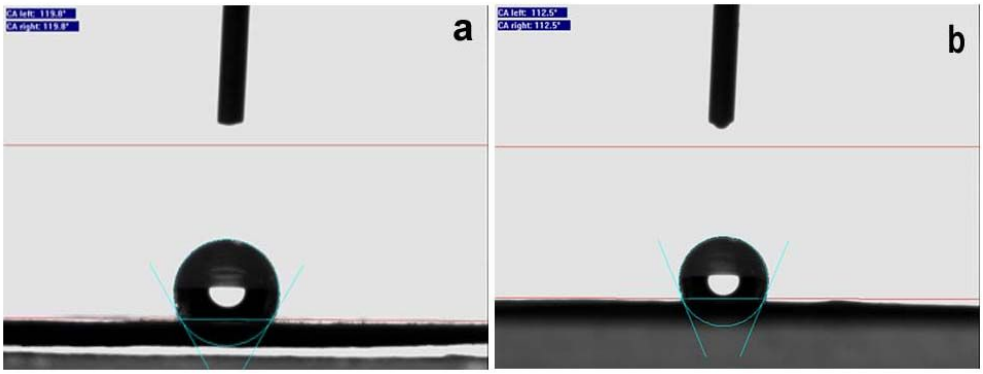

Figure 20. Contact angle measurements of (a) PCL and (b) PCL/nHAP

4.2.4. Static mechanical properties of scaffolds

The static mechanical properties (Table 7) of the scaffolds revealed that electrospun PCL exhibited inferior tensile strength owing to its very high porosity of about 92% and increased fiber diameter of 1.53 µm when compared to both PCL/CEC (80% porosity, 0.40µm fiber diameter) and PCL/nHAP (80% porosity, 0.66 µm fiber diameter) scaffolds. The tensile strength of PCL increased from 5.3 MPa to 7.0MPa with the addition of CEC and to 8.5 MPa with that of nHAP. The PCL/CEC/nHAP composite scaffold showed an ultimate tensile strength of 13.1 MPa. The tensile modulus decreased with CEC from 34 MPa to 19 MPa for PCL/CEC and to 21 MPa for PCL/nHAP scaffolds. PCL/CEC/nHAP composite scaffold showed a tensile modulus of 17.2 MPa. The reinforcing effect of nHAP particles in PCL matrix was reflected by an increase in tensile strength by 60%. The copolymer blended scaffold exhibited an enhancement in tensile strength by 32% whereas for PCL/CEC/nHAP scaffold the tensile strength increased by 149%. The superior tensile strength of this composite scaffold can be

attributed to the decreased porosity (48%) as well as fine fiber diameter (0.37µm) which may provide more contacts and stronger cohesion among these fibers.

Sample	Tensile strength (MPa)	Elongation at break (%)	Youngs modulus (MPa)
PCL	5.3 ± 0.20	144 ± 17	34 ± 1.9
PCL/CEC	7.0 ± 0.30	111 ± 62	19.± 2.0
PCL/nHAP	8.5 ± 1.40	182 ± 15	21 ± 2.7
PCL/CEC/nHAP	13.1 ± 0.80	189 ± 42	17 ±1.8

Table 7. Static mechanical properties of scaffolds

4.2.5. Dynamic mechanical properties of scaffolds

Figure 21 shows the result of DMA analysis showing variation of storage modulus with temperature for the scaffolds with temperature. Electrospun PCL exhibited storage modulus of 8.1 MPa which was found to increase with the incorporation of CEC and nHAP. The storage modulus of PCL/CEC blend and PCL/nHAP composite was of 9.5 MPa and 9.2 MPa respectively. The PCL/CEC/nHAP composite scaffold exhibited storage modulus of about 10.4 MPa.

The variation of tan delta with temperature for the scaffolds is shown in Figure 22. The temperature corresponding to the tan delta peak is taken as the glass transition temperature (T_g). It was observed that the T_g values of PCL and the PCL/CEC/nHAP composite scaffold were almost similar around – 47.7 °C and – 47.4 °C respectively where as for PCL/CEC and PCL/nHAP scaffolds, there was slight decrease in T_g to

−49.4 °C and -51.6 °C which may be due to the enhancement in the chain flexibility of PCL with the incorporation of both nHAP and CEC.

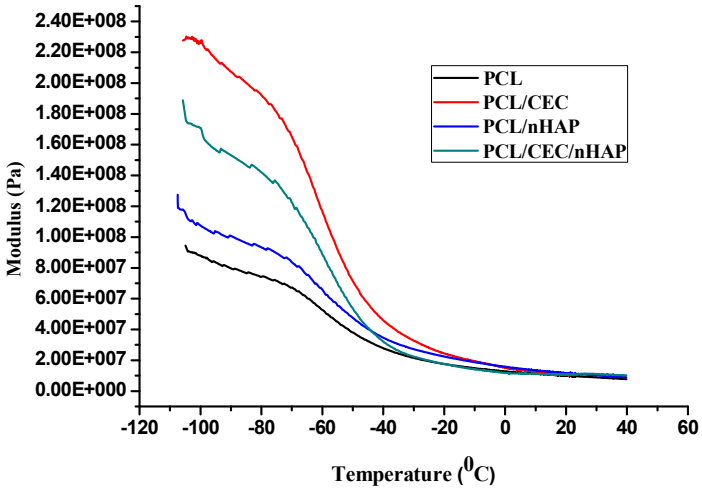

Figure 21. DMA analysis showing variation of storage modulus of scaffolds with temperature

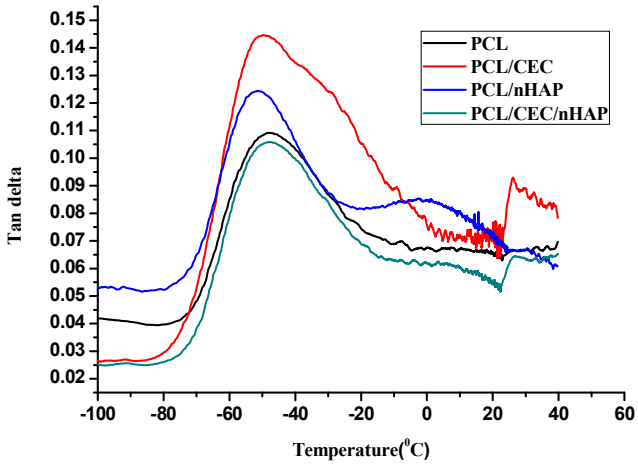

Figure 22. DMA analysis showing variation of tan delta of scaffolds with temperature

4.2.6. *In vitro* Hydrolytic Degradation Studies

SEM images (Figure 23) illustrates the effect of ageing in hydrolytic medium on the fibrous morphology of the scaffolds.

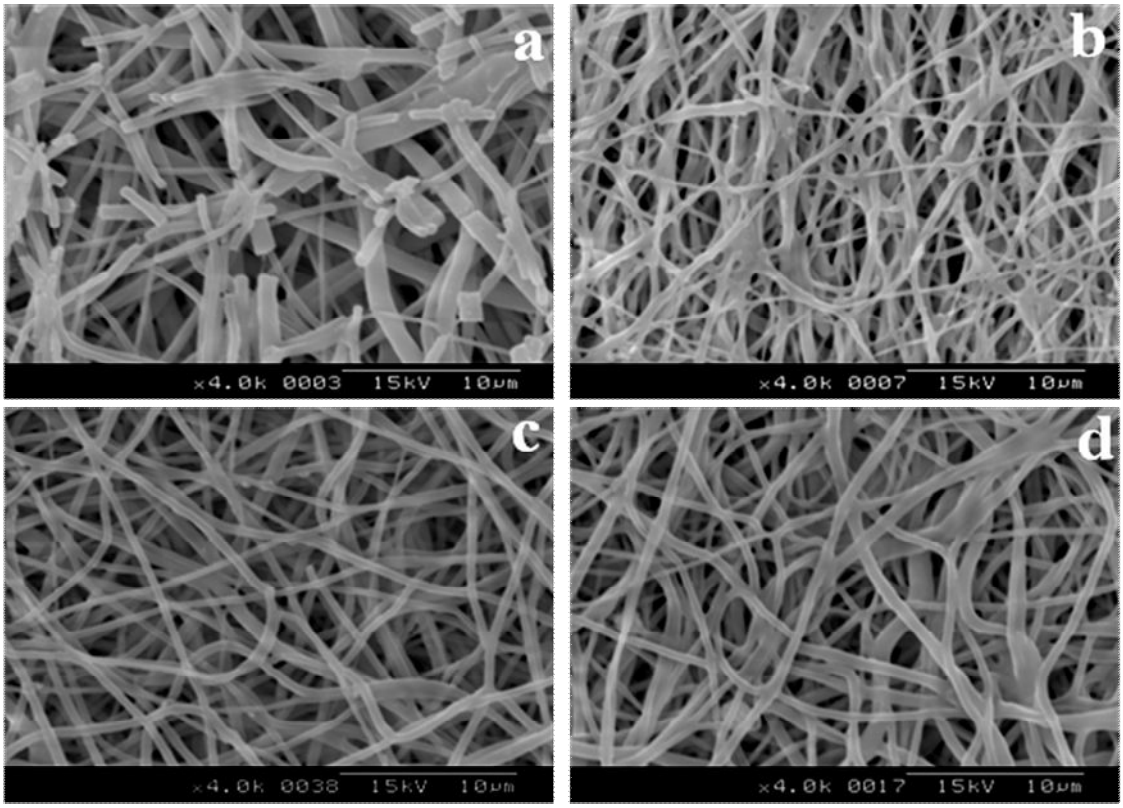

Figure 23. ESEM analysis showing effect of PBS ageing on morphology of scaffolds (a) PCL (b) PCL/CEC (c) PCL/nHAP and (d) PCL/CEC/nHAP

After 3 months of PBS ageing, thinning as well as rupture of fibers occurred indicating the biodegradation phenomenon. This was further confirmed by the significant drop in mechanical properties for all the scaffolds. On 3 months of PBS aging, the tensile strength of neat PCL decreased by 26%. The incorporation of CEC resulted in a decrease of strength by 40%. In the case of composite scaffolds, the

decrease in tensile strength was about 17% for PCL/nHAP and 35% for PCL/CEC/nHAP systems (Figure 24).

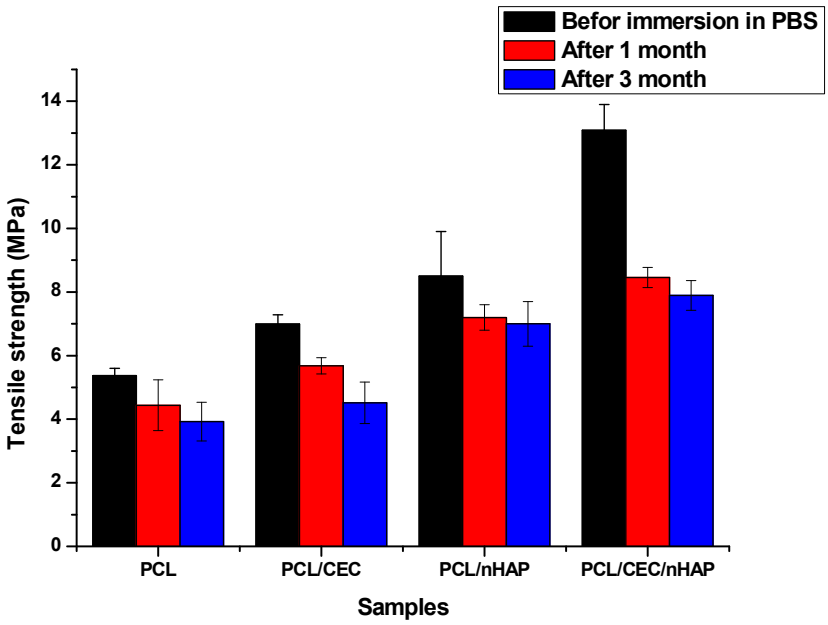

Figure 24. Effect of PBS ageing on tensile strength of scaffolds

4.2.7. Cytotoxicity Test: MTT Assay

Figure 25 shows the percentage metabolic activity of the L929 mouse fibroblast cells which were cultured with the extraction media in comparison with the control. All the scaffolds were found to be non-cytotoxic with more than 80% metabolic activity.

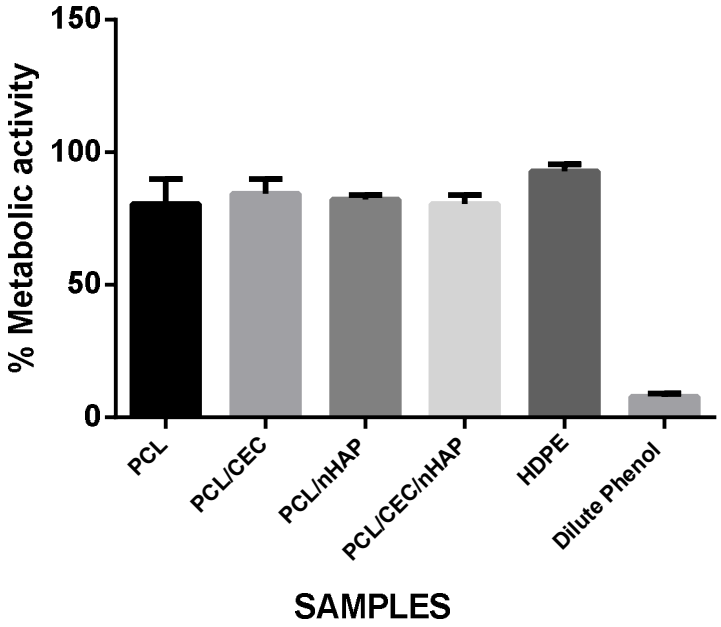

Figure 25. MTT assay on scaffolds

4.2.8. Cell Attachment Studies

The attachment of RADMSC on the scaffolds is shown in Figure 26. The cell morphology as well as the interaction between cells and scaffolds is well evident in the ESEM image. The cells that were cultured on the fibrous scaffolds expanded and stretched out to attach themselves on the fiber surface. After 2 h of cell seeding, SEM images depicted round morphology for the cells with few spread cells on all the scaffolds. The adhesion and spreading became more after 4 h seeding and the cells appeared well spread on all the scaffolds. Spreading of cells was more pronounced after 5 days of culture. The results suggested that the fibrous as well as porous nature of the scaffolds promote the attachment of RADMSCs. However in comparison with PCL, cells seeded on PCL/CEC/nHAP composite scaffold covered most of the pores and

formed a sheet like morphology. This indicates the better biocompatibility of the composite scaffold for attachment of RADMSCs.

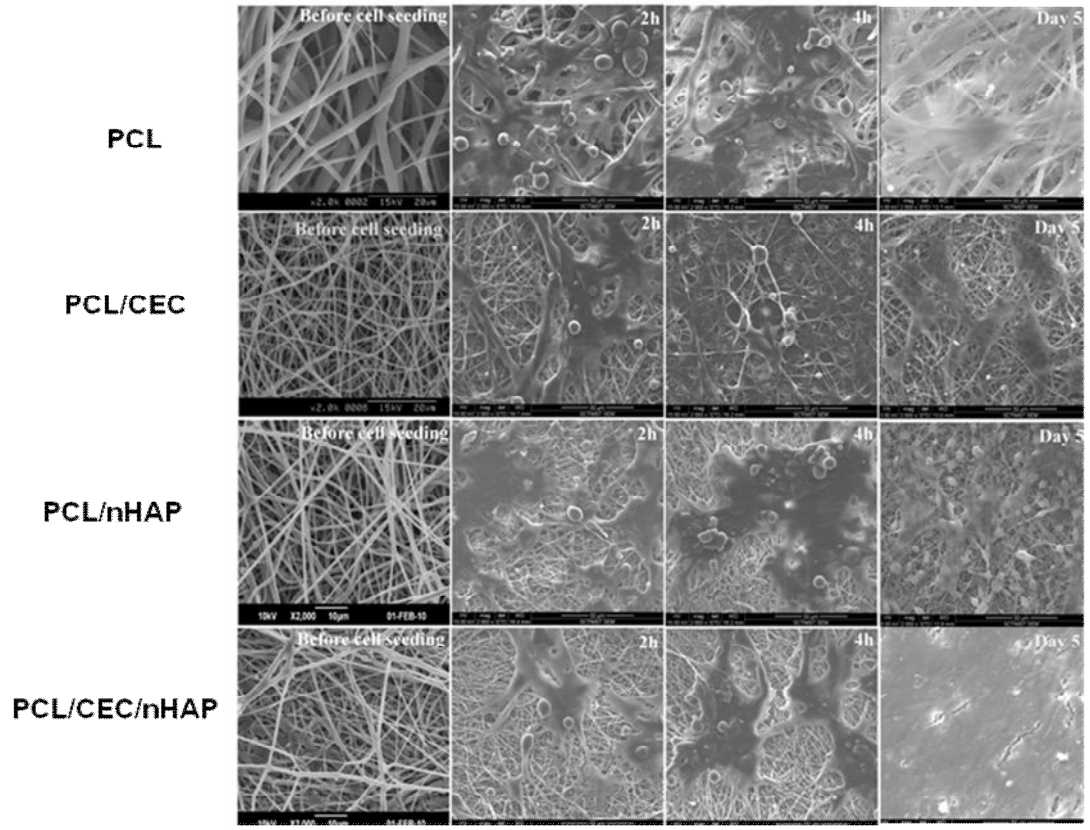

Figure 26. ESEM analysis showing adhesion of RADMSCs on scaffolds

4.2.9. Live/Dead Assay

The RADMSCs were viable on all the scaffolds as shown by the live dead staining (Figure 27). Acridine orange enters living cells that will appear bright green fluorescent, whereas ethidium bromide stains nuclei of dead cells orange. The elongated spindle morphology of the RADMSCs was also very well evident in the confocal images.

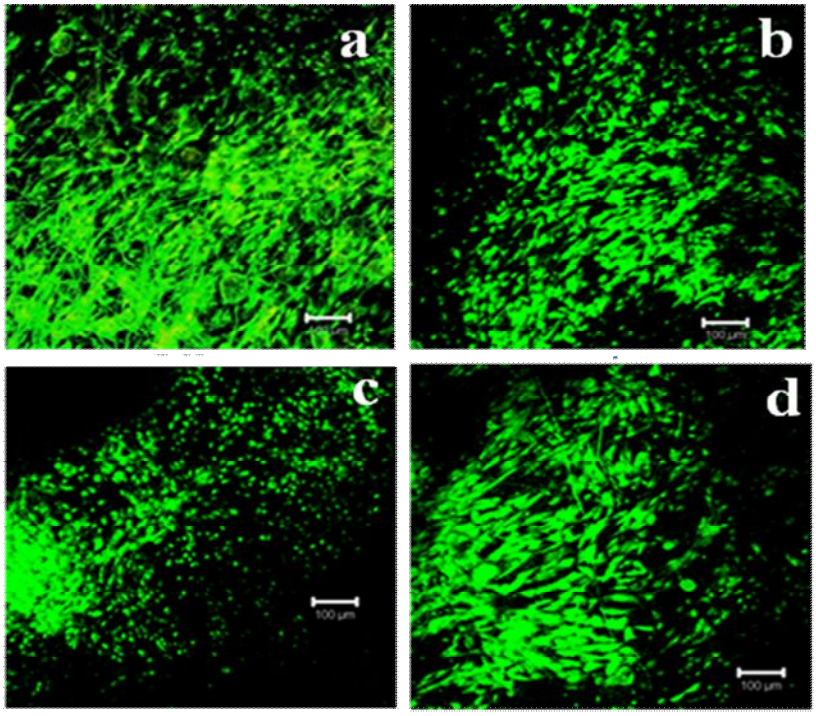

Figure 27. Live/ dead assay on scaffolds

(a) PCL (b) PCL/CEC (c) PCL/nHAP (d) PCL/CEC/nHAP

4.2.10. LDH Assay

Cell viability determined by LDH assay reveals the influence of both copolymer CEC and osteoconductive nHAP particles on PCL. Quantitative LDH activity measurement showed that all the scaffolds exhibited an increase in cell viability with culturing period (Figure 28). However, a significant increase was observed for PCL/CEC/nHAP scaffold at a later period of 28 days in comparison with other scaffolds.

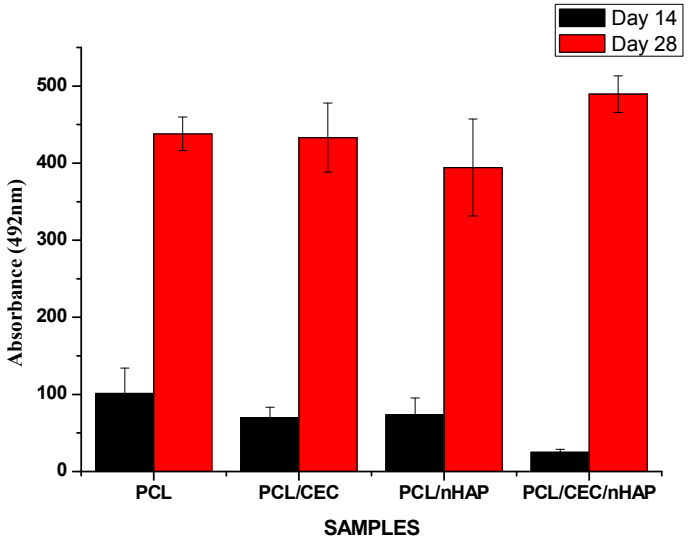

Figure 28. LDH assay on scaffolds

4.2.11. Picogreen assay

Cell proliferation determined by Picogreen assay further fortifies the results of LDH assay (Figure 29).

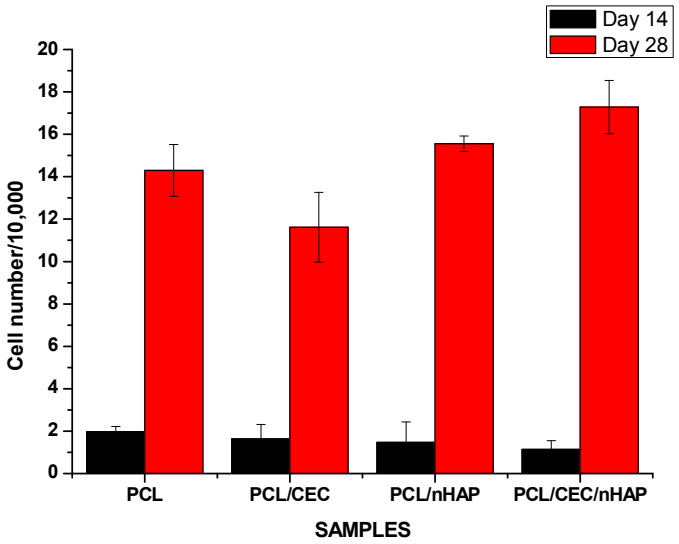

Figure 29. Picogreen assay on scaffolds

The results revealed that the cell number increased with increasing culturing period for all the scaffolds with PCL/CEC/nHAP scaffolds having a significant higher proliferation rate at a later period of 28 days when compared with other scaffolds. The enhanced proliferation of cells can be attributed to the scaffold's greater hydrophilicity (water contact angle dropped to zero), higher extent of degradation and the presence of osteoconductive nHAP.

4.2.10. Alkaline Phosphatase (ALP) activity of scaffolds

Confocal laser scanning micrographs depicted ALP activity of osteogenic induced cultured RADMSCs (Figure 30). Qualitative determination of ALP activity confirms the presence of osteogenic induced RADMSCs on all the scaffolds.

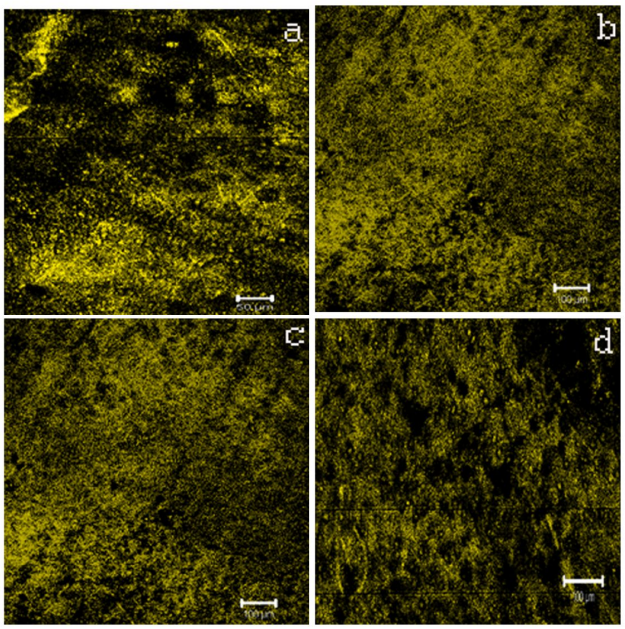

Figure 30. ALP activity of scaffolds

(a) PCL (b) PCL/CEC (c) PCL/nHAP (d) PCL/CEC/nHAP

4.3. Development and characterization of pamidronate (PDS) incorporated PCL based scaffolds

This section discusses the fabrication and characterization of pamidronate (PDS) incorporated PCL, PCL/CEC blend and PCL/CEC/nHAP composite scaffolds. The effect of PDS on the phyisco-mechanical and biological properties of PCL based scaffolds was analyzed in order to choose an appropriate scaffold for the *in-vivo* study.

4.3.1 Environmental scanning electron microscopy (ESEM) analysis

The morphology of PDS incorporated PCL based scaffolds observed using ESEM is depicted in Figure 31. All the scaffolds exhibited fibrous morphology characteristic of electrospinning process. The fiber diameter measured using image J analysis depicted that bare PCL scaffold exhibited non uniform fibers with an average fiber diameter of about 1.54 ± 0.5 μm. The PCL/CEC blend scaffold had an average fiber diameter of 0.40 ± 0.10 μm and the PCL/CEC/nHAP composite scaffolds exhibited an average fiber diameter of 0.37 ± 0.10 μm.

The conductivity of spinning dopes prior to spinning was also measured and the results are summarized in Table 8. The results indicated that the incorporation of CEC, nHAP and PDS has enhanced the solution conductivity of PCL which resulted in reduced fiber diameter. It was also observed that significant difference exist between fiber diameter of PCL and PDS incorporated PCL scaffolds (p value <0.001).

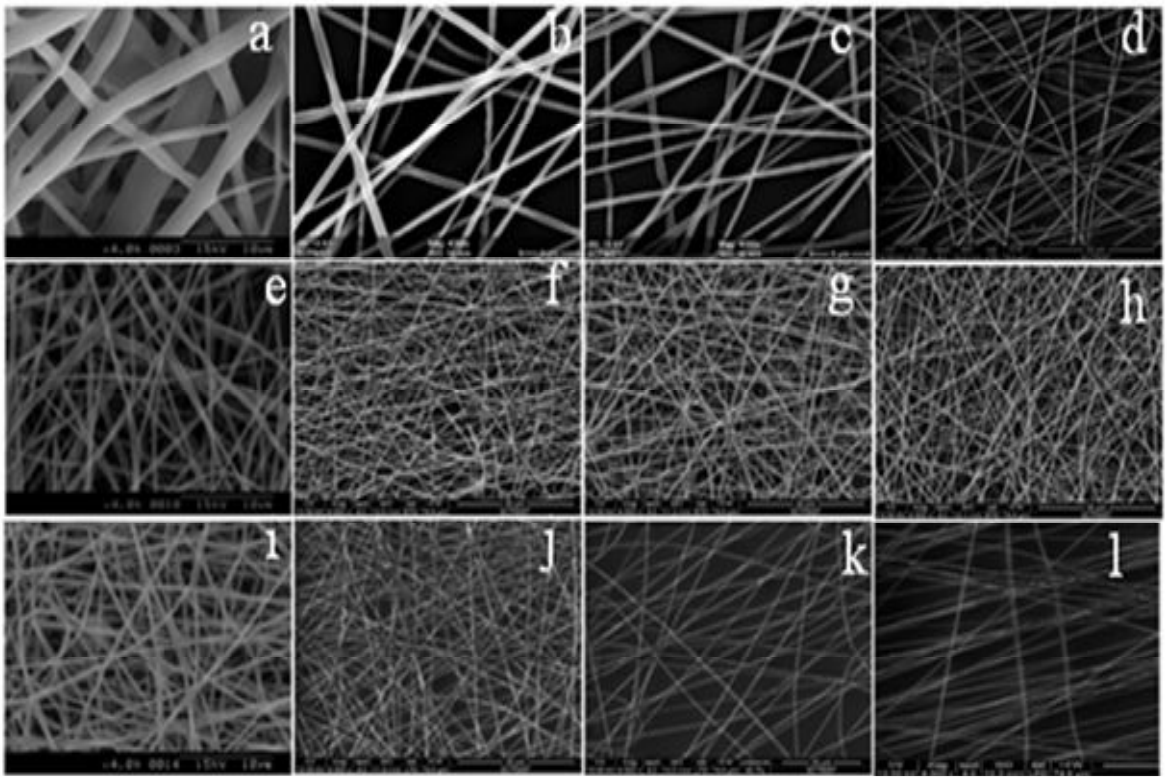

Figure 31. ESEM analysis showing morphology of PDS incorporated scaffolds (magnification: 4000x, scale bar = 10µm)

a. PCL **b.** PCL-PDS1 **c.** PCL-PDS3 **d.** PCL-PDS5**e.** PCL/CEC **f.** PCL/CEC-PDS1 **g.** PCL/CEC-PDS3 **h.** PCL/CEC-PDS5 **i.** PCL/CEC/nHAP **j.** PCL/CEC/nHAP-PDS1 **k.** PCL/CEC/nHAP-PDS3 **l.** PCL/CEC/nHAP-PDS5

Sample	Conductivity ($\mu S/cm^{-1}$)	Average fiber diameter (μm)
PCL	0.98 ± 0.05	1.53 ± 0.53
PCL-PDS1	5.40 ± 0.14	0.46 ± 0.20
PCL-PDS3	9.75 ± 0.21	0.42 ± 0.10
PCL-PDS5	9.85 ± 0.07	0.39 ± 0.10
PCL/CEC	2.87 ± 0.15	0.40 ± 0.10
PCL/CEC-PDS1	4.14 ±0.22	0.40 ± 0.20
PCL/CEC-PDS3	5.10 ± 0.48	0.30 ±.0.10
PCL/CEC-PDS5	9.91 ± 0.03	0.28 ± 0.20
PCL/CEC/nHAP	9.20 ± 0.05	0.37 ± 0.10
PCL/CEC/nHAP-PDS1	12.36 ± 0.20	0.33± 0.10
PCL/CEC/nHAP-PDS3	13.29 ± 0.07	0.30 ± 0.10
PCL/CEC/nHAP-PDS5	13.76 ± 0.14	0.32 ± 0.11

Table 8. Conductivity of spinning dopes and average fiber diameter of scaffolds

For PCL scaffolds, incorporation of PDS resulted in formation of smooth uniform beadless fibers with narrow fiber diameter distribution. The fiber diameter of PCL/PDS scaffolds varied in the range of 0.4-0.45 μm and no significant difference in fiber diameter exist between PDS incorporated scaffolds (p value = 0.4046). The average fiber diameter of PCL-PDS1, PCL-PDS3 and PCL-PDS5 was of 0.46 ± 0.2 μm, 0.42 ± 0.1 μm and 0.39 ± 0.10 μm respectively.

In case of PCL/CEC blend scaffolds, PDS incorporation resulted in formation of smooth bead free fibers with fiber diameter varying from 0.3-0.4 μm. The fiber diameter

of PCL/CEC blends reduced significantly with the incorporation of PDS (p value = 0.0001). The PCL/CEC-PDS1 scaffolds had an average fiber diameter of 0.4 ± 0.2 µm and that of PCL/CEC-PDS3 exhibited fiber diameter of 0.3 ±.0.1 µm. Significant difference in fiber diameter exist between PCL/CEC-PDS1 and PCL/CEC-PDS3 scaffolds (p value = 0.0153) and that of PCL/CEC-PDS1 and PCL/CEC-PDS5 scaffolds (p value = 0.013). The PCL/CEC-PDS5 scaffold had an average fiber diameter of 0.28 ± 0.2 µm. No significant difference exist in fiber diameter between PCL/CEC-PDS3 and PCL/CEC-PDS5 scaffolds (p value = 0.4430).

The fiber diameter of PCL/CEC/nHAP scaffolds was of 0.37 ± 0.10 µm. The fiber diameter of PCL/CEC/nHAP-PDS composite scaffolds varied from 0.3-0.37µm with PCL/CEC/nHAP-PDS1, PCL/CEC/nHAP-PDS3 and PCL/CEC/nHAP-PDS5 scaffolds having fiber diameter of about 0.33 ± 0.10 µm, 0.30 ± 0.1 and 0.32 ± 0.11 µm respectively. No significant difference observed in fiber diameter among PDS incorporated scaffolds (p value 0.0001)

4.3.2. Porosity evaluation using liquid intrusion method

The porosity evaluation using liquid intrusion method revealed that all the scaffolds were porous in nature with more than 80% porosity (Table 9). The bare scaffold exhibited increased porosity; however PDS incorporation has slightly lowered the porosity which may be due to the lower fiber diameter of PDS loaded scaffolds which resulted in effective fiber packing.

Sample	Porosity (%)
PCL	89 ± 0.8
PCL-PDS1	80 ± 3.1
PCL-PDS3	83 ± 0.3
PCL-PDS5	84 ± 0.2
PCL/CEC	82 ± 1.4
PCL/CEC-PDS1	80 ± 0.3
PCL/CEC-PDS3	82 ± 0.8
PCL/CEC-PDS5	85 ± 0.3
PCL/CEC/nHAP	79 ± 6.2
PCL/CEC/nHAP-PDS1	79± 1.9
PCL/CEC/nHAP-PDS3	76 ± 2.4
PCL/CEC/nHAP-PDS5	71 ± 1.6

Table 9. Porosity of scaffolds determined using liquid intrusion method

4.3.3. Surface wetting property by contact angle measurements

The inherent hydrophobic nature of PCL is depicted by its higher water contact angle of 97 ± 10º (Figure 32). Both PCL/CEC and PCL/CEC/nHAP scaffolds were found to be hydrophilic in nature with complete wetting of scaffolds. In case of PCL/PDS scaffolds, the incorporation of hydrophilic PDS has altered the surface wetting property of PCL which is reflected by the drop in the contact angle value with increasing PDS content. The PCL-PDS5 scaffolds exhibited contact angle value of 36 ± 4º indicating hydrophilic nature of PDS incorporated scaffolds. Both PCL/CEC-PDS and

PCL/CEC/nHAP-PDS scaffolds were found to be hydrophilic with water contact angle almost zero.

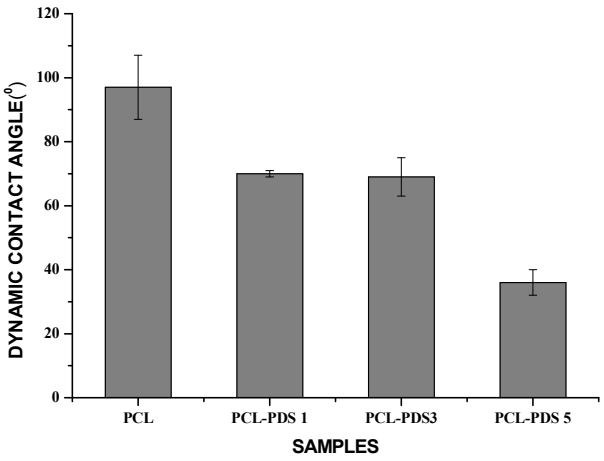

Figure 32. Contact angle of PCL & PCL-PDS scaffolds

4.3.4. Static mechanical properties using UTM

The PDS incorporated scaffolds demonstrated improved tensile properties on comparison with the bare scaffolds. The data obtained from UTM is summarized in Table 10. The tensile strength of PCL scaffolds was about 5.3 ± 0.2 MPa which was found to increase with the incorporation of PDS. The PCL-PDS scaffolds exhibited tensile strength in the range of 13 MPa. For PCL/CEC scaffolds, the tensile strength was about 7.0 ± 0.3MPa which was found to increase to 11 MPa with PDS incorporation. The PCL/CEC/nHAP composite scaffold exhibited tensile strength of 13.08 ± 0.8MPa which was found to increase to 15.02 ± 0.5 MPa for PCL/CEC/nHAP-PDS3 scaffolds. The PCL/CEC/nHAP-PDS5 composite scaffolds exhibited tensile strength of 11.00 ± 0.7 MPa.

Sample	Tensile strength (MPa)	Elongation at break (%)	Youngs modulus (MPa)
PCL	5.3 ± 0.20	144. ± 17	34 ± 1.9
PCL-PDS1	13.5 ± 1.60	174 ± 10	23 ± 5.8
PCL-PDS3	13.7 ± 0.04	172 ± 0.4	29 ± 5.9
PCL-PDS5	13.4 ± 0.16	186 ± 5.3	34 ± 5.3
PCL/CEC	7.0 ± 0.30	111 ± 62	19 ± 2
PCL/CEC-PDS1	11.2 ± 0.22	113 ± 20	23 ± 1.3
PCL/CEC-PDS3	11.4 ± 0.05	143 ± 28	17 ± 2.7
PCL/CEC-PDS5	11.5 ± 1.50	132 ± 56	20 ± 2.8
PCL/CEC/nHAP	13.12 ± 0.80	189 ± 42	17 ± 1.8
PCL/CEC/nHAP -PDS1	13.30 ± 0.45	111 ± 42	23 ± 4.4
PCL/CEC/nHAP -PDS3	15.02 ± 0.54	161 ± 68	32 ± 5.6
PCL/CEC/nHAP -PDS5	11.00 ± 0.71	129 ± 23	18 ± 4.4

Table 10. Static mechanical properties of scaffolds

4.3.5. Dynamic mechanical properties using DMA

The temperature dependence of storage modulus of PDS incorporated PCL scaffolds are depicted in Figure 33. The storage modulus of PDS incorporated scaffolds at 37 °C was higher than that of PCL scaffolds. For PCL scaffolds, the storage modulus at 37 °C was found to be 8.1 MPa , whereas for the PDS incorporated scaffolds storage modulus was of 14.3 MPa, 14.6MPa and 15.3 MPa for PCL-PDS1, PCL-PDS3 and PCL-PDS5 scaffolds respectively.

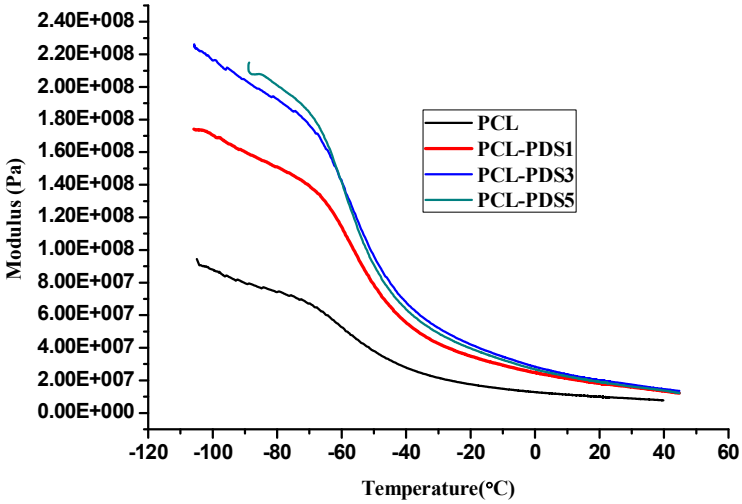

Figure 33. DMA analysis showing variation of storage modulus of PCL and PCL-PDS scaffolds with temperature

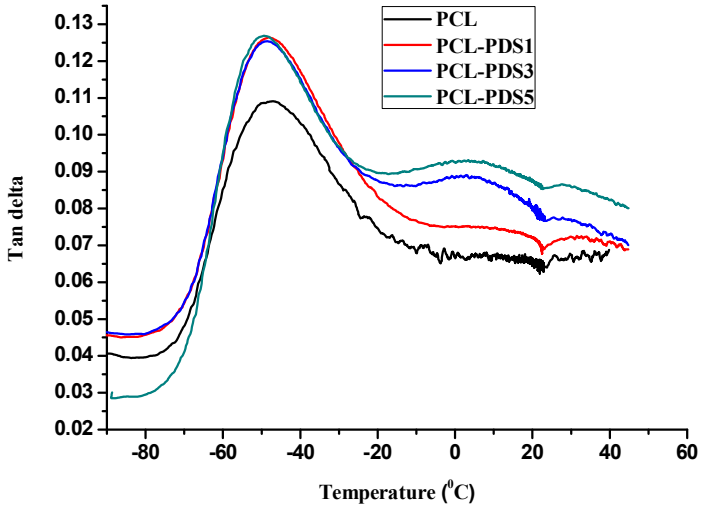

Figure 34. DMA analysis showing variation of tan delta of PCL and PCL-PDS scaffolds with temperature

Figure 34 represents the variation of tan delta of PDS incorporated PCL scaffolds. The PCL scaffold exhibited glass transition temperature (Tg) at - 47.7°C. The observed Tg values for PCL-PDS1, PCL-PDS3 and PCL-PDS5 scaffolds are - 48.2°C, - 48.7.°C and -49.2°C respectively.

The temperature dependence of storage modulus of PDS incorporated PCL/CEC blend scaffold is shown in Figure 35. The storage modulus of PCL/CEC blend scaffolds at 37 °C was higher than that of the PDS incorporated scaffolds. The storage modulus at 37 °C for PCL/CEC blend was found to be 9.5 MPa whereas for the PDS incorporated scaffolds the storage modulus was of 7.8 MPa, 6.3 MPa and 4.3 MPa for PCL/CEC-PDS1, PCL/CEC -PDS3 and PCL/CEC -PDS5 scaffolds respectively.

The temperature dependence of tan delta of PDS incorporated PCL/CEC blend scaffold is shown in Figure 36. The broadening of tan delta peak was observed with the incorporation of CEC on to PCL scaffolds. The PCL/CEC blend scaffold exhibited Tg around - 49.4°C whereas for PDS incorporated scaffolds increment in Tg was observed. The Tg values observed for PCL/CEC-PDS1 scaffolds was about - 44.5°C, and - 46.8 °C for PCL/CEC-PDS3 scaffolds and that of - 46.2.°C for PCL/CEC-PDS5 scaffolds.

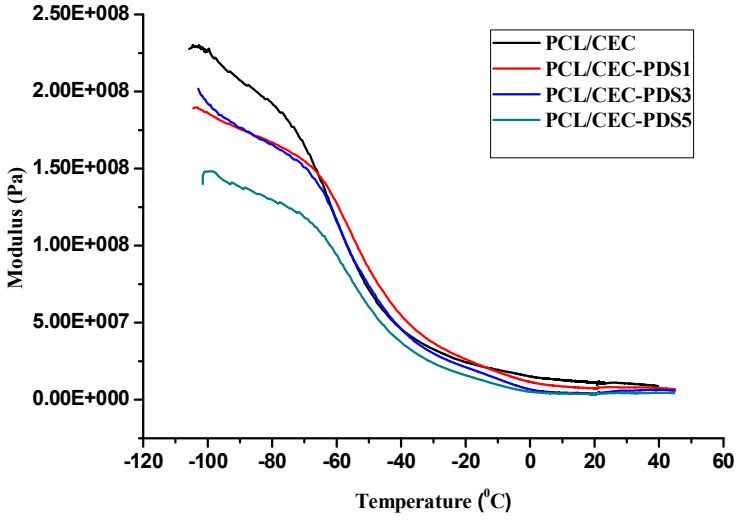

Figure 35. DMA analysis showing variation of storage modulus of PCL and PCL/CEC-PDS scaffolds with temperature

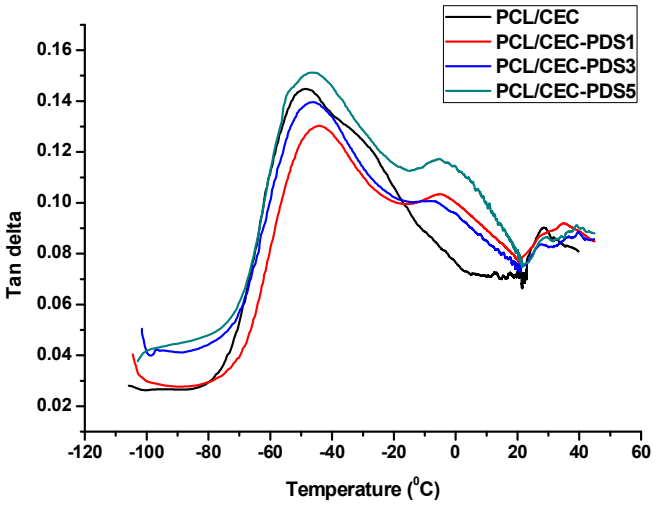

Figure 36. DMA analysis showing variation of tan delta of PCL and PCL/CEC-PDS scaffolds with temperature

The variation of storage modulus of PCL/CEC/nHAP composite scaffolds is represented in Figure 37. The storage modulus of PCL/CEC/nHAP scaffold at 37 °C was higher than that of PDS incorporated scaffolds. The storage modulus of PCL/CEC/nHAP composite scaffold was of 10.4 MPa whereas for the PDS incorporated scaffolds storage modulus was of 6.4 MPa, 7.4 MPa and 8.1 MPa for PCL/CEC/nHAP-PDS1, PCL/CEC/nHAP-PDS3 and PCL/CEC/nHAP-PDS5 scaffolds respectively.

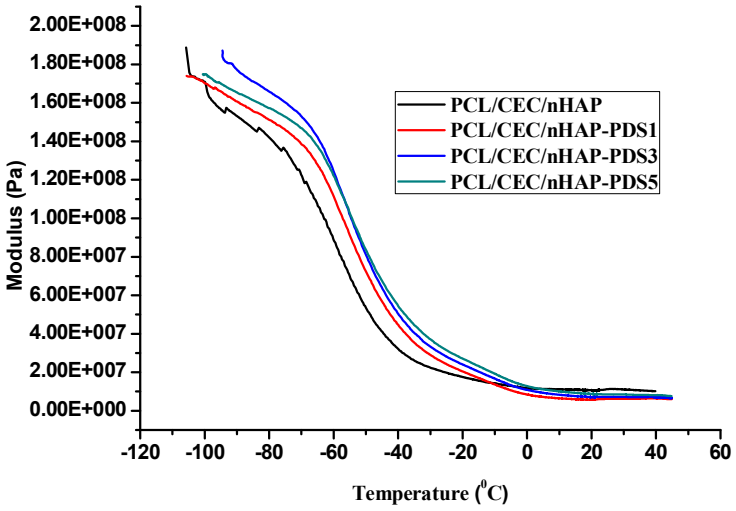

Figure 37. DMA analysis showing variation of storage modulus of PCL/CEC/nHAP and PCL/CEC/nHAP -PDS scaffolds with temperature

The temperature dependence of tan delta with temperature for PDS incorporated PCL/CEC/nHAP composite scaffolds is represented in Figure 38. The broadening of tan delta peak was also observed for the PCL/CEC/nHAP scaffolds. The PCL/CEC/nHAP composite scaffold exhibited Tg at - 47.4 °C whereas for PDS incorporated scaffolds increment in Tg was observed. The Tg values observed for PCL/CEC/nHAP-PDS1

scaffolds was about - 43.8°C, - 44.4°C for PCL/CEC/nHAP-PDS3 scaffolds and that of - 43.2.°C for PCL/CEC/nHAP-PDS5 scaffolds.

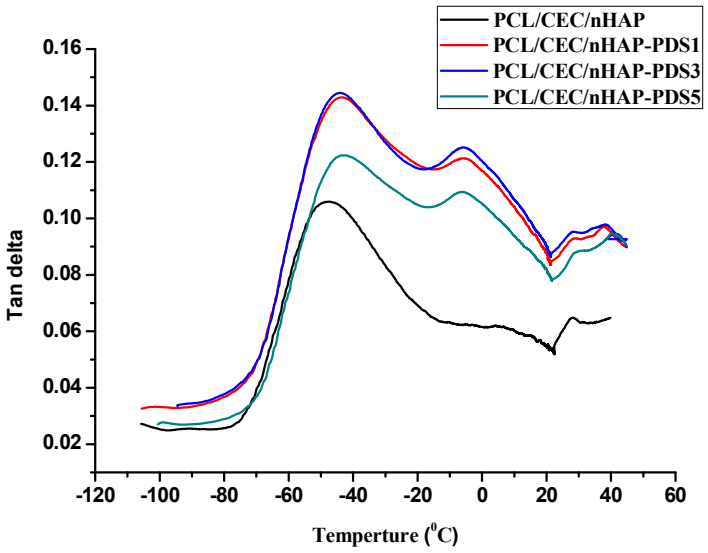

Figure 38. DMA analysis showing variation of tan delta of PCL/CEC/nHAP and PCL/CEC/nHAP-PDS scaffolds with temperature

4.3.6. *In vitro* release studies of PDS

The release profile of PDS from PCL, PCL/CEC and PCL/CEC/nHAP scaffolds is shown in figures 39 to 40. An initial burse release of PDS was observed from all the scaffolds for the first few hours. The amount of PDS released depends on the polymer composition as well as on the initial concentration of PDS and its distribution within the scaffold. The amount of PDS released form PCL scaffolds after 21 days were 197 µg/ml, 259 µg/ml and 290 µg/ml respectively for 1, 3 and 5 wt% PDS scaffolds. The PCL-PDS5 exhibited higher release rate compared to that of PCL-PDS1 and PCL-PDS3 scaffolds.

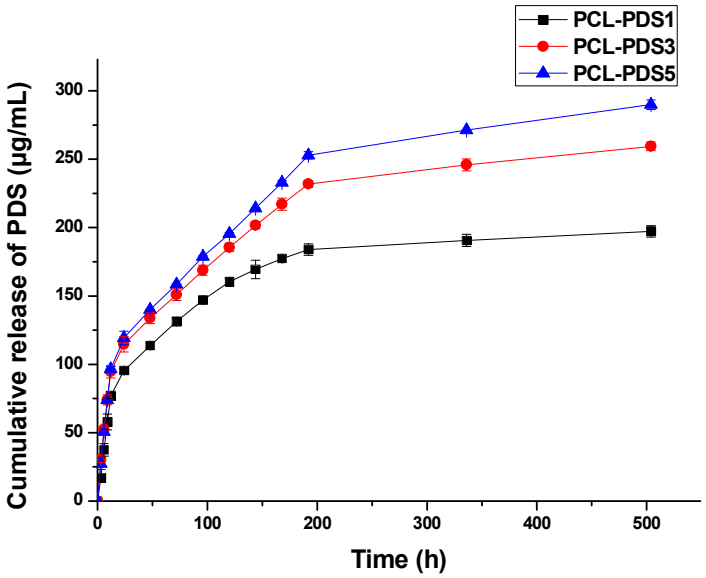

Figure 39. *In-vitro* release studies of PDS from PCL scaffolds

In case of PCL/CEC scaffolds, the amount of PDS released after 21 days were 245 µg/ml, 316 µg/ml and 324 µg/ml respectively for 1, 3 and 5 wt% PDS scaffolds. The PCL/CEC-PDS5 exhibited higher release rate compared to that of PCL/CEC-PDS1 and PCL/CEC-PDS3 scaffolds.

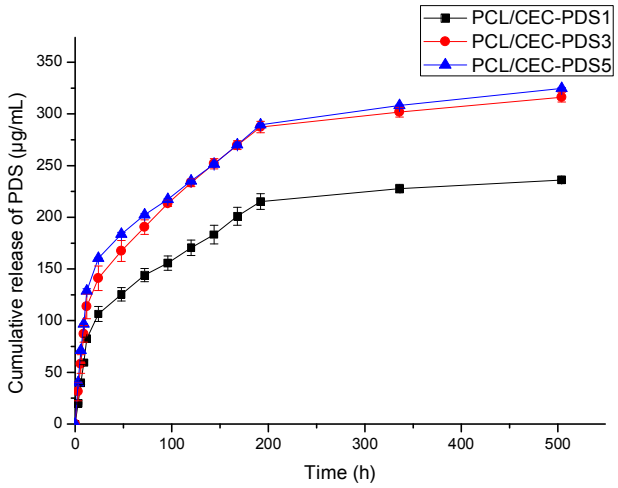

Figure 40. *In vitro* release studies of PDS from PCL/CEC blend scaffolds

For PCL/CEC/nHAP composite scaffolds, the amount of PDS released after 21 days were 214 µg/ml, 246 µg/ml and 265 µg/ml respectively for 1, 3 and 5 wt% PDS scaffolds. The PCL/CEC/nHAP -PDS5 exhibited higher release rate compared to that of PCL/ CEC/nHAP –PDS1 and PCL/ CEC/nHAP –PDS3 scaffolds.

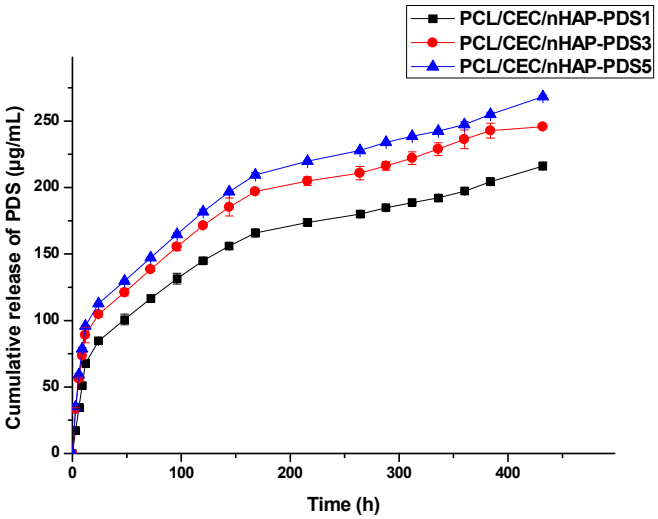

Figure 41. *In vitro* release studies of PDS from PCL/CEC/nHAP scaffolds

4.3.7 *In vitro* degradation studies in PBS

The effect of PBS ageing on bare and PDS incorporated scaffolds is depicted in Figure 42.

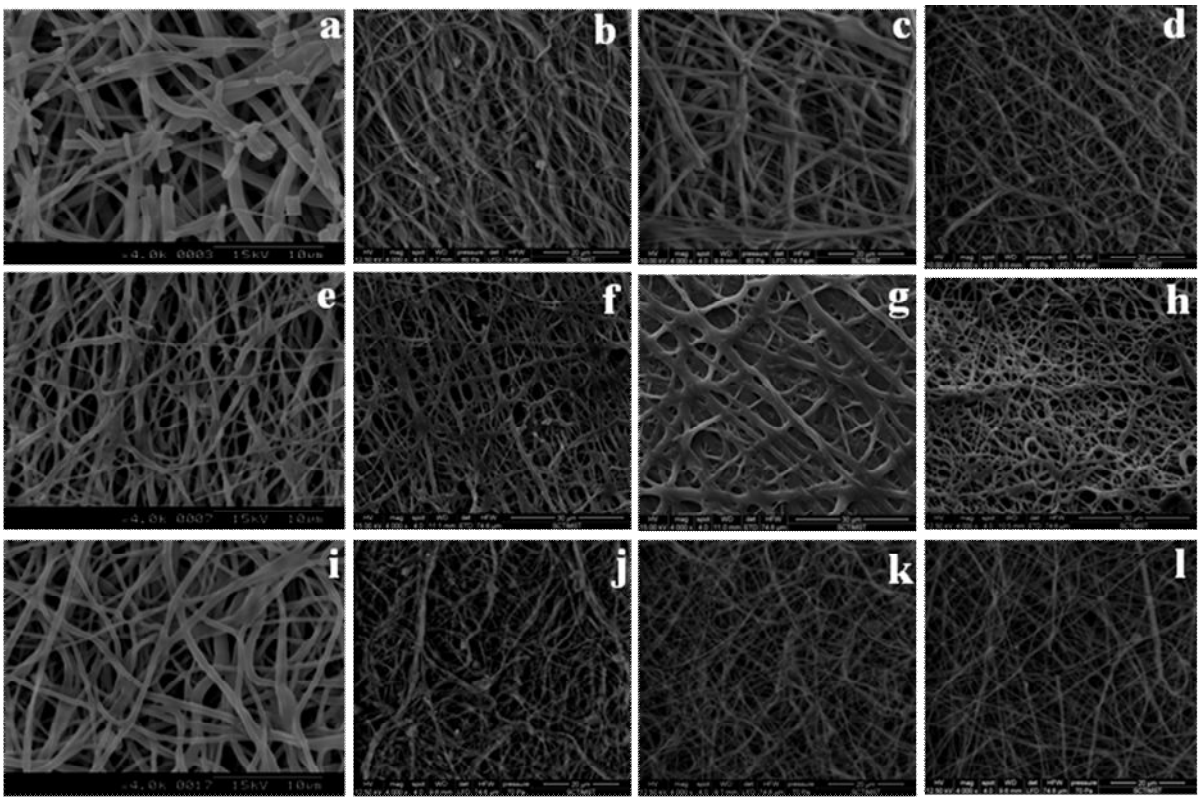

Figure 42. ESEM images showing fiber rupture after 3 months of PBS aging

a. PCL **b.** PCL-PDS1 **c.** PCL-PDS3 **d.** PCL-PDS5

e. PCL/CEC **f.** PCL/CEC-PDS1 **g.** PCL/CEC-PDS3 **h.** PCL/CEC-PDS5

i. PCL/CEC/nHAP **j.** PCL/CEC/nHAP-PDS1 **k.** PCL/CEC/nHAP-PDS3

l. PCL/CEC/nHAP-PDS5

The degradation behavior is well evident from the morphological changes occurred in scaffolds which is depicted by the ESEM images showing the fiber thinning and rupture. This was further supported by the drop in tensile strength observed after 90 days of PBS ageing. After 3 months of PBS ageing, in case of PCL scaffolds, the drop in tensile strength was of 26% (Figure 43-45). Compared to bare PCL scaffolds, drop in tensile strength was more prominent on PDS incorporated scaffolds. It was observed that drop in tensile strength was of 30% for PCL-PDS1, 56% for PCL-PDS3 and 68% for PCL-PDS5 scaffolds. For PCL/CEC blend scaffolds, drop in tensile strength observed after 3 months of PBS ageing was of 35%. The drop in tensile strength was of 52%, 67% and 77% for PCL/CEC-PDS1, PCL/CEC-PDS3 and PCL/CEC-PDS5 scaffolds. The drop in tensile strength observed for PCL/CEC/nHAP composite scaffolds was of 40%. It was observed that drop in tensile strength was of 47% for PCL/CEC/nHAP-PDS1, 51% for PCL/CEC/nHAP-PDS3 and 55% for PCL/CEC/nHAP-PDS5 scaffolds.

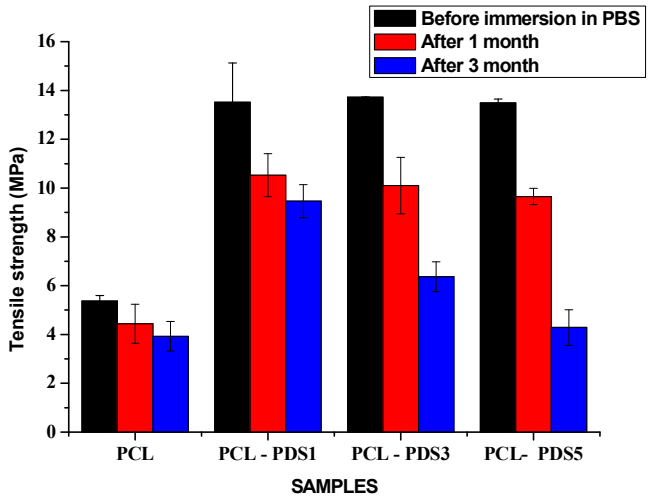

Figure 43. Tensile strength of PCL-PDS scaffolds after 3 months of PBS ageing

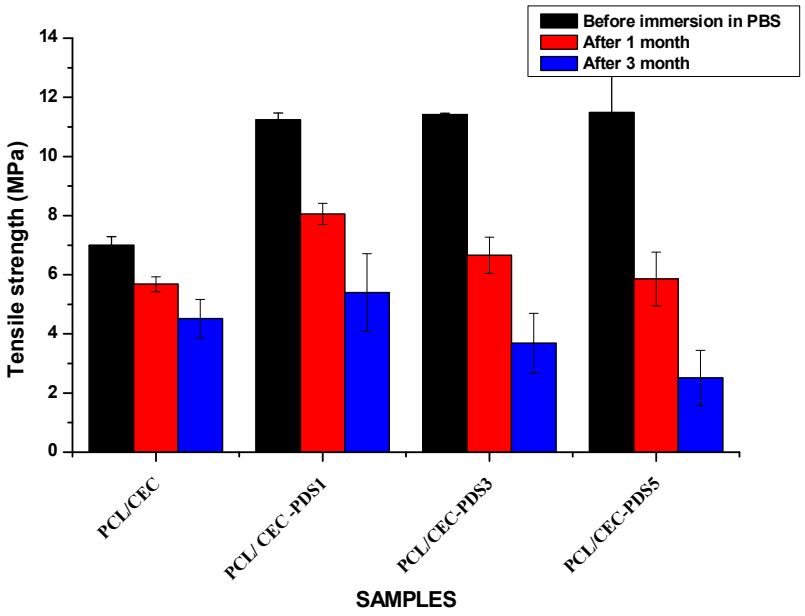

Figure 44 Tensile strength of PCL/CEC-PDS scaffolds after 3 months of PBS ageing

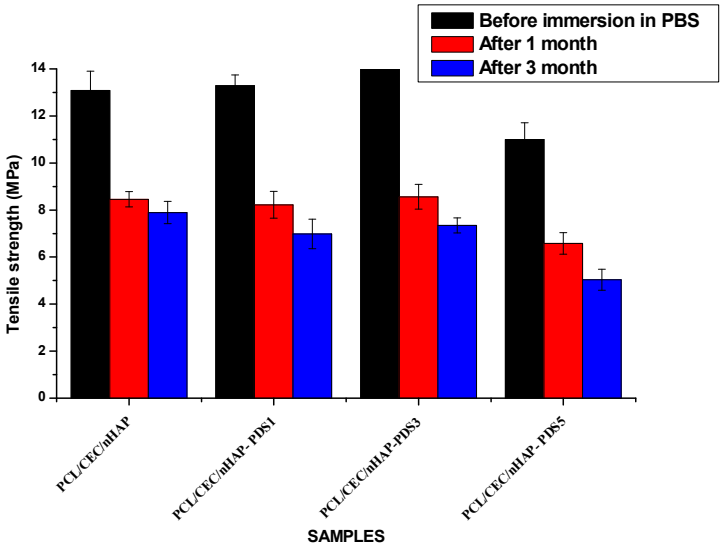

Figure 45 Tensile strength of PCL/CEC/nHAP-PDS scaffolds after 3 months PBS ageing

4.3.8. *In vitro* cell culture studies using human osteosarcoma (hOS) cell lines

4.3.8.1. Live/dead assay

The viability of hOS cells on PDS incorporated PCL scaffolds were analyzed using FDA /PI staining (Figure 46) in which the cytoplasm of the live cells stained with FDA appears green and that of nucleus of the dead cells stained with PI appears red.

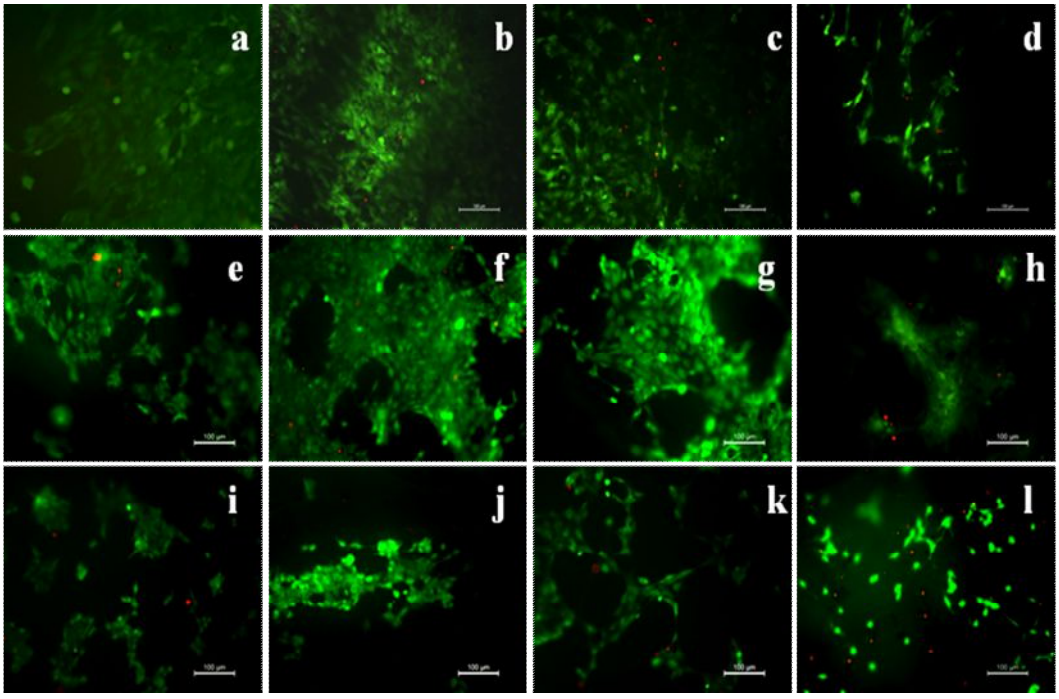

Figure 46. FDA/PI staining after 48 h showing viability of hOS cells on scaffolds (scale bar = 100 µm)

a. PCL **b.** PCL-PDS1 **c.** PCL-PDS3 **d.** PCL-PDS5

e. PCL/CEC **f.** PCL/CEC-PDS1 **g.** PCL/CEC-PDS3 **h.** PCL/CEC-PDS5

i. PCL/CEC/nHAP **j.** PCL/CEC/nHAP-PDS1 **k.** PCL/CEC/nHAP-PDS3

l. PCL/CEC/nHAP-PDS5

It was observed that hOS cells adhered well on both bare as well as PDS incorporated scaffolds (especially on scaffolds with PDS1 and PDS3). The assay revealed that majority of the adhered cells were viable (green) thus proving the cytocompatibility of scaffolds towards hOS cells. However, at higher PDS content, i.e, on scaffolds with PDS5, cells lost their characteristic spindle morphology which is well evident in the fluorescent microscopic images.

4.3.8.2. MTT assay

MTT assay (Figure 47), further fortify the results of live/dead assay showing that all the scaffolds supported cell proliferation with ~100 % metabolic activity especially in PDS incorporated scaffolds which further prove their non toxicity of scaffolds towards hOS cells. The metabolic activity of hOS cells were not affected even after 48 h of incubation. It was observed that in case of PCL-PDS scaffolds, significant difference exists in cell viability between PCL and PCL-PDS scaffolds (p value = 0.0004). On comparison among PCL-PDS scaffolds, no significant difference exist in cell viability between PCL-PDS1 and PCL-PDS5 scaffolds (p value = 0.07406) whereas significant difference exist between PCL-PDS1 and PCL-PDS3 (p value= 0.0057), PCL-PDS3 and PCl-PDS5 (p value= 0.0082) scaffolds. The PCL-PDS3 scaffolds exhibited higher percentage of metabolic activity.

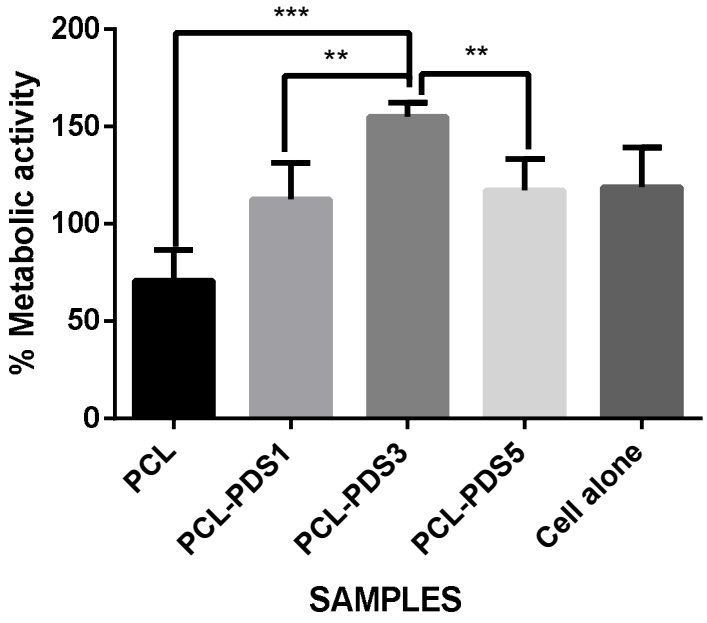

Figure 47. MTT assay using hOS cells on PCL & PCL-PDS scaffolds

In case of PCL/CEC-PDS scaffolds (Figure 48), all the scaffolds exhibited metabolic activty of ~ 100% and no significant difference in cell viability was obseved among bare PCL/CEC and PCL/CEC-PDS scaffolds (p value = 0.7935) as well as among PCL/CEC-PDS scaffolds (p value = 0.8549).

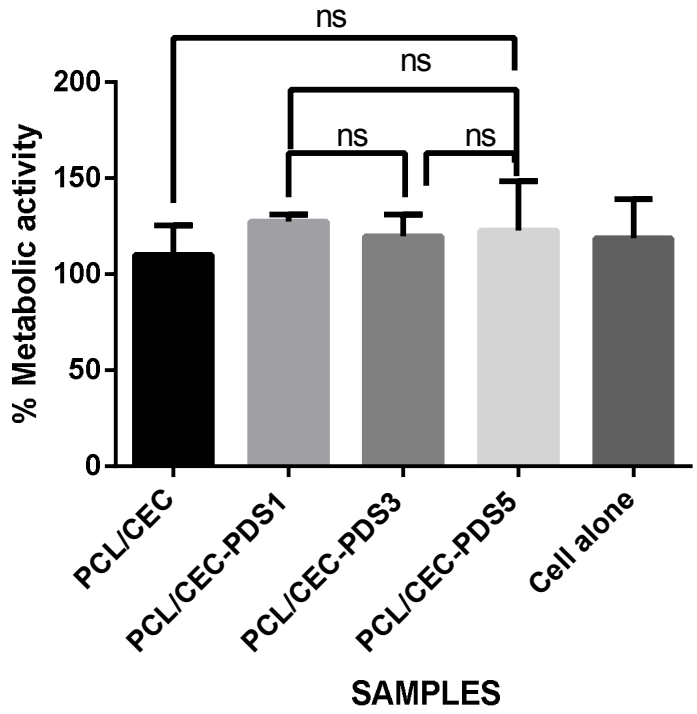

Figure 48. MTT assay scaffolds using hOS cells on PCL & PCL/CEC-PDS scaffolds

In case of PCL/CEC/nHAP scaffolds also (Figure 49), % metabolic activity was higher for PDS incorporated scaffolds and significant difference exist in cell viability among bare PCL/CEC/nHAP and PCL/CEC/nHAP-PDS scaffolds (p value = 0.0237) as well as among PCL/CEC/nHAP-PDS scaffolds (p value = 0.0453). On comparison among PCL/CEC/nHAP-PDS scaffolds, no significant difference exist in cell viability between PCL/CEC/nHAP-PDS1 and PCL/CEC/nHAP-PDS5 scaffolds (p value = 0.9381) as well between PCL/CEC/nHAP-PDS3 and PCL/CEC/nHAP-PDS5 scaffolds (p value = 0.0585) whereas significant difference exist between PCL/CEC/nHAP-PDS1 and PCL/CEC/nHAP-PDS3 (p value= 0.0071), PCL/CEC/nHAP and PCL/CEC/nHAP-

PDS3 scaffolds (p value= 0.0021). The percentage metabolic activity was higher for the PCL/CEC/nHAP-PDS3 composite scaffolds.

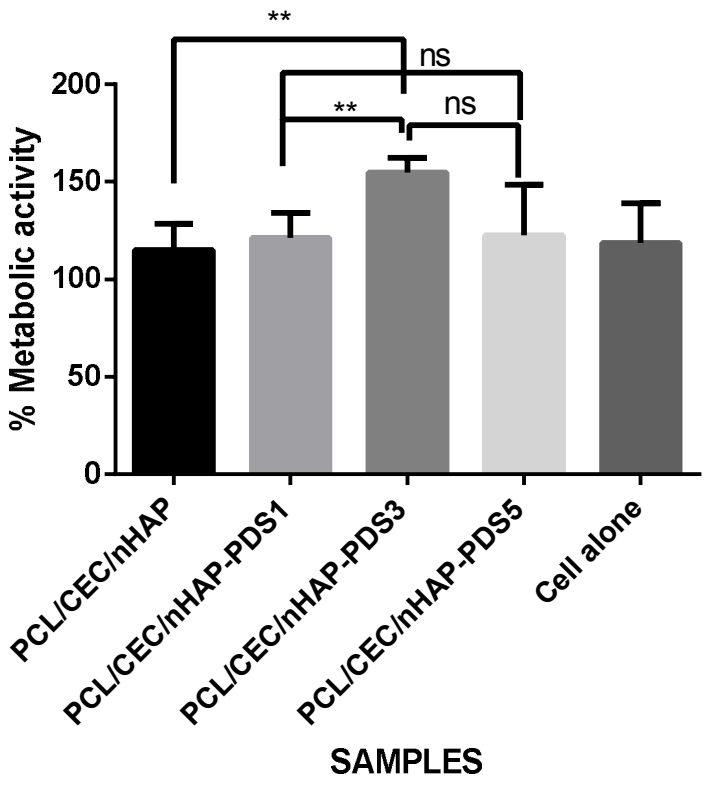

Figure 49. MTT assay using hOS cells on PCL/CEC/nHAP & PCL/CEC/nHAP-PDS scaffolds

4.3.9. *In vitro* cell culture studies rats adipose derived mesenchymal stem cells (rADMSC)

Based on the physico-mechanical properties, the PCL/CEC/nHAP composite scaffolds were selected for further *in-vitro* cytocompatibility evaluation using rat's adipose derived mesenchymal stem cells (rADMSC). Rat ADMSCs were chosen for the

study since the potential of the scaffolds has to be evaluated under *in vivo* conditions in a rat animal model.

4.3.9.1. MTT assay

The results of MTT assay (using un-induced rADMScs (Figure 50) after 24h revealed that all the scaffolds were found to be cytocompatible with more than 90% metabolic activity.

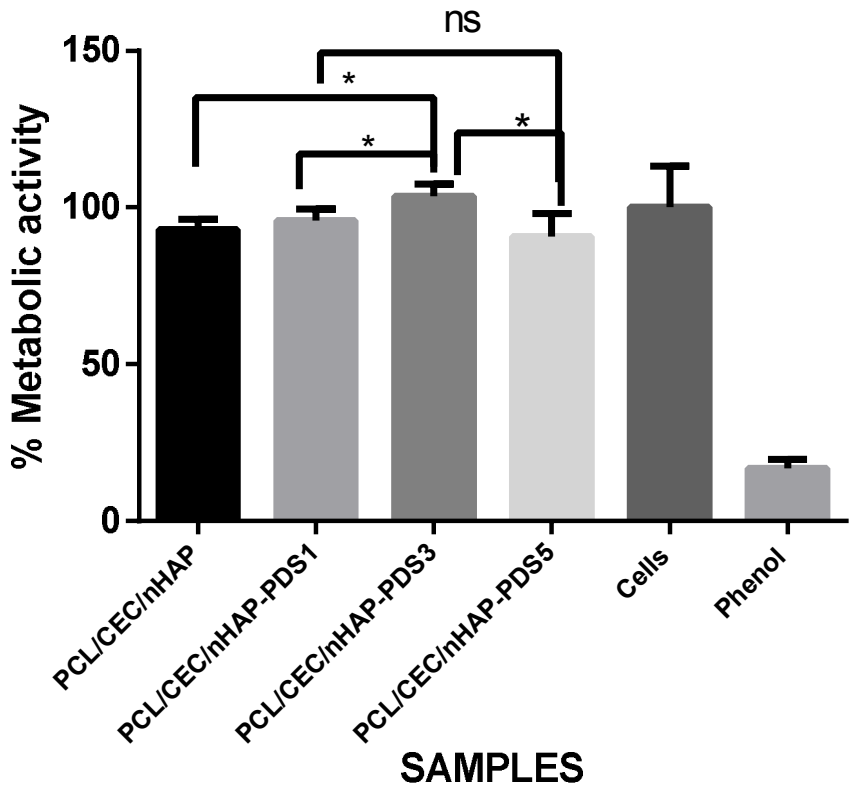

Figure 50. MTT assay using un-induced rADMSCs on PCL/CEC/nHAP-PDS PCL/CEC/nHAP-PDS scaffolds

The percentage metabolic activity was more pronounced on PCL/CEC/nHAP-PDS scaffolds than that of PCL/CEC/nHAP scaffold (p value = 0.0203). On comparison among PCL/CEC/nHAP-PDS scaffolds, significant difference exist in metabolic activity among PCL/CEC/nHAP-PDS1 and PCL/CEC/nHAP-PDS3 (p value = 0.0193) scaffolds as well as between PCL/CEC/nHAP-PDS3 and PCL/CEC/nHAP-PDS5 (p value = 0.0280). However no significant difference in viability was observed between PCL/CEC/nHAP-PDS1 and PCL/CEC/nHAP-PDS5 scaffolds (p value = 0.1519).

4.3.9.2. Live/dead assay

The rADMSCs adhered on the scaffolds and were found to be viable as depicted actin staining (Figure 51). The cells exhibited their characteristic spindle morphology on all the scaffolds except on PCL/CEC/nHAP-PDS5.

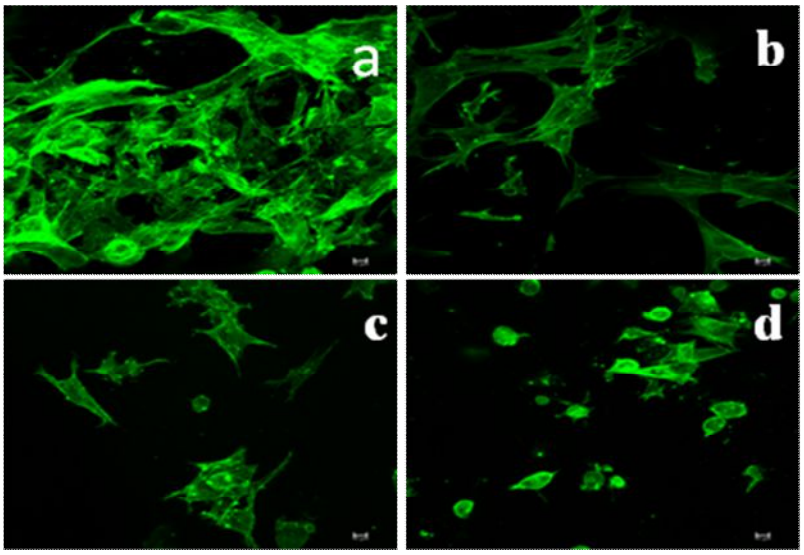

Figure 51. Actin staining showing adhesion and morphology of rADMSCs on scaffolds (scale bar = 10 µm) a. PCL/CEC/nHAP **b.** PCL/CEC/nHAP-PDS1 **c.** PCL/CEC/nHAP-PDS3 **d.** PCL/CEC/nHAP-PDS5

4.3.9.3. Cell adhesion

The adhesion of un-induced rADMSCs after 24 h (Figure 52) and osteogenic induced rADMSCs (Figure 53) after 14 days on the scaffolds was qualitatively analyzed by ESEM analysis. The rADMSc had favourable interraction on all the scaffold and they adhered and spread well on the fibroporous scaffold surface further proving their cytocompatibility. The *in vitro* osteogenic efficacy of scaffolds was depicted by the formation of mineralized nodules by osteogenic induced rADMSCs on scaffold surface.

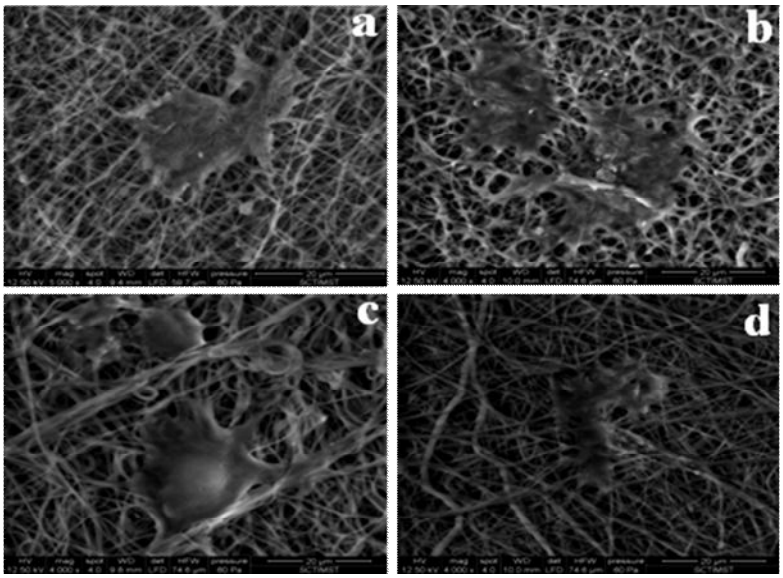

Figure 52. ESEM analyis showing adhesion of un induced rADMSCs on scaffolds scale bar = 20 µm) a. PCL/CEC/nHAP **b.** PCL/CEC/nHAP-PDS1 **c.** PCL/CEC/nHAP-PDS3 **d.** PCL/CEC/nHAP-PDS5

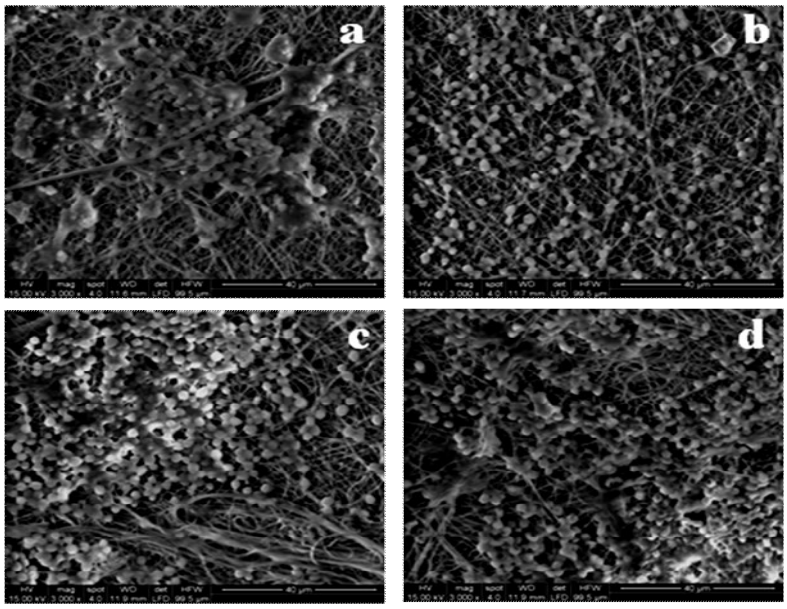

Figure 53. ESEM analyis showing formation of mineralized nodules by osteeogenic induced rADMSCs on scaffolds surface scale bar = 40 µm)

a. PCL/CEC/nHAP **b.** PCL/CEC/nHAP-PDS1 **c.** PCL/CEC/nHAP-PDS3 **d.** PCL/CEC/nHAP-PDS5

4.4. In vivo studies in rat animal model

The main objective of this section was to evaluate the osteogenic potential of the fabricated scaffold under *in vivo* conditions. The work is divided into two sections. The first section deals with the development and validation of osteoporotic rat animal model. The second section involves creating critical size calvarial defect (8 mm) in osteoporotic rats and implanting scaffolds (bare as well as PDS incorporated scaffolds) so as to evaluate their efficacy for bone regeneration. The test material was selected based on the results of preliminary *in vitro* cell culture studies. The created calvarial defect area was

treated with PCL/CEC/nHAP-PDS3 scaffold (test) and PCL/CEC/nHAP scaffold (control) to evaluate the effect of PDS on the calvarial bone defect regeneration.

4.4.1 Establishment of rat osteoporotic model

This section confirms the establishment of rat osteoporotic model by ovariectomy. The rat animal model was evaluated for the induction of osteoporosis after four months post ovariectomy.

4.4.1.1. Histological evaluation of excised tissue using H & E staining

Histological evaluation (Figure 54), of excised tissue using H & E staining confirmed that the excise tissue is of rat ovary showing typical follicular structures (primary and secondary) which are characteristic of ovarian structure and organization.

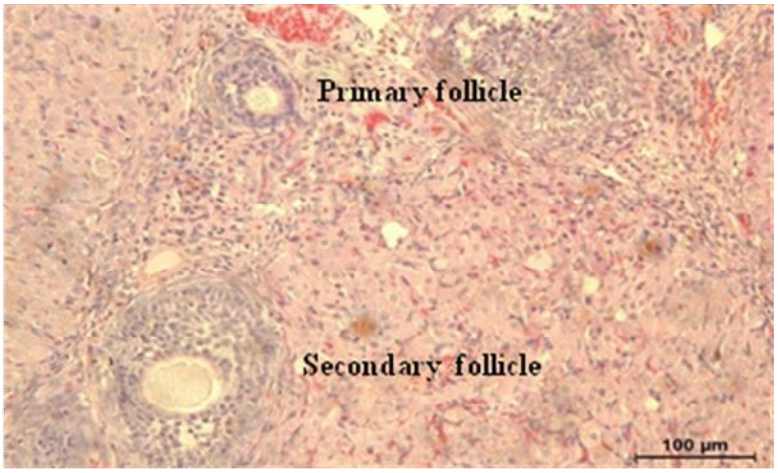

Figure 54. H & E staining of rat ovary (scale bar 100 µm)

4.4.1.2. Evaluation of trabecular bone loss using micro CT analysis

Micro CT analysis of metaphyseal cancellous bone of normal and ovariectomised rats (post 4 months) was carried out to evaluate the trabecular bone loss

both qualitatively and quantitatively. The analysis of 2D slices generated from micro CT revealed disruption of the trabecular structure and thereby confirming trabecular bone loss in ovariectomised rats which is evident from the Figure 55.

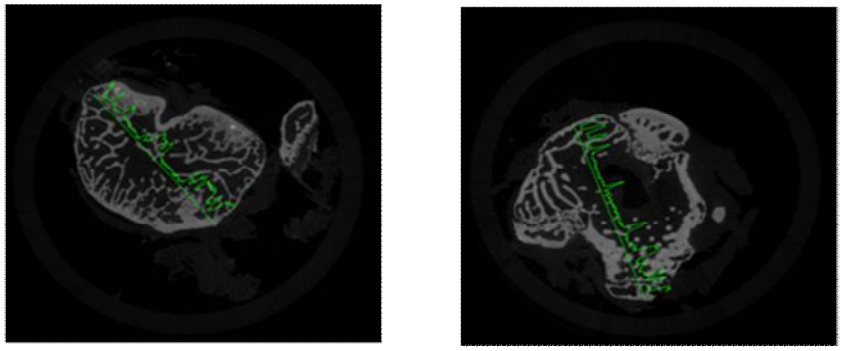

Figure 55. 2D slice from micro CT showing trabecular bone loss

The quantitative evaluation of various trabecular bone parameters such as trabecular number (Tb.N), trabecular thickness (Tb.Th), trabecular spacing (Tb.Sp), trabecular density and ratio of bone volume to total volume (BV/TV) of normal and ovariectomised rats is summarized in Table 11.

Sample	Tb.N 1/mm	Tb.Th mm	Tb.Sp Mm	Tb.density mg HA/ccm	BV/TV
Normal rat	**3.6846**	**0.1622**	**0.2832**	**374.17**	**0.3897**
Ovariectomised Rat	**1.5938**	**0.1247**	**0.6507**	**276.83**	**0.2596**

Table 11.Trabecular bone parameters measured from micro CT

On comparison with normal rats, decrease in Tb.N, Tb.Th, Tb.density and BV/TV and increase in Tb.Sp was observed for ovariectomised rats which validates the induction of osteoporosis in rat animal model

4.4.1.3. Biochemical analysis of blood serum

The level of calcium, phosphorus and alkaline phosphatase (Figure 56 - 58) in blood serum was evaluated before and after ovariectomy (2 & 4 week post ovariectomy). The initial calcium level in blood serum before ovariectomy was of 8.17 ± 0.1 mg/dl and which was found to increase significantly to 9.0 ± 0.4 mg/dl and 11.4 ± 0.8 mg/dl respectively after 2 and 4 week post ovariectomy. The phosphorus level in blood serum before ovariectomy was 4.04 ± 0.5 mg/dl which was found to increase significantly to 4.63 ± 0.2 mg/dl and 6.2 ± 0.6 mg/dl respectively after 2 and 4 week post ovariectomy. The initial value of ALP activity was of 145 ± 4.7 IU/L and after 2 and 4 weeks post ovariectomy, the ALP activity decreased to 132 ± 5.6 IU/L and 128 ± 4.7 IU/L respectively. Hence the increase in level of calcium and phosphorus after ovariectomy and decrease in ALP activity confirms the osteoporotic model induction.

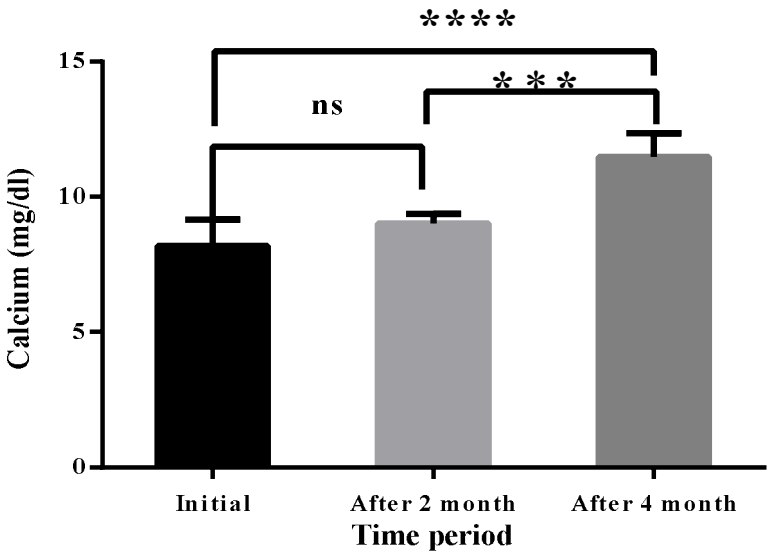

Figure 56. Biochemical analysis of serum for calcium

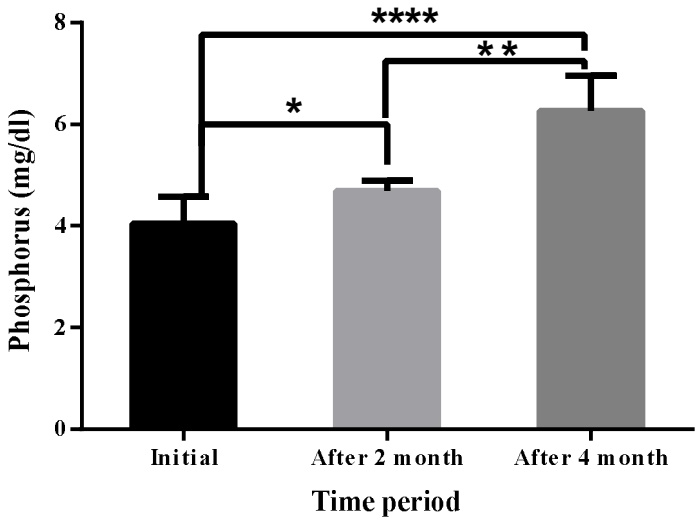

Figure 57. Biochemical analysis of serum for phosphorus

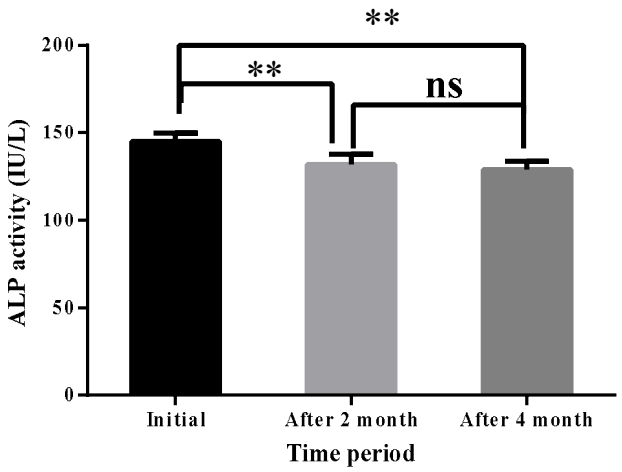

Figure 58. Biochemical analysis of serum for ALP activity

4.4.1.4. Body weight

The weight of rats was monitored before and after 1, 2 and 4 months post ovariectomy. The loss of ovarian function in rats resulted in hyperphagia which resulted in increased weight gain and adiposity which is evident in Figure 59. The percentage weight gain observed in rats after 1, 2 and 4 months post ovariectomy was of 6.5 ± 3.5% , 16.4 ± 3.1% and 24.9 ± 4.3% respectively.

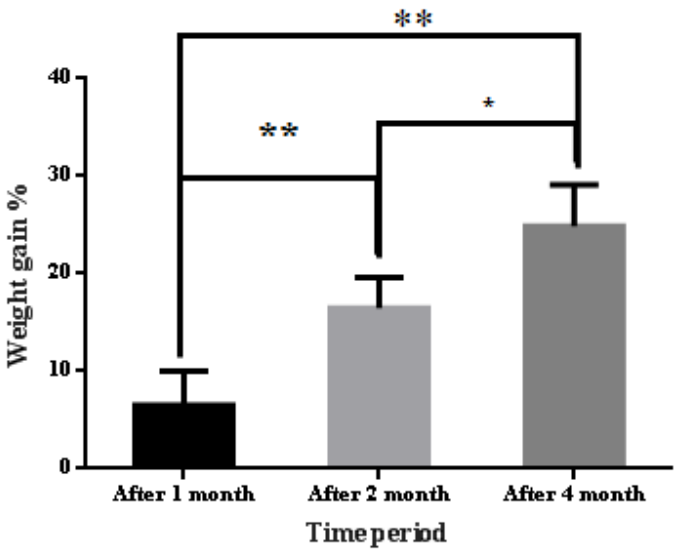

Figure 59. Weight gain in osteoporotic rats

4.4.2. *In vivo* bone formation evaluation

4.4.2.1. Gross evaluation of explants:

There were no complications observed in animals in association with the surgical procedure to create the calvarial defect followed by the scaffold implantation. All the animals survived and were available during the experiment period for further evaluation. At definite time period (3, 6 and 12 weeks post implantation), the animals were euthanized and the gross evaluation of the retrieved explants confirmed the absence of any fibrous / inflammataory tissue formation (Figure 60). The gross evaluation also confirmed the stern adherence of scaffolds to the defect area within the host tissue even without any fixation and no signs of scaffold disintegration were observed.

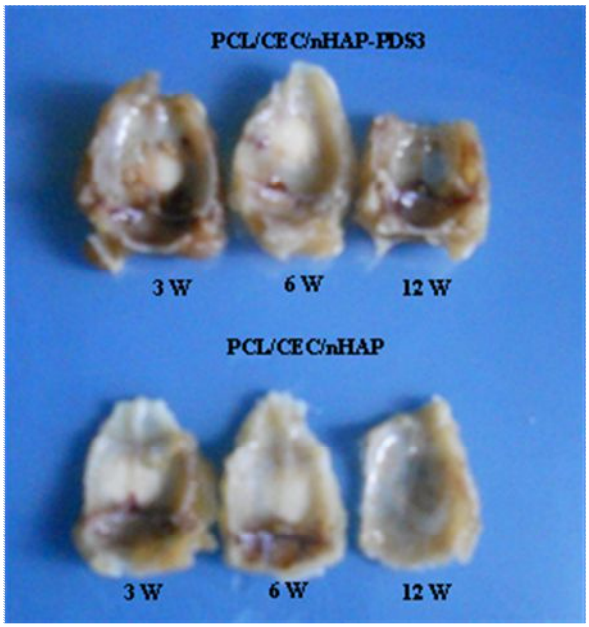

Figure 60.: Gross morphology of explants

4.4.2.2. Radiographic evaluation

The qualitative analysis of bone mineralization using radiographic analysis (Figure 61) depicted bone formation at the rounded edge of the rat calvarium with increasing time period. The images revealed that the use of PCL/CEC/nHAP-PDS3 scaffolds (test group) enabled the regeneration of calvarial defect after 12 weeks post implantation. The presence of PDS on PCL/CEC/nHAP scaffolds has promoted better bone formation and had better healing effect on the defect area and on comparison with PCL/CEC/nHAP scaffolds (control group), almost complete bridging of the defect site was observed in PCL/CEC/nHAP-PDS3 scaffolds (test group).

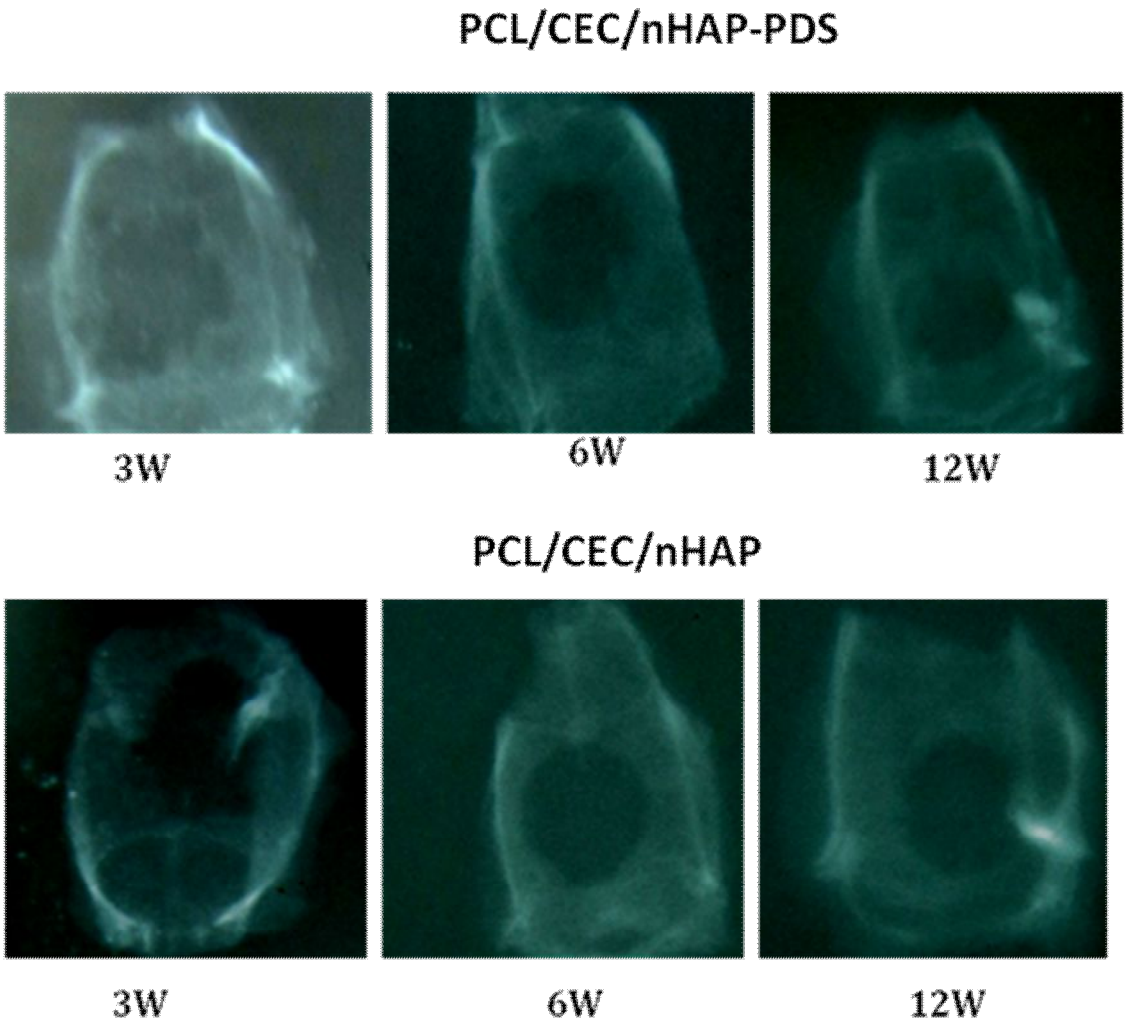

Figure 61. Radiographic analysis of explants

4.4.2.3. Micro CT evaluation

The 3D morphometric images (Figure 62) obtained from micro CT analysis clearly depicts the extend of new bone formation within the defect area. The level of bone formation varied among the test and control group at different time periods. The formation and integration of new bone tissue was more profound with the use of PCL/CEC/nHAP-PDS3 scaffolds (test group) than that of PCL/CEC/nHAP scaffolds

(control group). It is clearly evident from the figure that almost complete bridging of defect area with new bone was observed for test group after12 weeks post implantation.

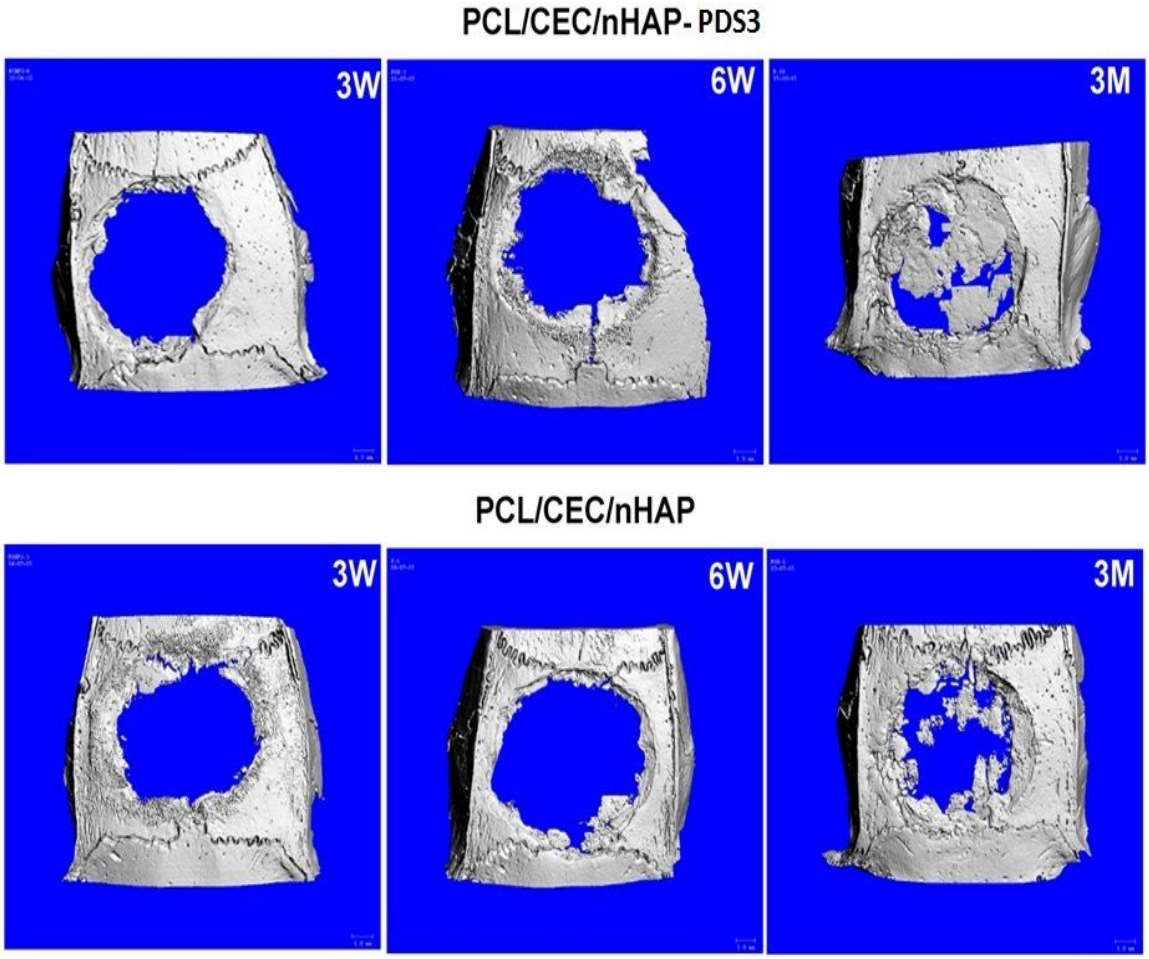

Figure 62. Micro CT analysis of explants

The analysis of 2D slice of the defect area followed by the evaluation of bone mineral density from micro CT further confirms the improved bone formation using the test group at 12 weeks post implantation (Figure 63). The defect size got reduced and

more bony islands were observed thereby indicating the better osteogenic efficacy of PCL/CEC/nHAP-PDS3 scaffolds. The quantitative measurement of density from the 2 D slice reveals that the newly formed bone exhibited density which was almost comparable to the host bone in the test group. Whereas in the case of control group (Figure 64), i.e., for defect area treated with PCL/CEC/nHAP scaffolds, bone formation was more prominent on one of the interface of defect area.

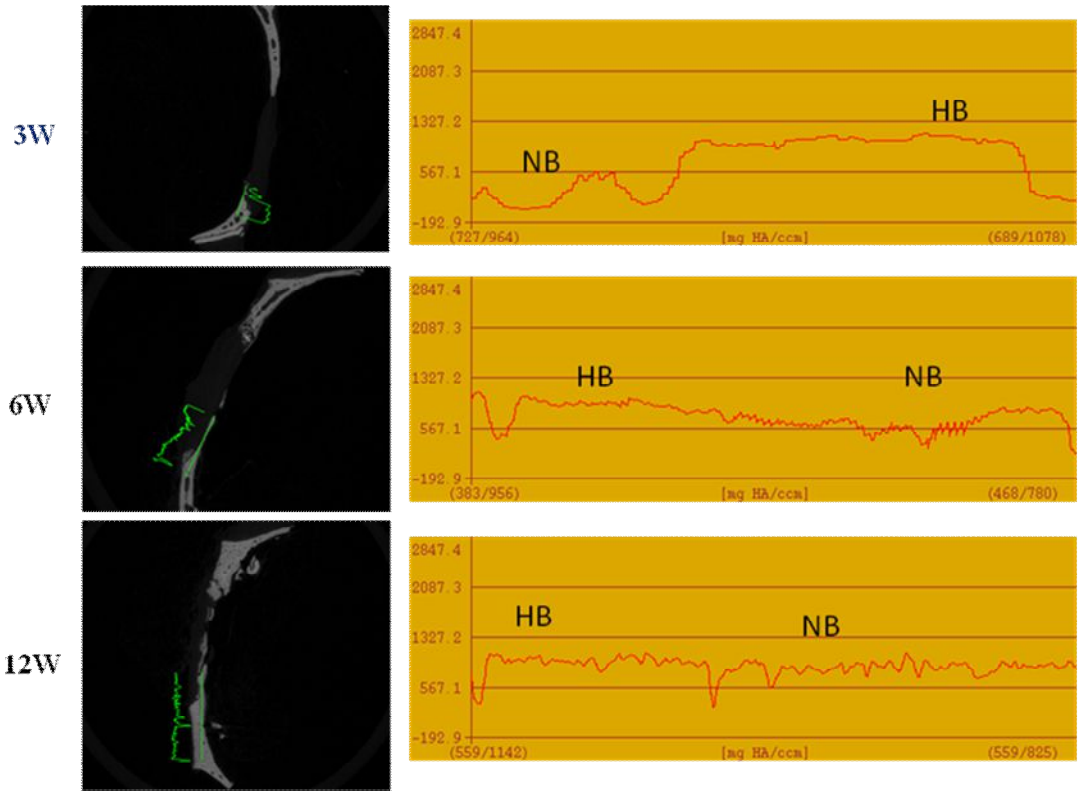

Figure 63. Density of new bone at the defect area of test group measured using micro CT

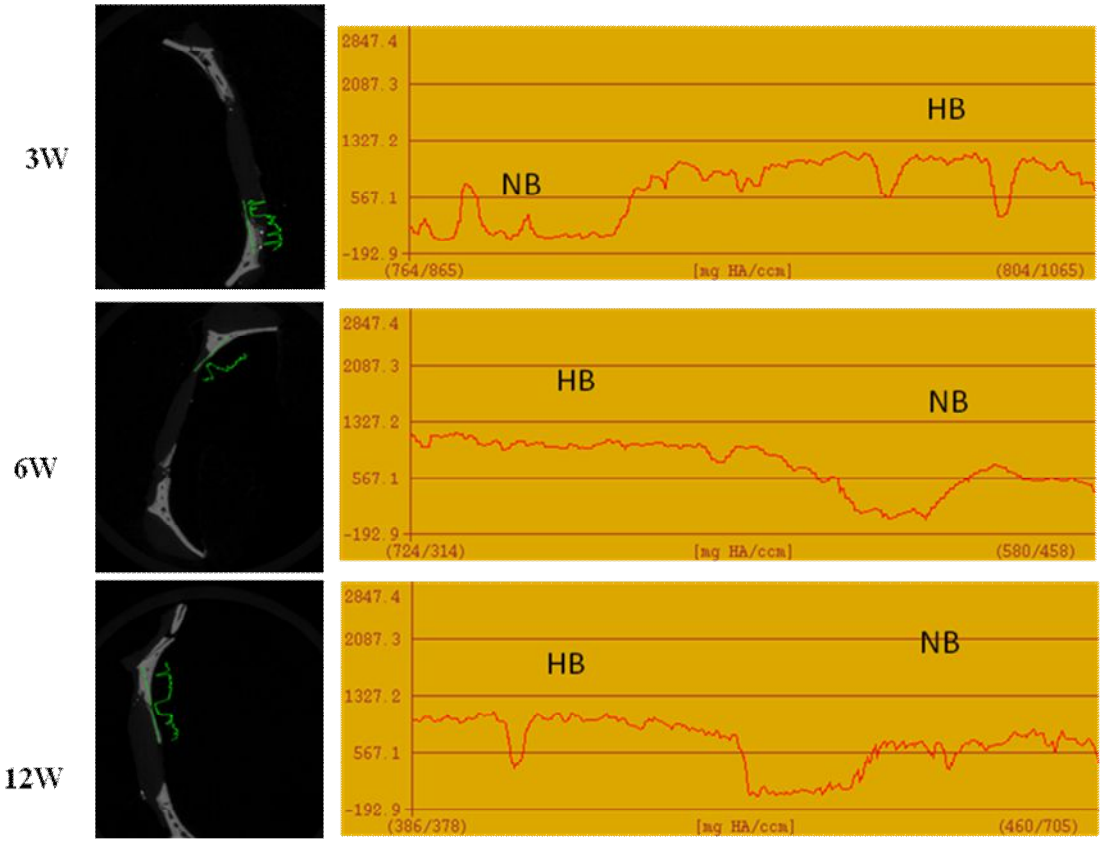

Figure 64.Density of new bone at the defect area of control group measured using micro CT

4.4.2.4. Histology analysis

The explants after processing were stained with Stevenal's blue & van Gieson's picrofuchsin and were analyzed. The stitched image showing the entire defect area and one of the bone-implant interface is depicted in the figures 65 and 66. It was observed that the level of healing was much slower in the control group compared to that of test group. After 3 and 6 week post implantation, not much improvement in bone formation was observed and at 12 weeks post implantation, the new bone formation at the bone implant interface with cellular infiltration was observed.

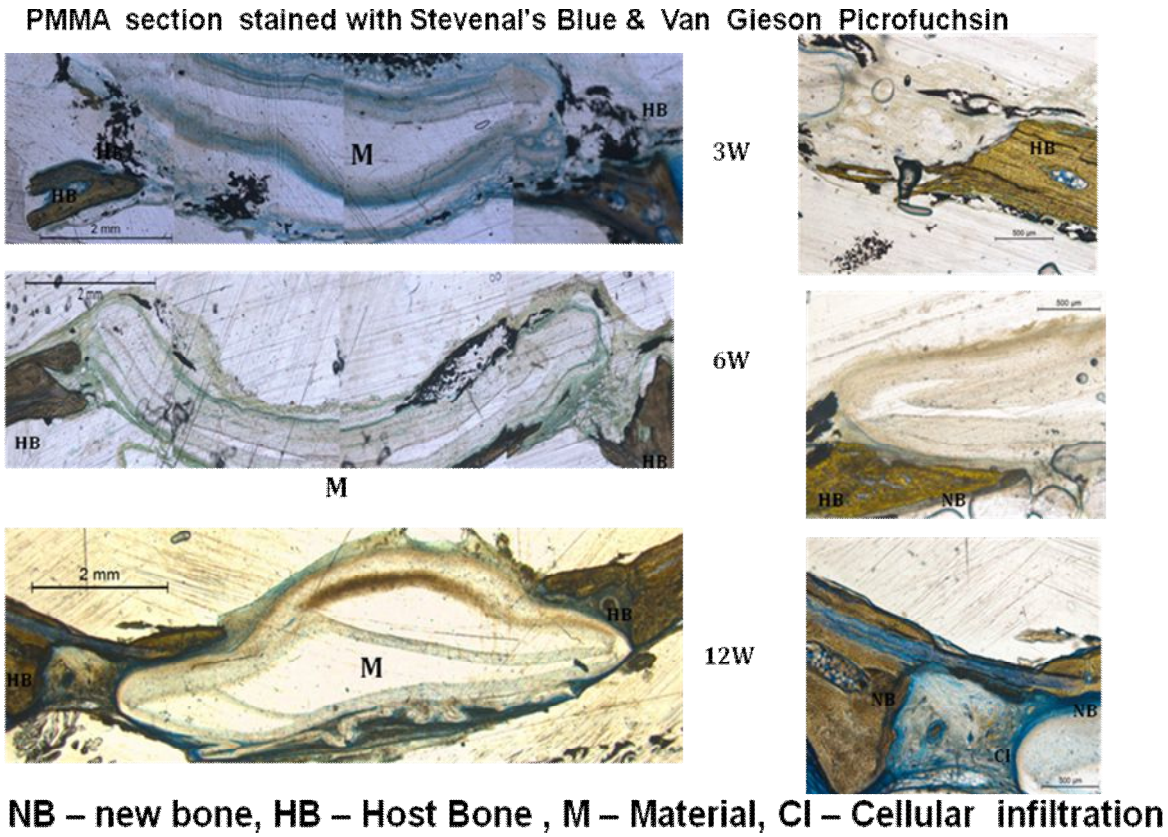

Figure 65. Histological analysis of control group

However in the test group (defect area treated with PCL/CEC/nHAP-PDS3 scaffolds), the healing effect was more effective and even at 3weeks, new bone formation was evident at the bone-implant interface. The better osteoingeration of test group was revealed by the observation of bone formation within the defect area as well as at the bone material at 6 and 12 week post implantation.

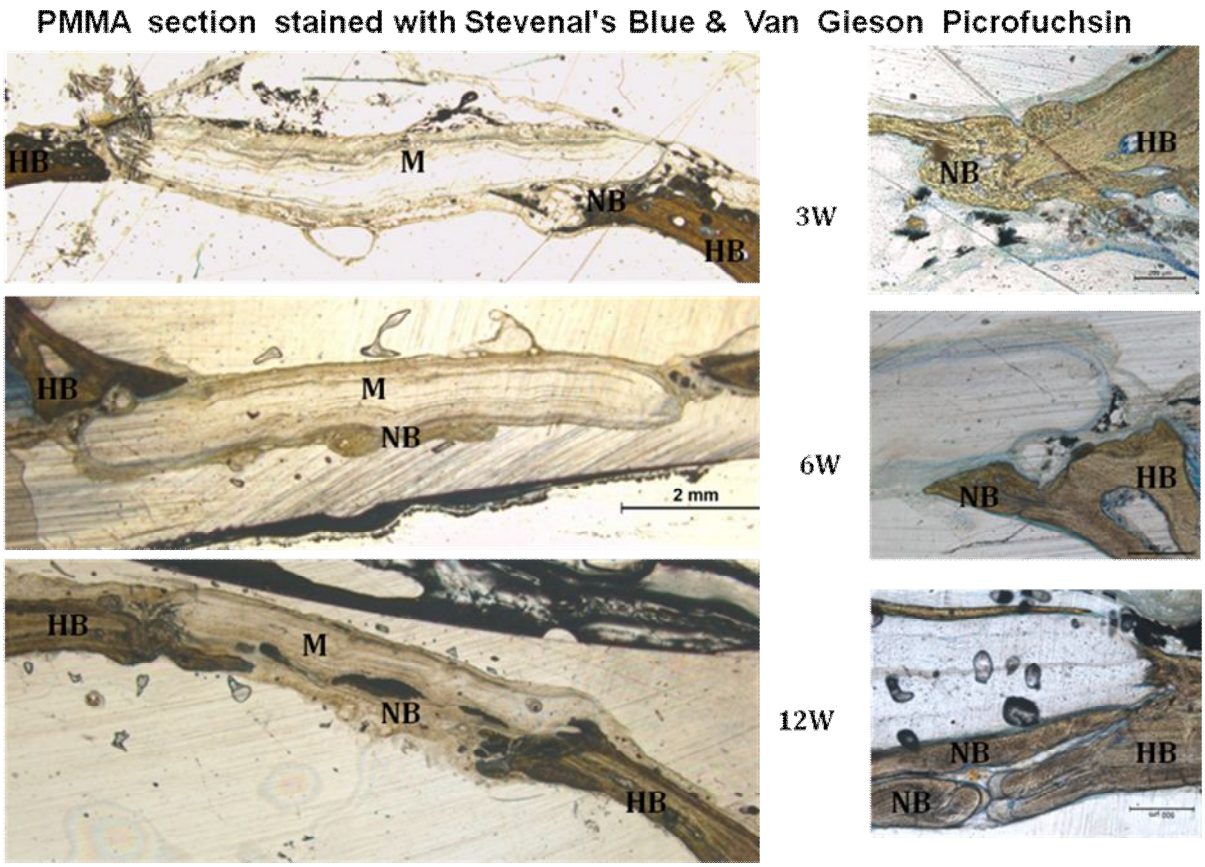

Figure 66. Histological analysis of test group

4.4.2.5. Histomorphometry

The results of histomorphometric analysis (Figure 67.) further confirm that the new bone formation was more pronounced with the use of PCL/CEC/nHAP-PDS3 scaffolds rather than that of PCL/CEC/nHAP scaffolds. The regeneration ratio observed after 12 weeks was of 0.159 ± 0.006 for PCL/CEC/nHAP-PDS3 scaffolds and 0.058 ± 0.005 for PCL/CEC/nHAP scaffolds respectively.

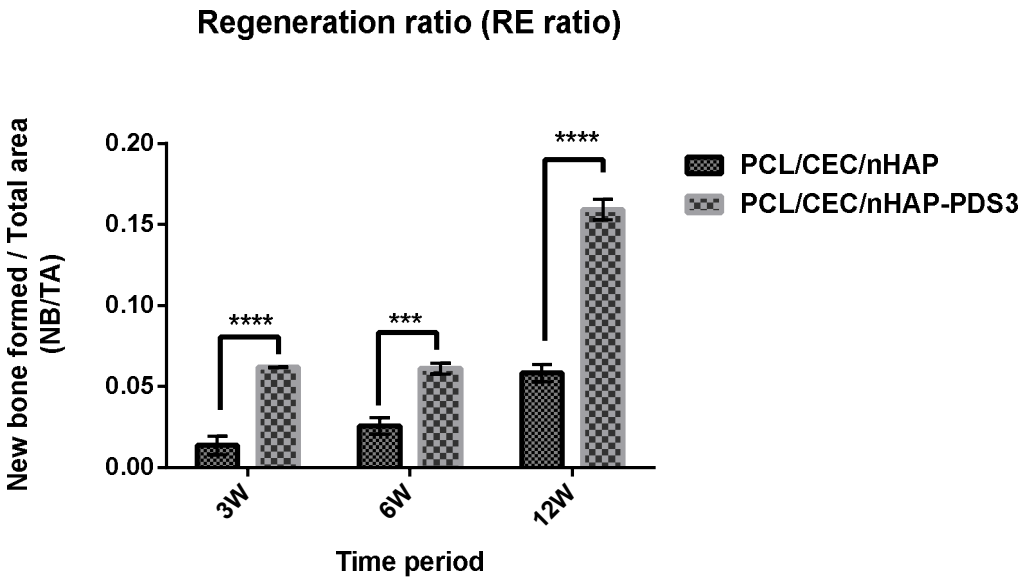

Figure 67. Histomorphometrical analysis showing regeneration ratio of test and control group at different time period

CHAPTER 5

DISCUSSION

Chapter 5 details the discussion and interpretation of the results presented in Chapter 4. The major findings of this study are correlated with published literature in the relevant field and interpretations made wherever possible.

5.1. Development of biodegradable and bioactive scaffolds based on PCL with improved hydrophilicity, biodegradability and better cell viability

PCL is one of the widely explored polymers for biomedical application especially in the area of bone tissue engineering as well as drug delivery. The major feature which attracts the biomaterial researchers is its FDA approval which allows its safer use in humans. Moreover, its compatibility with wide variety of polymers along with good processability, excellent biocompatibility, biodegradability and relatively low cost makes PCL an excellent candidate as scaffolding material for tissue engineering and drug delivery applications (Shalumon *et al.,* 2010; Wutticharoenmongkol *et al.,* 2006). The inherent hydrophobic nature of PCL results in long degradation period of about 2-3 years which recommends its suitability for long term implants (Bölgen *et al.,* 2005; Nam *et al.,* 2007).

However the hydrophobicity of PCL limits its use as a functional scaffold as it is unfavourable for cell adhesion, migration, proliferation, and differentiation (Fabbri *et al.,* 2010; Kim *et al.,* 2006)). Different strategies have been adopted by researchers to

improve hydrophilicity of PCL scaffolds which includes blending or copolymerizing with hydrophilic polymers (Wang *et al.,* 2011; Bajgai *et al.,* 2008; Shafiee et al., 2011; Chong *et al.,* 2007; Oh *et al.,* 2003)).

Besides improving the hydrophilicity, the cellular response as well as the mechanical properties of PCL can be improved by incorporating bioactive nHAP particles. The excellent biocompatibility, bioactivity, osteoconductivity and direct involvement in bone cell differentiation and mineralization makes nHAP suitable for bone tissue engineering applications. The advantage of using nHAP is its structural similarity to the mineral component of the bone. Moreover nHAP has the ability to induce mesenchymal stem cells differentiation towards osteoblasts. Studies have shown that nHAP particles enhance protein adsorption and cell adhesion to the internal surfaces of the scaffold and improve both mechanical and biological properties. However the use of nHAP alone is limited due to its inherent brittle nature. Hence studies involving composites based on nHAP and biodegradable polymers are promising and are being carried out extensively with the aim to confer high bioactivity and adequate mechanical properties to the scaffolds.

In this section, the study focus on improving the hydrophilicity, degradation behaviour and cellular response of PCL scaffolds by blending with the synthesized copolymer CEC as well as by incorporating nHAP particles. The copolymer CEC was successfully synthesized by the ring-opening copolymerization of ε-CL initiated by PEG using stannous octoate as catalyst. The reaction was carried out in bulk with a monomer to initiator ratio of 2:1 (w/w) at 130^{o}C for a period of 3 hours. Yield obtained (90%)

indicates that the feed ratio was almost retained in the prepared polymer. PEG is a non toxic biocompatible polymer which is soluble in water and organic solvents. The absence of antigenicity and immunogenicity allows PEG to be used for many clinical applications (Bramfeldt *al.,*2007). Though PEG is not susceptible to hydrolysis; its incorporation into the polymer backbone has been shown to enhance the rate of degradation by improving the hydrophilicity (Shafieyan *et al.,* 2011).

With the aim to modify PCL, the copolymer CEC was synthesized and chemically characterized and confirmed using FTIR and NMR analysis.. The GPC analysis revealed that the copolymer CEC exhibited narrow molecular weight distribution with number and weight average molecular weight of 5508 and 7305 respectively. The nHAP particles gifted by Bioceramic Laboratory was characterized for its size using TEM and particle size analyzer. TEM analysis depicted rod shaped particles of 12-35 nm width and 90-120 nm length. The average particle size of nHAP particles measured by particle size analyzer was of 89 nm with polydispersity index of 0.292.

Electrospinning technique provides a simple and direct way for developing novel functional biomaterials. The proper choice of material components and their combination in appropriate ratio enables one to tailor the physical and biological properties of the resultant electrospun fibers such as hydrophilicity, mechanical modulus and strength, biodegradability, biocompatibility, and specific cell interactions (Liang *et al.,* 2007). In this study, electrospinning technique has been explored to fabricate scaffolds based on PCL, PCL/CEC blend and their nHAP filled composites.

Comparative evaluation of the physical and biological properties of the scaffolds (PCL, PCL/CEC, PCL/nHAP and PCL/CEC/nHAP) was carried out to evaluate their applicability for bone tissue engineering applications. The PCL/CEC blend ratio and nHAP weight percentage used for the study was of 80:20 ratio and 2 wt% (optimized based on preliminary mechanical property evaluation).

The selection of suitable solvent for electrospinning is crucial since it affects the fiber morphology and diameter. DCM is a good solvent for PCL, however using it alone results in formation of fibers with large fiber diameter. Hence the solvent DMF with high dielectric constant was also added so as to improve the fiber formation as well as to get fine fibers. The spinning was done using DCM/DMF solvents mixtures in 80:20 v/v ratio at predetermined optimized condition of 10 % concentration, feed rate of 1mL/h, applied voltage of 10-13 kV, mandrel speed of 500 rpm and needle to collector distance of 13 cm so as to get bead free fine fibers.

The morphology and diameter of fibers depends on the conditions of electrospinning process (Han et al, 2010, Huang et al., 2003). The morphological features of the scaffolds analyzed by SEM (Figure 16) revealed random nonwoven fibrous architecture with PCL having a fiber diameter around 1.53 μm. It was observed that blending PCL with the copolymer CEC resulted in smooth fibers with reduced fiber diameter. This reduced fiber diameter observed for the blend scaffold can be attributed to the difference in solution viscosity between PCL and PCL/CEC (80/20) blend. The nHAP incorporation has altered the surface texture of PCL fibers. Similar phenomenon was observed by Wutticharoenmongkol *et al.* in electrospun PCL with incorporation of

nHAP particles (Wutticharoenmongkol *et al.,* 2006). Lao *et al.* has reported that PLGA nanofibers with varying HAP content have introduced surface roughness (Lao *et al.,* 2011). The decreased fiber diameter exhibited by PCL/nHAP composite scaffold can be attributed to the presence of calcium and phosphate ions in nHAP which has imparted higher conductivity (Jose *et al.,* 2010). Chuenjitkuntaworn *et al.* has reported regarding decrease in fiber diameter of PLLA/HAP composite fibers in comparison with neat PLLA which was reported to be observed due to the increase in the restriction to flow due to the presence of HAP particles Chuenjitkuntaworn et al., 2010).

The porosity of scaffolds plays vital role in their biological performance as it determines both cell–cell as well as cell scaffold interaction. High porosity, adequate pore size and interconnected pore network are essential criteria for a tissue engineering scaffold as it enables better cell infiltration and vascularisation. Micro CT analysis revealed the porous nature of the scaffolds and it was observed that electrospun PCL was highly porous with percentage porosity of about 92 % and an average pore size of 48 μm. Compared to PCL, both copolymer blended and nHAP incorporated composite scaffolds exhibited reduced percentage porosity and average pore size. The reduction in pore size occurs as more layers of fibers might overlap with each other, especially when the fiber diameter is smaller, resulting in smaller pore diameter (Li *et al.,* 2002). It was observed that the pore size distribution lies in a range below 100 μm for all the scaffolds (Figure 19). The preferable pore size for osteoblast cells ranges from 200 to 400 μm for encouraging migration, attachment and proliferation. However for electrospun matrices pores formed are much smaller than the normal cell size of a few to tens of micrometer.

Pores in an electrospun structure are formed by the randomly oriented fibers lying loosely upon each other. Cells can migrate through pores by their amoeboid movement and can push surrounding fibers aside to expand the pore. This dynamic architecture of fibers allows cells to adjust according to pore size and grow into nanofiber matrices (Li *et al.,* 2002).

Surface properties of scaffolds such as wettability, chemistry and roughness have significant influence on appropriate cell response. The hydrophilic/hydrophobic characteristic of scaffold can influence the initial cell adhesion and cell migration to a greater extend (Masaeli *et al.,* 2012; Cao *et al.,* 2011). Surfaces with moderate hydrophilicity will promote better cell adhesion, proliferation and cellular activities. The surface of PCL and PCL/nHAP scaffolds were hydrophobic indicated by their higher contact angle value of 119 ± 2° and 112 ± 1° respectively. Blending PCL with copolymer CEC resulted in imparting hydrophilicity which was reflected by the complete wetting of scaffolds by the water drop within few seconds. It has been reported by Li *et al.* that incorporating PEG moiety in the polymer backbone improves the hydrophilicity of multiblock copolymers with respect to PCL homopolymer (Li *et al.,* 1998).

The mechanical properties of scaffolds are significant as the scaffold must be strong enough to resist the forces from body movement or outer environment and must also keep its structural integrity during the initial stages of the new bone formation. For electrospun fibers, the mechanical properties are closely related to the fiber orientation, bonding between fibers and fiber slippage rather than the mechanical properties of

individual fibers. The evaluation of both static and dynamic mechanical properties of the scaffolds confirmed the enhancement of mechanical properties of electrospun PCL with incorporation of both CEC and nHAP. Liao *et al.* in their studies with Poly (L-lactide)/Poly(ε-caprolactone) blend fibers observed that the tensile strength of the blend was reduced owing to the porous nature of the electrospun membranes which were compared with that of cast film (Liao *et al.,* 2011). Studies on PCL/multiwalled carbon nanotubes (MWCNTs) composites by Meng *et al.* reported that nanocomposite fibers of PCL with 0.5 wt.% MWCNTs with less agglomeration and finest fiber size had better mechanical properties (Meng *et al.,* 2010). The dynamic mechanical properties of the scaffolds evaluated using DMA also revealed the significant enhancement in the storage modulus of PCL with incorporation of both CEC and nHAP. As discussed earlier, scaffolds with smaller fiber diameters will provide higher overall relative bonded areas between fibers due to the increased surface area, bonding density, and better distribution of bonds. PCL and PCL/CEC/nHAP composite scaffold exhibited comparable glass transition temperature. However, slight decrease in T_g for both nHAP and CEC incorporated scaffolds was observed which may be due to the enhancement in the chain flexibility of PCL. Bianco *et al.* has reported that decrease in T_g of electrospun poly(L-lactic acid)/Ca-deficient-hydroxyapatite composites with increasing filler content may be due to the enhancement in the chain mobility of poly(L-lactic acid) (Bianco *et al.* 2009*)*. In comparison, results of both static and dynamic mechanical properties reveals that blending with copolymer CEC and incorporation of nHAP has significantly

increased the strength of PCL scaffold. On comparison, the PCL/CEC/nHAP composite exhibited superior mechanical properties.

Apart from favourable physico-chemical and mechanical properties, the most important requirement for a biomaterial is its biocompatibility in a specific environment, together with the non cytotoxicity of its degradation products (Gomes *et al.,* 2001). One of the main reasons for choosing PCL for the present study is its slow degradation. Degradation of PCL occurs mainly by hydroxylation and fragmentation of high molecular weight chains, followed by changing to carbondioxide and water in the environment of water or body fluid with or without enzyme. ESEM analysis of the scaffolds after 3 months of of PBS incubation depicted fibre rupture as well as fiber thinning. The incorporation of CEC has enhanced the degradation of PCL which was reflected by the significant drop in the tensile strength of the PCL/CEC/nHAP composite scaffold. This was mainly due to the hydrophilicity imparted by the introduction of copolymer CEC which allows the more water molecules to diffuse into the polymer and thereby enhancing degradation.

As a preliminary step towards the evaluation of cytocompatibility of the scaffold, MTT assay was performed using L929 cell lines and the result revealed the non-cytotoxic nature of all the scaffolds with more than 80 % viability. The attachment, viability and proliferation of cells on the scaffold determine the suitability of the material for the intended application. The electrospun fibrous scaffolds were assessed for its ability for cell attachment, viability and proliferation *in vitro* using RADMSCs which showed favourable interaction with all the fibrous scaffolds. The initial cell

attachment and spreading are significant factors in developing scaffolds for tissue engineering. The morphology of the cells after seeding provides a wealth of information regarding the interaction between the scaffold and cells. The morphology of RADMSCs that adhered to the scaffold at different time period was examined using ESEM (Figure 31). The RADMSC cells expanded on the scaffolds with anchoring ligands stretching out to attach themselves on the fiber surface. ESEM micrographs revealed that the electrospun fibroporous architecture of PCL, PCL/CEC and their nHAP incorporated scaffolds could provide a suitable ECM-like environment for the cells to attach and proliferate. During 2 h, the RADMSCs exhibited a small spherical shape, a typical non-adherent and non-spreading morphology. With increasing time period cells actively proliferated on the scaffolds and after 5days the spreading of cells was more pronounced on the PCL/CEC/nHAP composite scaffold indicating their superior cellular response. The fibroporous architecture of scaffold allowed the cells to adhere, proliferate and to migrate into the scaffold and confirmed that the porosity and pore size of the scaffolds were sufficient for tissue engineering applications.

The qualitative determination of viability of ADMSCs using cLSM depicts high ratio of viable green cells homogenously distributed over all the scaffolds (Figure 27). All the fibrous scaffolds showed increase in cell viability and cell number with culturing period. The higher LDH value of PCL/CEC/nHAP composite scaffold suggests that more viable cells were present on this composite scaffold compared to neat PCL. The cell number on the fibrous scaffolds determined by picogreen analysis was also found to increase during the culture period of 28 days. The number of osteogenic-induced

RADMSCs was also significantly higher on PCL/CEC/nHAP composite scaffold at a later time period of 28 days than other scaffolds. The enhanced viability and proliferation of cells on PCL/CEC/nHAP composite scaffold can be attributed to the scaffold's greater hydrophilicity, and the presence of osteoconductive nHAP particles which may be responsible for stimulating cell proliferation and differentiation. ALP activity of osteogenic induced ADMSC on fibrous scaffolds was further demonstrated by ELF-97 staining followed by cLSM investigation (Figure 30). Alkaline Phosphatase (ALP) is an enzyme secreted by osteoblasts that is normally present in high concentration in growing bone, essential for the deposition of minerals and is considered as an early bone marker (Nair *et al.,* 2009). These observations confirm the bioactivity and osteoconductivity of the PCL/CEC/nHAP composite scaffold and its usefulness in bone tissue engineering as a template for cell adhesion, proliferation and differentiation into the specific bone lineage.

5.2 Development of pamidronate incorporated PCL based scaffolds

The simplicity of electrospinning technique has been utilized for fabricating PDS loaded PCL based scaffolds so as to enhance the biofunctionality of the scaffold. Three different loadings of drug PDS has been incorporated on PCL, PCL/CEC blend and PCL/CEC/nHAP composite scaffold and a comparative evaluation was carried out to choose an appropriate scaffold for *in vivo* studies.

PDS belongs to the family of aminobisphosphonate drug which is widely used for the clinical treatment of bone related loss associated with osteoporosis, paget diseae, hypercalcemia etc (Wilkinson and Little, 2011; Groff *et al.,* 2001; Wang *et al.,* 2014;

Fan *et al.,* 2005) Since the oral administration of bisphosphonate drugs is associated with drawbacks such as poor bioavailability and gastrointestinal ulcerations, it is expected that the local delivery of these drugs at the defect site can enhance its efficacy. On reviewing literature, only a few works has been reported on the developments of electrospun polymeric scaffolds for the delivery of bisphosponates (Puppi *et al.,* 2010; Lu *et al* 2011; Yun *et al* 2014) To the best of our knowledge, no studies have been reported in literature on the delivery of PDS from electrospun PCL scaffolds.

The successful incorporation of drug PDS on to PCL, PCL/CEC blend and PCL/CEC/nHAP composite scaffolds were revealed by the morphological anaysis using ESEM. All the scaffolds exhibited beadless smooth fibers with reduced fiber diameter. The significant reduction in the fiber diamter observed for PDS incorporated scaffolds could be related to the conductivity measurement values (Table 8). The PDS incorporation has improved the solution conductivity of PCL based scaffolds. Generally during electrospinning process, increased solution conductivity will impart more electric charges to the electrospinning jet which results in higher elongation forces under electric field. Moreover increased solution conductivity will also cause more bending instability which increases the jet path and more stretching of spinning solution. Hence this reduction in fiber dimater observed for PDS incorporated scaffolds also suggest the homogenous distribution of the drug PDS in the scaffolds. There was no aggregates of drug on the fiber surface.

An ideal tissue engineering scaffold must be porous so as to facilitate cell seeding and to enable gaseous and nutrient exchange. Porosity measurement by ethanol

intrusion method revealed the porous nature of PCL and PDS incorporated scaffolds. The surface wetting behaviour of PCL scaffolds was influenced by the incorporation of hydrophilic PDS. PCL is inherently hydrophobic in nature owing to presence of five CH_2 groups. Imaparting hydrophilicity can have positive impact on the biological performance of the scaffolds. The incorporation of hydrophilic PDS altered the surface wetting behaviour of PCL scaffolds which is indicated by the decreased contact angle value of 36° for PCL-PDS5 scaffolds. However for PCL/CEC and PCL/CEC/nHAP scaffolds, contact angle couldnot be measured as complete wettiing of scaffolds with water was observed.

Besides improving surface wettability, mechanical perfomance of scaffolds were also enhanced with PDS incorporation. When PDS content was of 5 %, the tensile strength of PCL scaffolds increased from 5.2 MPa to 13.4 MPa and for that of PCL/CEC scaffolds, tensile strength increased from 7 MPa to 11.5 MPa. However for the PCL/CEC/nHAP composite scaffolds, there was no significant difference in tensile strength after PDS incorporation. The superior mechanical properties of PDS scaffolds observed in PCL and PCL/CEC blend scaffolds can be attributed to the improved solution conductivity which favoured the formation of fibers with reduced fiber diameter.

Dynamical mechanical analysis showed that storage modulus of scaffolds enhanced with PDS incorporation for PCL scaffolds and there was not much difference in the Tg values observed for scaffolds. PCL exhibited Tg around - 47.7 °C whereas for PDS incorporated scaffolds Tg ranged from - 48 °C to - 49 °C. For PCL/CEC blend and

PCL/CEC/nHAP composites scaffolds, storage modulus dropped with PDS incorporation and increase in Tg was observed.

It is difficult to dissolve hydrophilic PDS into hydrophobic PCL scaffolds. Hence the successful incorporation and sustained release of hydrophilic PDS is a challenge. Studies have shown that amphiphilic block copolymers like PEG-b-PCL have been reported to incorporate hydrophilic drugs into hydrophobic polymers by electrospinning to produce controlled-release nanofibrous scaffolds (Kim *et al.,* 2004). *In vitro* relase studies in PBS at 37 °C showed that all the scaffolds exhibited quick release of PDS during the initial time period of about 12 h. The initial amount of drug release vary as a function of PDS content and its distribution in the scaffold. The initial quick release of PDS can be attributed to the release of drug which is localized on the fiber surface. When the drug concentration is increased, the drug molecules may aggregate more on the fiber surface, which would lead to an even larger initial burst of drug as seen in the scaffold with 5 wt% of drug loading. In our study it was observed that the drug release from PCL/CEC blend scaffolds was higher than that of PCL and PCL/CEC/nHAP composite scaffolds suggesting the enhancement in drug release with incorporation of CEC. However, the presence of nHAP in the composite scaffold enabled sustained release of drug from the scaffold.

The incorporation of PDS has influence on the degradation behaviour of scaffolds. PCL is a slow degrading polymer having a degradation time of about 2 to 3 years owing to its inherent hydrophobic nature. It was observed that PDS incorporation

accelerated the degradation behaviour which was revealed by the thinning and rupture of fibers observed after 3 months of PBS ageing (Figure 43). This was further substantiated by the results of tensile strength of scaffolds observed after 3 months of PBS ageing. The tensile strength of scaffolds decreased with PBS ageing and the drop in tensile strength was more prominent on PDS incorporated scaffolds. For PCL, after 3 months of PBS ageing, tensile strength dropped by 26 % whereas in case of PCL-PDS scaffolds, the drop in tensile strength was more prominent on PCL-PDS5 scaffolds which was about 68%. This drastic drop in tensile strength of PCL-PDS5 scaffolds was mainly due to the improved hydrophilicity imparted by PDS incorporation which is reflected by its lower contact angle value of 36°. The study also demonstrated that higher the PDS content, the more is the chance of PDS to be located on the scaffold surface which can be easily dissolved and washed out using PBS resuting in faster degradation. For PCL/CEC blend scaffolds, incorporation of hydrophilic CEC and PDS further enhanced the degradation profile of PCL scaffold showing about 77% drop in tensile strength for PCL/CEC-PDS5 scaffolds. In case of PCL/CEC/nHAP composite scaffolds, owing to the presence of nHAP particles the drop in PCL/CEC/nHAP-PDS5 scaffolds was of only 55 %. However all the scaffolds maintained their structural integrity in the original dimension till the end of the experiment.

The *in vitro* biocompatibility of PDS loaded scaffolds were assessed using hOS cell lines to evaluate the effect of PDS on the cell viability and proliferation. The hOS cells were used for the study as they maintain the cellular features of osteoblasts. The results suggested that PDS was not toxic to hOS cells, highlighting that PDS loaded

scaffolds provides a favourable microenvironment for osteogeneic ability. The scaffolds favoured the adhesion of hOS and maintained their typical spindle morphology as revealed by the live/dead assay (Figure 46). However at higher PDS content, cells lost their spindle morphology. The quantification of cell viability using MTT assay after 48h indicated that all the scaffolds had favorable interaction with cells and the cells were viable on all the scaffolds proving their cytocompatibility.

The PCL/CEC/nHAP composite scaffolds were selected for the *in vivo* study based on the physico-mechanical properties and was further evaluted for *in vitro* cytocompatibility using rat's adipose derived mesenchymal stem cells (rADMSC). Rat ADMSCs were chosen since the potential of the scaffolds has to be evaluated in a rat animal model. The MTT assay using un-induced rADMSC proved the cytocompatibility of the scaffolds with more than 90% cell viability and on comparison it was observed that cell viability was more prominent on PCL/CEC/nHAP-PDS3 scaffolds. Studies by Ponader *et al* have showed that pamidronate has the ability to affect positively the vitality of human osteoblasts in a concentration dependent manner. It was observed that the lowest pamidronate accumulation led to the highest enhancement of osteoblast vitality. Higher concentrations of pamidronate seem to block the anabolic effect (Ponader *et al.,* 2008). This finding correlates with the conclusion of Correia *et al*., who found a cytotoxic effect of alendronate, one of the most potent osteoclast inhibitors among bisphosphonates, in higher concentrations (Correia *et al.,* 2006). This effect could be explained by the dual effect of bisphosphonates, influencing the calcification,

which seems to be elevated in low bisphosphonate doses and the bone resorption, which is dominant in higher doses.

Live/dead assay using actin staining depicted the viable rADMSCs adhered on the fibrous scaffolds (Figure 51). It was observed that cells maintained their characteristic spindle morphology only at lower PDS content. The disruption in morphology at higher PDS i.e. on PCL/CEC/nHAP-PDS5 scaffolds was observed.

The ability of scaffolds to support the attachment of un-induced rADMScs after 24 h (Figure 52) and osteogenic induced rADMSCs after 14 days was analyzed using ESEM analysis (Figure 53). The cells adhered well on all the scaffolds and interestingly it was observed that the un-induced rADMSCs after 14 days of osteogenic induction synthesized mineralized nodules on scaffold surface proving their osteogenic efficacy. Similar findings were observed by Venugopal *et al* in which mineralization was observed in PCL/HAP-modified nanofibrous scaffolds (Venugopal *et al.,* 2008). Hence the PCL/CEC/nHAP-PDS3 scaffolds were chosen for the *in vivo* based on its enhanced physico-mechanicl and biological properties..

5.3. *In vivo* evaluation of PDS incorporated PCL based scaffold in a rat animal model

After the *in vitro* biofunctional assessment, the *in vivo* osteogenic potential of the fabricated PCL/CEC/nHAP-PDS3 scaffolds was evaluated under *in vivo* conditions as a critical indicator for future clinical translational application. The present study is an attempt to explore the potential of local delivery of PDS in healing rat calvarial bone

defect under osteoporotic conditions. Rat animal model was chosen for the study as it is the FDA recommended preclinical small animal model for evaluating the potential of pharmaceutical agents intended for osteoporosis treatment (Reinwald & Burr, 2008, Colman, 2003). No single animal model precisely mimics all the characteristics of human osteoporosis. However there are different strategies for inducing osteoporotic conditions in animals which includes ovareiectomy, low calcium diet, steroid usage etc. Among these, ovariectomized animals are widely accepted for bone loss related research since they closely mimics the physiological condition of postmenopausal osteoporosis. The high reproducibility of ovariectomized animal model and the bone loss associated with estrogen deficiency makes rat an ideal candidate for inducing osteoporosis.

The first phase of the *in vivo* study was to develop osteoporosis in rat animal model and to validate the model induction. To induce osteoporosis, 4 months aged female wistar rats were subjected to bilateral ovariectomy and kept for a period of four months for model induction. A time period of 3 to 4 months is usually provided after ovariectomy for inducing osteoporotic condition. The surgical procedure adopted was bilateral ovariectomy in order to remove the ovaries so as to induce estrogen deficiency which could result in osteoporosis. There were no signs of complications observed during as well as after the surgery.

The removed ovarian tissue after surgery was further analyzed by histology using H & E staining (Figure 54) which depicted typical follicular structures thereby confirming that the excised tissue is of rat ovary. In order to further validate the trabecular bone loss associated with ovariectomy, the metaphyseal cancellous bone area

at the tibial head of normal rats and ovariectomised rats after 4 months of induction was quantitatively and qualitatively analyzed and compared by micro CT analysis.

Since bone loss associated with osteoporosis is more evident in trabecular area, measurement of trabecular bone parameters enables the confirmation of osteoporotic model induction. As expected, the effect of ovariectomy was marked by the disruption of trabecular network in case of ovariectomised rats (Figure 55) as well as decrease in various trabecular parameters such as Tb.N, Tb.Th Tb.density and BV/TV. Similar observations were reported by Majumdar *et al* on the effect on trabecular micro-architecture after osteoporosis induction (Majumdar *et al.,* 1997).

The analysis of serum showed increase in serum calcium and phosphorus level as well decreased serum ALP level which further supports the bone loss in the induced rat animal model. As a secondary effect of ovariectomy, weight gain was observed in animals which further confirm the model induction. Hence the results of histological analysis, μ-CT and blood serum analysis confirm the development and validation of osteoporosis in rat animal model.

The second phase of the *in vivo* study was to create calvarial defect in the developed osteoporotic rat animal model and to evaluate the efficacy of the fabricated scaffolds in healing the defect. The PCL/CEC/nHAP-PDS3 scaffold was chosen as the test material and that of PCL/CEC/nHAP composite scaffold as the control material for the study based on the physico-mechanical properties and *in vitro* assessment. The defect site chosen was of calvaria and 8 mm critical size defect (Szpalski *et al,* 2010) was created using dental burr. The calvarial defect site offers advantage of not requiring

any internal fixation devices and eliminates the dislocation of implant associated with the motion of animal.

The gross evaluation of explants confirms the proper fixation of scaffold to the defect site and absence of any inflammatory responses. The implanted scaffolds were well integrated into the calvarial bone defect. The scaffolds adhered strictly to the host bone tissue even without any fixation. There were no mortality or complications observed in animals during the period of our study. No signs of bleeding, wound fester, infection, scalp edema, or effusion were seen at the site of surgery.

The bone regenerative capacity of scaffolds analyzed by radiography revealed bony infiltrations in the cavity after 12 week post implantation with the use of PCL/CEC/nHAP-PDS3 scaffolds (test group). These results were further confirmed by the μ-CT data which presented more detailed bone regeneration. Almost complete bridging of the defect site was evident after 12 weeks post implantation with the use of PCL/CEC/nHAP-PDS3 scaffolds (test group) in comparison with that of PCL/CEC/nHAP(control group).

The extend of mineralization (in-terms of bone density) was assessed from the density histograms generated from 2 D slice of the defect area treated with control and test group (included host bone and *de novo* bone). The defect area treated with PCL/CEC/nHAP-PDS3 scaffolds (test group) exhibited better osteointegration as the bone density (in terms of mg HA/ccm) of the new bone equalised to that of the host bone, indicating improved mineralization efficiency. However, new bone formed with the use of control group scaffolds in the defect area exhibited poor mineralization

efficiency as compared to the mineral content of host bone. Results indicate that PDS loaded PCL/CEC/nHAP scaffolds exhibited better matrix formation, with promising results which is probably as a result of release of PDS at the defect area from the test group. The PDS released from PCL/CEC/nHAP-PDS3 scaffolds may have positively regulated the excessive mineralization along with the inherent bioactivity of nHAP. Similar findings were observed by Yu *et al* in which the local co-delivery of BMP / pamidronate using poly-D, L-lactic-acid implants have improved calvarial bone defect healing in healthy rat models (Yu *et al.,* 2010).

Histological analysis using Stevenal's blue and van Gieson's picrofuchsin staining was carried out to determine the area of cells infiltered around and within the defect area as well as the newly formed bone area (Figure 65-66). Stevenal's blue stains cells and extracellular structures in a subtle gradation of blue tones and van Giesen's picrofuchsin bone as orange or purple and osteoid matrix as yellow green. It was observed that defect area treated with test group scaffolds exhibited new bone formation at the bone implant interface after 3 week post implantation. With increasing time period, i.e., after 12 week post implantation new bone formation was observed within the defect area (bridging of defect site) as well as at the bone implant interface further confirming the better osseointegration. In case of defect area treated with control scaffolds, cellular infiltration with new bone formation was observed only at the bone implant interface after 12 week post implantation and no bridging of defect site was observed. The osteogenic efficacy of scaffolds in terms of regeneration efficiency (RE) ratio (New bone formed per total defect area of the implant materials) obtained from the

histomorphometric analysis further substantiate the results of histology data revealing that the new bone formation was more pronounced with the use of test scaffolds and significant difference exist in new bone formation between test and control scaffolds after 3, 6 and 12 week post implantation (Figure 67). The result of *in vivo* bone regeneration studies reveals that the PDS incorporated scaffolds promoted the reconstruction of calvarial defect in osteoporotic rat. This study shows proof-of concept that the local delivery of pamidronate using PCL based scaffold have the potential to improve bone formation and thus may have translational applications for maximising bone formation in mechanically unfavourable environments.

5.4. Limitations of Study

The present study explored the feasibility of electrospinning technique for the fabrication scaffolds based on PCL for bone tissue engineering application. The study undertook the modification of PCL scaffolds in order to improve its surface wettability, mechanical properties, degradation behaviour and cellular response and evaluated its applicability for osteoporotic bone defect repair. It was also made sure that the relevant properties required for a scaffolding material to be used for bone tissue engineering applications have been evaluated. However, the study lacks the effect of PDS on osteoclast activity, which is an important criteria which could not be evaluated due to limitations.

5.5. Future perspectives

Extension of the work into large animal models will be the final criteria in deciding the potential application of these scaffolds in clinical practice.

CHAPTER 6

SUMMARY AND CONCLUSIONS

Bone fractures associated with osteoporosis is becoming a major concern all over the world especially in the elderly population and in postmenopausal women. Conventional treatment modality involves use of autografts, allografts, synthetic grafts as well as pharmaceutical agents for treating osteoporotic fractures. However, the scarcity of availability of tissues and organs for transplantation, donor site morbidity, immune rejection, pathogen transfer associated with the use of grafts and that of poor bioavailability and undesirable toxic side effects of pharmaceutical agents is a major concern.

Tissue engineering emerged as a promising alternative to traditional osteoporosis therapy. The scaffold based tissue engineering approach enables the delivery of cells, growth factors as well as bioactive drugs at the defect site which helps in stimulating bone formation. The main focus of the study was to design a scaffold based on PCL with appropriate combination of mechanical properties, cellular response and at the same time serving as matrix for sustained delivery of a pharmaceutical agent which can be used for osteoporotic bone defect repair.

The present study utilized the electrospinning technique for fabricating nanofibrous scaffolds based on synthetic biodegradable polymer PCL. The relatively low cost, inherent biocompatibility and biodegradability, along with its FDA approval makes PCL an ideal candidate as scaffolding material. The main concern in using PCL

as scaffolding material is its inherent hydrophobicity which results in slow degradation rate as well as poor cellular response.

The primary objective of the present study is to address the above problem by blending PCL with a hydrophilic polymer. With this aim, the copolymer PCL-PEG-PCL (CEC) was successfully synthesized by the ring opening polymerization of ε-caprolactone monomer using PEG as the macro initiator. The chemical characterization of CEC using FTIR and NMR confirms its formation and GPC analysis revealed its Mw as 7305. The copolymer CEC was incorporated on PCL scaffolds to modify its physical and biological properties. In addition to the blending approach, developing composites based on bioactive ceramics is an effective strategy to improve the cellular response and mechanical performance of the scaffolds. Hence the present study also focussed on incorporating nHAP particles into PCL and PCL/CEC blend scaffolds. The nHAP particles used in the study was of rod shaped and the size was found to be in the range of 12-35 nm width and 90-120 nm length as revealed by the TEM analysis.

Nanofibrous scaffolds using PCL, PCL/CEC blend and their nHAP filled composites were fabricated by electrospinning technique and evaluated for their physical and biological properties to identify scaffold with superior properties suitable for bone tissue engineering applications. The morphological features of the scaffolds analyzed by SEM showed bead free fibers confirming that the spinning parameters were optimal. The blending of PCL with the synthesized copolymer CEC resulted in smooth fibers with reduced fiber diameter, improved hydrophilicity, superior mechanical properties and enhanced degradation behavior. The nHAP incorporation resulted in fibers with rough

surface which may encourage better cellular response and reduced fiber diameter thereby improved mechanical properties. The effect of CEC and nHAP incorporation on the morphological properties, fiber diameter, pore size, percentage porosity, wettability, mechanical properties and degradation behaviour of PCL scaffolds were also well established in the study. The *in vitro* studies using RADMSCs revealed that fibroporous architecture of scaffold allowed the cells to adhere, proliferate and migrate into the scaffold and confirmed that the porosity and pore size of the scaffolds were sufficient for bone tissue engineering applications. An overall enhanced performance was shown by PCL/CEC/nHAP composite scaffold in cell viability (LDH assay) and proliferation (Picogreen assay) studies. Among the different scaffolds, the PCL/CEC/nHAP composite scaffolds exhibited superior performance in terms of physico-mechanical and biological properties which can be attributed to the combined effect of hydrophilic CEC and osteoconductive nHAP particles. Hence the results suggest that the PCL/CEC/nHAP composite scaffold can be a promising candidate for bone tissue engineering applications.

Pamidronate (PDS) is found to be an effective antiresorptive drug which has been used clinically in treating fractures associated with osteoporosis. Studies have shown that local delivery of PDS can improve the bone growth around dental and orthopedic implants. As an initial step towards developing scaffolds for osteoporotic bone defect repair, the study demonstrated the incorporation of different loadings of PDS onto PCL, PCL/CEC blend and PCL/CEC/nHAP composite scaffolds and evaluated the effect of PDS on the physico-mechanical and biological properties of

scaffolds. The study was designed to choose an appropriate scaffold with effective PDS loading that can be for used *in vivo* studies. The drug PDS was successfully incorporated on PCL, PCL/CEC blend and PCL/CEC/nHAP composite scaffolds which were reflected by the reduced fiber diameter and enhanced surface wettability of scaffolds. *In vitro* release study in PBS showed that sustained release of PDS was observed with the PCL/CEC/nHAP composite scaffolds. It was observed that PDS incorporation didn't elicit any cytotoxic response towards hOS cells during *in vitro* studies. However it was observed that at higher loadings of PDS, hOS cells lost their spindle morphology. Similar findings were observed with *in vitro* studies using osteogenic induced rADMSCs on PCL/CEC/nHAP composite scaffolds. The PCL/CEC/nHAP-PDS3 composite scaffold was selected for the *in vivo* studies based on the physico mechanical properties and *in vitro* release behavior.

The performance of the scaffolds under *in vivo* conditions was further evaluated by developing and validating an osteoporotic rat animal model. The potential of PCL/CEC/nHAP-PDS3 scaffold (test group) in healing 8 mm critical size calvarial defects created in osteoporotic was evaluated for different time period and was compared with that of the PCL/CEC/nHAP scaffolds (control group). Micro CT evaluation of the explants confirmed the improved osteointegrative ability of PDS incorporated scaffolds after 12 week post implantation. Histological analysis further supports the results of μ-CT data and shows the better osteointegration of test group indicated by the presence of bony islands within the defect area as well as at the bone-material interface after 6 and 12 week post implantation.The PDS incorporation in

PCL/CEC/nHAP scaffolds aided osteogenesis which was further depicted quantitatively in terms of regeneration efficiency ratio (new bone formed /total defect area).

The concept of local delivery of PDS at the implant site *via* PCL/CEC/nHAP composite scaffolds demonstrated better osteogenesis and osteointegration under osteoporotic condition. Our results suggest that incorporating PDS onto PCL/CEC/nHAP scaffolds is a promising and effective method to construct tissue engineering scaffolds utilising the combined effect of bioactivity of nHAP and the anti-osteoporotic effect of PDS.

The study suggests that PCL/CEC/nHAP-PDS composite scaffolds can be used as bone substitutes for local implantation into critical sized osteoporotic defects, owing to the enhanced *in vitro* cell attachment, proliferation and osteogenic differentiation, and accelerated *in vivo* healing progress on compared with PCL/CEC/nHAP scaffolds (control group). The better cytocompatibility of scaffolds under *in vitro* conditions supported by its performance under *in vivo* conditions in rat osteoporotic model predicts the clinical application of tissue engineered PDS incorporated PCL/CEC/nHAP scaffolds for osteoporotic bone defect repair.

BIBILOGRAPHY

Aggarwal N, Raveendran A, Khandelwal N, Sen RK, Thakur JS, Dhaliwal LK, Singla V, Manoharan SR (2011) Prevalence and related risk factors of osteoporosis in peri-and postmenopausal Indian women. *Journal of mid-Life health*. 2(2):81.

Aghdam RM, Najarian S, Shakhesi S, Khanlari S, Shaabani K, Sharifi S (2012) Investigating the effect of PGA on physical and mechanical properties of electrospun PCL/PGA blend nanofibers. *Journal of Applied Polymer Science.* 124(1):123-31.

Babel B. *Investigations on bone metabolism in intact and ovariohysterectomised miniature pigs* (Doctoral dissertation, lmu).

Bagi CM, Ammann P, Rizzoli R, Miller SC (1997) Effect of estrogen deficiency on cancellous and cortical bone structure and strength of the femoral neck in rats. *Calcified tissue international*. 61(4):336-44.

Bajgai MP, Aryal S, Bhattarai SR, Bahadur KC, Kim KW, Kim HY (2008) Poly (ϵ-caprolactone) grafted dextran biodegradable electrospun matrix: A novel scaffold for tissue engineering. *Journal of Applied Polymer Science*.108(3):1447-54.

Bianco A, Di Federico E, Moscatelli I, Camaioni A, Armentano I, Campagnolo L, Dottori M, Kenny JM, Siracusa G, Gusmano G (2009) Electrospun poly (ε-caprolactone)/Ca-deficient hydroxyapatite nanohybrids: microstructure, mechanical properties and cell response by murine embryonic stem cells. *Materials Science and Engineering: C.* A29(6):2063-71.

Blitch EL, Ricotta PJ. (1996) Introduction to bone grafting. *The Journal of foot and ankle surgery*. 35(5):458-62.

Bölgen N, Menceloğlu YZ, Acatay K, Vargel I, Pişkin E (2005) In vitro and in vivo degradation of non-woven materials made of poly (ε-caprolactone) nanofibers prepared by electrospinning under different conditions. *Journal of Biomaterials Science, Polymer Edition*. 16(12):1537-55.

Bramfeldt H, Sarazin P, Vermette P (2007) Characterization, degradation, and mechanical strength of poly (D, L-lactide-co-ϵ-caprolactone)-poly (ethylene glycol)-poly (D, L-lactide-co-ϵ-caprolactone). *Journal of Biomedical Materials Research Part A*. 83(2):503-11.

Cao D, Wu YP, Fu ZF, Tian Y, Li CJ, Gao CY, Chen ZL, Feng XZ. (2011) Cell adhesive and growth behavior on electrospun nanofibrous scaffolds by designed multifunctional composites. *Colloids and Surfaces B: Biointerfaces*. 84(1):26-34.

Cauley JA, Chalhoub D, Kassem AM, Fuleihan GE (2014) Geographic and ethnic disparities in osteoporotic fractures. *Nature Reviews Endocrinology*. 10(6):338-51.

Chandran S, Babu S S, Varma HK, John A (2016) Osteogenic efficacy of strontium hydroxyapatite micro-granules in osteoporotic rat model. Journal of biomaterials applications. 31(4):499-509.

Cheng N, Dai J, Cheng X, Li SE, Miron RJ, Wu T, Chen W, Zhang Y, Shi B (2013) Porous CaP/silk composite scaffolds to repair femur defects in an osteoporotic model. *Journal of Materials Science: Materials in Medicine*. 24(8):1963.

Chong EJ, Phan TT, Lim IJ, Zhang YZ, Bay BH, Ramakrishna S, Lim CT (2007) Evaluation of electrospun PCL/gelatin nanofibrous scaffold for wound healing and layered dermal reconstitution. *Acta biomaterialia*.3(3):321-30.

Chuenjitkuntaworn B, Supaphol P, Pavasant P, Damrongsri D (2010) Electrospun poly (L-lactic acid)/hydroxyapatite composite fibrous scaffolds for bone tissue engineering. *Polymer International*. 59(2):227-35.

Colman EG (2003) The Food and Drug Administration's osteoporosis guidance document: past, present, and future. *Journal of Bone and Mineral Research*. 18(6):1125-8.

Correia VD, Caldeira CL, Marques MM. (2006) Cytotoxicity evaluation of sodium alendronate on cultured human periodontal ligament fibroblasts. *Dental Traumatology*. 22(6):312-7.

Cunha MR, Santos Jr AR, Petinari L, Goissis G, Nonaka KO, Wang CC, Genari SC (2010) Characterization of the physical and mechanical properties of femoral bone defects filled with polyanionic collagen scaffolds in ovariectomized rats. *Materials Research*. 13(2):239-44.

Elsalanty ME, Genecov DG (2009) Bone grafts in craniofacial surgery. *Craniomaxillofacial Trauma and Reconstruction*. 2(03):125-34.

Fabbri P, Bondioli F, Messori M, Bartoli C, Dinucci D, Chiellini F(2010) Porous scaffolds of polycaprolactone reinforced with in situ generated hydroxyapatite for bone tissue engineering. *Journal of Materials Science: Materials in Medicine*. 21(1):343-51.

Fan TM, Lorimier LP, Charney SC, Hintermeister JG. (2005) Evaluation of intravenous pamidronate administration in 33 cancer-bearing dogs with primary or secondary bone involvement. *Journal of veterinary internal medicine*. 19(1):74-80.

Fischer RL, McCoy MG, Grant SA. (2012) Electrospinning collagen and hyaluronic acid nanofiber meshes. *Journal of Materials Science: Materials in Medicine*. 23(7):1645-54.

Gan Z, Liang Q, Zhang J, Jing X (1997) Enzymatic degradation of poly (ε-caprolactone) film in phosphate buffer solution containing lipases. *Polymer degradation and stability*. 56(2):209-13.

Galia CR, Moreira LF (2012) The Biology of Bone Grafts. InRecent Advances in Arthroplasty InTech.

Ghasemi-Mobarakeh L, Prabhakaran MP, Morshed M, Nasr-Esfahani MH, Ramakrishna S (2008)Electrospun poly (ε-caprolactone)/gelatin nanofibrous scaffolds for nerve tissue engineering. *Biomaterials*. 29(34):4532-9.

Giannoudis PV, Schneider E. (2006) Principles of fixation of osteoporotic fractures. *Bone & Joint Journal*. 88(10):1272-8.

Giger EV, Castagner B, Leroux JC (2013) Biomedical applications of bisphosphonates. *Journal of controlled release.* 167(2):175-88.

Goldhahn J, Féron JM, Kanis J, Papapoulos S, Reginster JY, Rizzoli R, Dere W, Mitlak B, Tsouderos Y, Boonen S (2012) Implications for fracture healing of current and new osteoporosis treatments: an ESCEO consensus paper. *Calcified tissue i nternational*. 90(5):343-53.

Gomes ME, Reis RL, Cunha AM, Blitterswijk CA, De Bruijn JD (2001) Cytocompatibility and response of osteoblastic-like cells to starch-based polymers: effect of several additives and processing conditions. *Biomaterials.* 22(13):1911-7.

Groff L, Zecca E, De Conno F, Brunelli C, Boffi R, Panzeri C, Cazzaniga M, Ripamonti C. (2001) The role of disodium pamidronate in the management of bone pain due to malignancy. *Palliative medicine.* 15(4):297-307.

Gross TP, Cox QG, Jinnah RH (1993) History and current application of bone transplantation. *Orthopedics.* 16(8):895-900.

Han J, Branford-White CJ, Zhu LM (2010) Preparation of poly (ε-caprolactone)/poly (trimethylene carbonate) blend nanofibers by electrospinning. *Carbohydrate Polymers.* 79(1):214-8.

Heath CA. (2000) Cells for tissue engineering. *Trends in biotechnology*. 18(1):17-9.

Hollinger JO, Battistone GC. (1985) Biodegradable bone repair materials: synthetic polymers and ceramics. ARMY INST OF DENTAL RESEARCH WASHINGTON DC;

Huang ZM, Zhang YZ, Kotaki M, Ramakrishna S (2003) A review on polymer nanofibers by electrospinning and their applications in nanocomposites. *Composites science and technology.* 63(15):2223-53.

Jakob F, Ebert R, Ignatius A, Matsushita T, Watanabe Y, Groll J, Walles H (2013) Bone tissue engineering in osteoporosis. *Maturitas*. 75(2):118-24.

Jee WS, Yao W (2001) Overview: animal models of osteopenia and osteoporosis. *J Musculoskelet Neuronal Interact.*1(3):193-207.

Jose MV, Thomas V, Xu Y, Bellis S, Nyairo E, Dean D (2010) Aligned bioactive multi-component nanofibrous nanocomposite scaffolds for bone tissue engineering. *Macromolecular bioscience.* 10(4):433-44.

Kajiwara H, Yamaza T, Yoshinari M, Goto T, Iyama S, Atsuta I, Kido MA, Tanaka T (2005) The bisphosphonate pamidronate on the surface of titanium stimulates bone formation around tibial implants in rats. *Biomaterials.* 26(6):581-7.

Kim CH, Khil MS, Kim HY, Lee HU, Jahng KY (2006) An improved hydrophilicity via electrospinning for enhanced cell attachment and proliferation. *Journal of Biomedical Materials Research Part B: Applied Biomaterials.* 78(2):283-90.

Kim GM, Huyen K, Le T, Giannitelli SM, Lee YJ, Rainer A, Trombetta M. (2013) Electrospinning of PCL/PVP blends for tissue engineering scaffolds. *Journal of Materials Science: Materials in Medicine.* 24(6):1425.

Kim KH, Cui GH, Lim HJ, Huh J, Ahn CH, Jo WH. (2004) Synthesis and Micellization of Star-Shaped Poly (ethylene glycol)-block-Poly (ε-caprolactone). *Macromolecular Chemistry and Physics*. 205(12):1684-92.

Kumar KS, Bhaskar P. (2012) Osteoporosis-An Emerging Disease of the 21st Century, Part 1: An Overview. *Journal of family medicine and primary care*. 1(1):66.

Labow RS, Meek E, Matheson LA, Santerre JP (2002) Human macrophage-mediated biodegradation of polyurethanes: assessment of candidate enzyme activities. *Biomaterials*. 23(19):3969-75.

Lao L, Wang Y, Zhu Y, Zhang Y, Gao C (2011) Poly (lactide-co-glycolide)/hydroxyapatite nanofibrous scaffolds fabricated by electrospinning for bone tissue engineering. *Journal of Materials Science: Materials in Medicine*. 22(8):1873-84.

Larsson S. Treatment of osteoporotic fractures. (2002) *Scandinavian journal of surgery*. 1(2):140-6.

Laurencin C, Khan Y, El-Amin SF (2006) Bone graft substitutes. *Expert review of medical devices*. 3(1):49-57.

Laverna C, Schoenung JM. (1991) Calcium phosphate ceramics as bone substitutes. American Ceramic Society Bulletin. 70(1):95-100.

Li S, Garreau H, Vert M, Petrova T, Manolova N, Rashkov I (1998) Hydrolytic degradation of poly (oxyethylene)–poly-(ε-caprolactone) multiblock copolymers. *Journal of applied polymer science*. 68(6):989-98.

Li WJ, Laurencin CT, Caterson EJ, Tuan RS, Ko FK (2002) Electrospun nanofibrous structure: a novel scaffold for tissue engineering. *Journal of Biomedical Materials Research Part A*. 60(4):613-21.

Liang D, Hsiao BS, Chu B (2007) Functional electrospun nanofibrous scaffolds for biomedical applications. *Advanced drug delivery reviews*.59(14):1392-412.

Liao GY, Chen L, Zeng XY, Zhou XP, Xie XL, Peng EJ, Ye ZQ, Mai YW (2011) Electrospun poly (L-lactide)/poly (ε-caprolactone) blend fibers and their cellular response to adipose-derived stem cells. *Journal of applied polymer science*. 120(4):2154-65.

Lu J, Liu JG, Song XF, Chen XS, Wu XD (2011) Sandwich structure-like meshes fabricated via electrospinning for controllable release of zoledronic acid. *Chem Res Chin Univ*. 27:524.

Luhmann T, Germershaus O, Groll J, Meinel L. (2016) Bone targeting for the treatment of osteoporosis. *Journal of controlled release.* 1(2):198-213.

LYET JP. (2006) Fragility Fractures in the Osteoporotic Patient: Special Challenges. *The Journal*. 1(3):91.

Majumdar, S., Genant, H.K., Grampp, S., Newitt, D.C., Truong, V.-H., Lin, J.C., Mathur, A., 1997. Correlation of Trabecular Bone Structure with Age, Bone Mineral Density, and Osteoporotic Status: In Vivo Studies in the Distal Radius Using High Resolution Magnetic Resonance Imaging. *J. Bone Miner. Res*. 12, 111–118.

Masaeli E, Morshed M, Rasekhian P, Karbasi S, Karbalaie K, Karamali F, Abedi D, Razavi S, Jafarian-Dehkordi A, Nasr-Esfahani MH, Baharvand H (2012) Does the tissue engineering architecture of poly (3-hydroxybutyrate)scaffold affects cell–material interactions?. *Journal of Biomedical Materials Research Part A*. 100(7):1907-18.

Meng ZX, Zheng W, Li L, Zheng YF (2010) Fabrication and characterization of three-dimensional nanofiber membrance of PCL–mwcnts by electrospinning. *Materials Science and Engineering: C*. 30(7):1014-21.

Mithal A, Bansal B, Kyer CS, Ebeling P (2014) The Asia-pacific regional audit-epidemiology, costs, and burden of osteoporosis in India 2013: a report of international 18(4):449

Morabito N, Gaudio A , Lasco, A, Vergara C, Tallarida F, Crisafulli G, Trifiletti A, Cincotta M., Pizzoleo MA, Frisina N. (2003) Three-year effectiveness of intravenous pamidronate versus pamidronate plus slow-release sodium fluoride for postmenopausal osteoporosis. *Osteoporosis international*. 14(6):500-506.

Mukherjee D, Bharath S (2013) Design and characterization of double layered mucoadhesive system containing bisphosphonate derivative. *ISRN pharmaceutics*. 19;2013.

Murugan R, Ramakrishna S (2005) Development of nanocomposites for bone grafting. Composites Science and Technology. 65(15):2385-406.

Nair MB, Bernhardt A, Lode A, Heinemann C, Thieme S, Hanke T, Varma H, Gelinsky M, John A (2009) A bioactive triphasic ceramic-coated hydroxyapatite promotes proliferation and osteogenic differentiation of human bone marrow stromal cells. *Journal of Biomedical Materials Research Part A*. 90(2):533-42.

Nam J, Huang Y, Agarwal S, Lannutti J (2007) Improved cellular infiltration in electrospun fiber via engineered porosity. *Tissue engineering*. 13(9):2249-57.

Natta FJ, Hill JW, Carothers WH (1934) Studies of polymerization and ring formation. XXIII. 1 ε-Caprolactone and its polymers. *Journal of the American Chemical Society*. (2):455-7.

Oh SH, Kang SG, Kim ES, Cho SH, Lee JH (2003) Fabrication and characterization of hydrophilic poly (lactic-co-glycolic acid)/poly (vinyl alcohol) blend cell scaffolds by melt-molding particulate-leaching method. *Biomaterials*. 24(22):4011-21.

Pitt CG. (1990) Poly-ε-caprolactone and its copolymers. *Drugs and the pharmaceutical sciences*. 45:71-120.

Ponader S, Brandt H, Vairaktaris E, von Wilmowsky C, Nkenke E, Schlegel KA, Neukam FW, Holst S, Müller FA, Greil P. (2008) In vitro response of hFOB cells to pamidronate modified sodium silicate coated cellulose scaffolds. *Colloids and Surfaces B: Biointerfaces*. 64(2):275-83.

Ponader S, Brandt H, Vairaktaris E, von Wilmowsky C, Nkenke E, Schlegel KA, Neukam FW, Holst S, Müller FA, Greil P (2008) In vitro response of hFOB cells to pamidronate modified sodium silicate coated cellulose scaffolds. *Colloids and Surfaces B: Biointerfaces*. 64(2):275-83.

Prabhakaran MP, Venugopal JR, Chyan TT, Hai LB, Chan CK, Lim AY, Ramakrishna S (2008) Electrospun biocomposite nanofibrous scaffolds for neural tissue engineering. *Tissue Engineering Part A*. 14(11):1787-97.

Puppi D, Chiellini F, Piras AM, Chiellini E (2010) Polymeric materials for bone and cartilage repair. *Progress in Polymer Science*. 35(4):403-40.

Raisz LG. (2005) Pathogenesis of osteoporosis: concepts, conflicts, and prospects. *Journal of Clinical Investigation*. 115(12):3318.

Reid IR, Wattie DJ, Evans MC, Gamble GD, Stapleton JP, Cornish JI. (1994) Continuous therapy with pamidronate, a potent bisphosphonate, in postmenopausal osteoporosis. *The Journal of Clinical Endocrinology & Metabolism*. 79(6):1595-9

Reinwald S, Burr D *(*2008) Review of nonprimate, large animal models for osteoporosis research. *Journal of Bone and Mineral Research*. 23(9):1353-68.

Salgado AJ, Coutinho OP, Reis RL (2004) Bone tissue engineering: state of the art and future trends. *Macromolecular bioscience*. 4(8):743-65.

Sartori AR, Moreira JA, Santos AM, Cintra DE, Sartori LR, Baraúna MA, Canto RS (2008) Bone repair process in normal and osteopenic female rats' tibiae: a comparative study. *Acta Ortopédica Brasileira*, *16*(1), 37-40.

Schneider E, Goldhahn J, Burckhardt P (2005) The challenge: fracture treatment in osteoporotic bone. *Osteoporosis International*. 16:S1-2.

Shafiee A, Soleimani M, Chamheidari GA, Seyedjafari E, Dodel M, Atashi A, Gheisari Y (2011) Electrospun nanofiber-based regeneration of cartilage enhanced by mesenchymal stem cells. *Journal of biomedical materials research Part A*. 99(3):467-78.

Shafieyan Y, Sharifi S, Imani M, Shokrgozar MA, Aboudzadeh N, Atai M. A (2011) biocompatible composite based on poly (ε-caprolactone fumarate) and hydroxyapatite. *Polymers for Advanced Technologies*. 22(12):2182-90.

Shalumon KT, Binulal NS, Deepthy M, Jayakumar R, Manzoor K, Nair SV. (2010) Preparation, characterization and cell attachment studies of electrospun multi-scale poly (caprolactone) fibrous scaffolds for tissue engineering. *Journal of Macromolecular Science, Part A*. 48(1):21-30.

Shen V, Birchman R, Wu DD, Lindsay R(2000) Skeletal effects of parathyroid hormone infusion in ovariectomized rats with or without estrogen repletion. *Journal of Bone and Mineral Research*. 15(4):740-6.

Shin YS, Borah JS, Haider A, Kim S, Huh MW, Kang IK (2013) Fabrication of pamidronic acid-immobilized TiO 2/hydroxyapatite composite nanofiber mats for biomedical applications. *Journal of Nanomaterials*. 2013:152.

Son SR, Linh NT, Yang HM, Lee BT (2013) In vitro and in vivo evaluation of electrospun PCL/PMMA fibrous scaffolds for bone regeneration. *Science and technology of advanced materials*. 14(1):015009.

Son SR, Linh NT, Yang HM, Lee BT. (2013) In vitro and in vivo evaluation of electrospun PCL/PMMA fibrous scaffolds for bone regeneration. *Science and technology of advanced materials.* 14(1):015009.

Sridevi A, Ragi V. Management of osteoporosis in women-A prevalence and interventional study.

Staiger MP, Pietak AM, Huadmai J, Dias G (2006) Magnesium and its alloys as orthopedic biomaterials: a review. *Biomaterials.* 27(9):1728-34.

STANLEY L, BALL KE. Pamidronate therapy as prevention of bone loss following renal transplantation1. Hypertension. (2000);50:2.

Subia B, Kundu J, Kundu SC. Biomaterial scaffold fabrication techniques for potential tissue engineering applications. InTissue engineering (2010). InTech.

Szpalski C, Barr J, Wetterau M, Saadeh PB, Warren SM (2010) Cranial bone defects: current and future strategies. *Neurosurgical focus.* 29(6):E8.

Thiebaud D, Burckhardt P, Melchior J, Eckert P, Jacquet AF, Schnyder P, Gobelet C (1994) Two years' effectiveness of intravenous pamidronate (APD) versus oral fluoride for osteoporosis occurring in the postmenopause. *Osteoporosis international.* 4(2):76-83.

Thulkar J, Singh S. (2015) Overview of research studies on osteoporosis in menopausal women since the last decade. *Journal of mid-life health*. 6(3):104.

Venugopal J, Low S, Choon AT, Kumar AB, Ramakrishna S (2008) Electrospun-modified nanofibrous scaffolds for the mineralization of osteoblast cells. *Journal of biomedical materials research Part A*. 85(2):408-17.

Verron E, Gauthier O, Janvier P, Pilet P, Lesoeur J, Bujoli B, Guicheux J, Bouler JM. (2010) In vivo bone augmentation in an osteoporotic environment using bisphosphonate-loaded calcium deficient apatite. *Biomaterials.* 31(30):7776-84.

Wang JH, Cheng XB, Huang G, Dong FC, Jia YT (2011) Preparation and Characterization of PCL/PVP Blend Membrane. InAdvanced Materials Research (Vol. 311, pp. 1638-1641). Trans Tech Publications.

Wang Z, Han Z, Tao J, Lu P, Liu X, Wang J, Wu B, Huang Z, Yin C, Tan R, Gu M (2014) Clinical efficacy and safety of pamidronate therapy on bone mass density in early post-renal transplant period: a meta-analysis of randomized controlled trials. *PloS one.* Se9(9):e108106.

Wilkinson JM, Little DG (2011) Bisphosphonates in orthopedic applications. *Bone.* 49(1):95-102.

Williams A, Szaso RM (2004) Bone transplantation. *Orthopedics.* 27(5):488-95.

Wronski TJ (1991) The ovariectomized rat as an animal model for postmenopausal bone loss. *Cells Materials.* 1:69-74.

Wronski TJ, Lowry PL, Walsh CC, Ignaszewski LA (1985) Skeletal alterations in ovariectomized rats. *Calcified tissue international*. 37(3):324-8.

Wutticharoenmongkol P, Sanchavanakit N, Pavasant P, Supaphol P (2006)Preparation and characterization of novel bone scaffolds based on electrospun polycaprolactone fibers filled with nanoparticles. *Macromolecular bioscience*.6(1):70-7.

Xie Z, Buschle-Diller G. (2010) Electrospun poly (D, L-lactide) fibers for drug delivery: The influence of cosolvent and the mechanism of drug release. *Journal of applied polymer science*. 115(1):1-8.

Yang S, Leong KF, Du Z, Chua CK. (2001) The design of scaffolds for use in tissue engineering. Part I. Traditional factors. *Tissue engineering.* 7(6):679-89.

Yu NY, Schindeler A, Peacock L, Mikulec K, Baldock PA, Ruys AJ, Little DG (2010) In vivo local co-delivery of recombinant human bone morphogenetic protein-7 and pamidronate via poly-D, L-lactic acid. *Eur Cell Mater.* 20:431-1.

Yun YP, Kim SJ, Lim YM, Park K, Kim HJ, Jeong SI, Kim SE, Song HR (2014) The effect of alendronate-loaded polycarprolactone nanofibrous scaffolds on osteogenic differentiation of adipose-derived stem cells in bone tissue regeneration. *Journal of biomedical nanotechnology.* 10(6):1080-90.

Zhang Y, Wei L, Chang J, Miron RJ, Shi B, Yi S, Wu C (2013) Strontium-incorporated mesoporous bioactive glass scaffolds stimulating in vitro proliferation and differentiation of bone marrow stromal cells and in vivo regeneration of osteoporotic bone defects. *Journal of Materials Chemistry B.* 1(41):5711-22.

LIST OF PUBLICATIONS

Remya K. R., Joseph, J., Mani, S., John, A., Varma, H. K., & Ramesh, P. Nanohydroxyapatite incorporated electrospun Polycaprolactone/Polycaprolactone – Polyethyleneglycol - Polycaprolactone Blend Scaffold for Bone Tissue Engineering Applications (2013). *Journal of biomedical nanotechnology*, *9*(9), 1483-1494.

Remya K.R., Sunitha Chandran, Annie John and P.Ramesh, Pamidronate encapsulated electrospun nanofibrous polycaprolactone scaffolds as a potential drug eluting scaffold for the treatment of osteoporotic bone defects. (manuscript submitted)

Remya K.R., Sunitha Chandran, Annie John and P.Ramesh, Hybrid Polycaprolactone/Polyethylene oxide scaffolds with tunable fiber surface morphology, improved hydrophilicity and biodegradability for bone tissue engineering application. (under revision)

Remya K.R., Sunitha Chandran, Harikrishnan V.S, Annie John and P.Ramesh. *In-vitro* and *in-vivo* evaluation of pamidronate incorporated PCL based scaffolds in an osteoporotic rat animal model. (manuscript to be submitted)

Conference presentations

Remya K.R. and P. Ramesh, Controlled release of Pamidronate from electrospun Polycaprolactone nanofibrous mats for orthopaedic application, National seminar on Biopolymers & Green Composites (BPGC 2015), October 9-10, 2015 organized by Centre for Biopolymer Science & Technology, Kochi.

Remya K.R, Sunitha Chandran, Annie John, Harikrishna Varma P.R. and Ramesh P , Pamidronate loaded electrospun Polycaprolactone/ Polycaprolactone – Polyethyleneglycol-Polycaprolactone / nanohydroxyapatite composite scaffold for orthopaedic application , National Conference on Material Science & Technology (NCMST 2015),July 6-8,2015 organized by IIST Thiruvananthapuram.

Remya K.R. and P. Ramesh, In-vitro degradation behaviour of electrospun Polycaprolactone/Polyethyleneoxide blends for tissue engineering applications , an international conference FAPS – MACRO, May 15-18, 2013 organized by Indian Institute of Science, Bangalore.

CURRICULUM VITAE

Personal

Name	:	Remya K R
Date of birth	:	30th April 1985
Marital status	:	Unmarried
Phone number	:	9847226094
Address	:	Raj Bhavan
		Chithrapuzha
		Irumpanam P. O.
		Ernakulam-682309
		Kerala, India
E-mail	:	remyaraj85@gmail.com

Education

Ph.D Scholar (January 2011- present) at Sree Chitra Tirunal Institute for Medical Sciences and Technology, BioMedical Technology Wing, Thiruvananthapuram, Kerala, India. Supervisor : Dr. P. Ramesh

Master of Technology in Polymer Technology (2007-2009) Cochin University of Science and Technology, Cochin, Kerala, India

Master of Science in Chemistry (Polymer science) (2005-2007), School of Chemical Sciences, Mahatma Gandhi University, Kottayam, Kerala, India

Bachelor of Science in Chemistry (2002-2005), St Teresa's College, (Mahatma Gandhi University), Kochi, Kerala, India

Professional Experience

August 2009- December 2010: Junior Research Fellow at Sree Chitra Tirunal Institute for Medical Sciences and Technology, Trivandrum, Kerala, India. Project Supervisor: Dr. P. Ramesh.

July 2008 – April 2009: MTech Project at HLL Lifecare, Trivandrum. Project Supervisor: Dr. Abi Santosh Aprem

February 2007 – May 2007: MSc Project at National Chemical Laboratory (NCL) , Pune, Maharashtra Project Supervisor: Dr. Jyoti P.Jog

Achievements

Prestegious SCTIMST Institute Fellowship 2011

Best oral presentation award, National conference on Biopolymers and Green composites (BPGC) 2015, organized by Centre for Biopolymer Science & Technology , Kochi

First prize in Quiz competition during National Conference on Biopolymers and Green composites 2015, organized by Centre for Biopolymer Science & Technology , Kochi

APPENDIX

PBS (1000ml) pH 7.4

NaCl - 8g
KCl - 0.2g
Na_2HPO_4 - 1.44g
KH_2PO_4 - 0.24g

(Added distilled water to a final volume of 1000 ml, solution is filtered and stored at room temperature)

Ninhydrin reagent (0.2 %)

Ninhydrin - 0.2 % w/v in methanol

Stevenal's blue stain

Methylene Blue – 1 gm in 75 ml distilled water
Potassium permanganate – 1.5 gm in 75 ml distilled water

Van Gieson's Picrofuchsin stain

Acid Fuchsin – 0.1 gm in 10 ml distilled water
Saturated picric acid – 100ml